Platinum promotion in supported gold catalysts for glycerol oxidation

Mariam Royker

Submitted in partial fulfilment of the requirements for the degree of

Master of Science in Chemical Engineering

Centre for Catalysis Research
Department of Chemical Engineering
University of Cape Town

Synopsis

There has been recently a drive toward cleaner fuels, with biodiesel proving to be a viable option. It is obtained by the transesterification of triglycerides, with glycerol as the main co-product. Approximately 100kg of glycerol is formed per ton of biodiesel produced. The commercial viability of biodiesel production also depends on the availability of a suitable market for the co-product. Traditional glycerol markets are in the food and drink industry, pharmaceuticals, personal care products, polymers and explosives. Glycerol oxidation follows a complex reaction pathway leading to a range of products which can be used in the synthesis of fine chemicals. These materials are currently being produced by processes that are expensive and harmful to the environment. Due to the increase of glycerol stocks world-wide and the need to create value added glycerol products, catalytic glycerol oxidation has become an area of great importance in research. This study focuses on the promotion of alumina supported gold catalysts with platinum for glycerol oxidation.

Alumina supported gold catalysts were prepared by ion-exchange with $HAuCl_4$. Bimetallic AuPt catalysts were prepared by impregnating the gold catalyst with Pt (by using $(NH_3)_4PtCl_2$ as a precursor). Catalysts were characterised by atomic absorption spectroscopy (AAS) and transmission electron microscopy (TEM). Three different catalysts were synthesized:

Catalyst	W_{Au} [wt-%]	W_{Pt} [wt-%]	d_{Au} [nm]	d_{Pt} [nm]
Au_{100}	2.2	0	4.2 ± 1.3	-
$Au_{63}Pt_{37}$	1.4	0.8	2.9 ± 1.0	1.5
$Au_{28}Pt_{72}$	0.6	1.6	2.8 ± 1.1	8.7

Glycerol oxidation experiments were performed in a semi-batch reactor at a temperature of 60°C, atmospheric pressure, an initial glycerol concentration of 0.03 M and a controlled pH of 10 by addition of NaOH. The three different catalysts were tested at these conditions. Monometallic Au_{100} was also tested in the oxidation of glycerol where the pH was varied from 7 to 10 as well as runs where the initial glycerol concentration was varied (0.003M, 0.03M, 0.16M & 0.6M). All reactions were run for 60 minutes and filtered samples were taken every 10 minutes. The samples were analysed using HPLC and products were identified using external standards of possible oxidation products.

The highest glycerol conversion achieved with monometallic Au was ca. 35% with hardly any activity after 10 minutes. This points toward strong rate of deactivation of the gold catalyst. After an hour, a 20% greater conversion is seen with the bimetallic catalysts and a slower rate of deactivation is observed. Four main products were identified from the oxidation reaction, i.e. dihydroxyacetone, glyceric acid, glycolic acid and tartronic acid. A carbon balance confirmed that these products and the unconverted glycerol account for 90% of the carbon in the system when using the bimetallic catalysts. For the monometallic Au catalyst, only 70% of the carbon is accounted for by the unconverted glycerol and the above four products. Reaction samples were tested for the presence of CO_2 in the form of carbonic acid and none was found. The 30% missing carbon is therefore thought to be coke which is also responsible for the deactivation of the catalysts. The bimetallic catalysts are less prone to coke formation and therefore sustain a lower degree of deactivation. A greater selectivity to dihydroxyacetone and glyceric acid was observed with the bimetallic catalysts compared to monometallic gold. In the catalysts investigated it was found that the fraction of platinum in the bimetallic catalyst has no significant effect on conversion and selectivity. However, the rate of deactivation of the catalyst decrease with an increase in platinum content with the lowest deactivation observed at ca. 80 wt-% platinum in the metal.

I know the meaning of plagiarism and declare that all the work in the document, save for that which is properly acknowledged, is my own

_____

Acknowledgements

I begin in the Name of God, the Most Beneficent, Most Merciful. All praise is due to God, Lord of all the worlds, Who has blessed me with so much.

A note of gratitude is owed to my supervisor, Prof Eric van Steen, not only for his technical expertise and outstanding knowledge and experience in the field of catalysis, but also for his constant encouragement and guidance throughout. A vote of appreciation is also due to Prof Jenni Case, the co-supervisor to this project, for her unending support and words of encouragement and for all the enthusiasm she imparted to me and this project. It has been an honour to work with both of them.

I am grateful for all the assistance I received with the laboratory work. The Centre for Catalysis Research provided a pleasant and accommodating environment for the laboratory work (catalyst preparation and testing). A fellow post-graduate student, Tracey Van Heerden, helped me find my feet in the laboratory during the initial phase of the project. The team in the Analytical Lab in the Department of Chemical Engineering made up of Mrs Helen Divey, Mrs Suzana Vasic and Mr Lonwabo Mtebeni performed all AAS work and H_2-chemisorption. Mr Mohammed Jaffer and Mr Franscious Cummings at the Electron Microscopy Unit at UCT aided in producing TEM images. HRTEM work was performed at the UWC Electron Microscopy Unit with assistance from Dr Subelia Botha. All HPLC work was performed in the CeBER laboratories and thanks is due to Mrs Frances Pocock for accommodating me in her labs and assistance with ordering of materials. Training on the HPLC unit was conducted by Dr Caryn Fenner, Dr Clive Garcin and Vinayak Bhardwaj in the CeBER group.

To my closest and dearest friend, Nabeel Hussain, thank you for all the support, encouragement and most importantly, for always believing in me.

My deepest appreciation is reserved for my parents and siblings. Without their unlimited love, support, patience and guidance none of this would have been possible.

Table of Contents

List of Figures

List of Tables

Chapter 1. Introduction

The production of biodiesel via trans-esterification of triglycerides yields glycerol as a side-product (Ma and Hanna, 1999). Approximately 100 kg of glycerol is formed per ton of biodiesel produced. Hence, the commercial viability of biodiesel production also depends on the available market for the side product, glycerol. Although glycerol itself is a useful chemical used in drugs, oral care products and food (Morrison, 2000), its market is far too small to take up the significant amount of glycerol produced from a growing biodiesel market necessitating the development of glycerol as a platform chemical (Zhou et al., 2008). Selective oxidation of glycerol (preferably using air) is the preferred method to generate other chemical building blocks, such as dihydroxyacetone, glyceric acid, and tartronic acid.

Supported gold catalysts have been shown to be active catalysts for the selective oxidation of glycerol to glyceric acid using oxygen (Carrettin et al., 2003; Porta and Prati, 2004; Demirel-Gülen et al., 2005; Demirel et al., 2007a). The oxidation of alcohols and polyols over gold catalysts requires alkaline conditions (Carretin et al., 2003), since the first step in the oxidation is the proton abstraction from glycerol (Ketchie et al., 2007). Furthermore, oxygen from the hydroxyl ion is incorporated into the product acid. The hydroxyl ion is regenerated via O_2 reduction with water (Zope et al., 2010).

The catalytic oxidation of glycerol can yield a multitude of products via a series of consecutive and parallel reactions. Control of product selectivity is of great importance to minimize the required separation processes to obtain the pure product compounds. Glycerol can be oxidized to glyceraldehyde, which is under basic conditions rapidly converted into dihydroxyacetone. Glyceric acid can either be formed directly from glycerol or in a consecutive reaction involving glyceraldehyde. The consecutive oxidation of glyceric acid yields tartronic acid. The oxidation of glycerol may lead to the formation of degradation products such as glycolic acid, oxalic acid, acetic acid, formic acid and CO_x. Supported gold catalysts have been reported to be selective towards the formation of glyceric and glycolic acid (Porta and Prati, 2004; Ketchie et al., 2007) with the latter formed directly from glycerol in a parallel pathway.

Bimetallic gold-platinum catalysts have been reported to be more active than mono-metallic gold based catalysts (Bianchi et al., 2005; Demirel et al., 2007a) increasing the activity (expressed per g of metal) by up to 80%. A similar enhancement was observed by alloying gold with palladium (Dimitratos et al., 2009a).

Supported gold catalysts are typically supported on carbon. However, the harsh conditions experienced typically in liquid phase reactions require a highly mechanically stable support (Villa et al., 2010). Not much research into alumina supported gold nanoparticles has been performed. In this study, the performance of monometallic gold and bimetallic Au-Pt catalysts supported on alumina for the liquid phase oxidation of glycerol is investigated.

Chapter 2. Literature Review

2.1 Gold as Heterogeneous Catalyst

Until the late 1980's gold was thought to be catalytically inert. This was until it was discovered (Haruta et al., 1987, Haruat et al.,1989) that supported nano-sized gold particles are catalytically active in the low temperature oxidation of CO. The catalytic behaviour of gold depends on forming these very small particles since large particles and bulk gold cannot chemisorb reactant molecules strongly enough (Bond et al., 1999).

Since this discovery, it has been reported that supported nano-sized gold particles are able to catalyse a range of reactions including redox reactions (Haruta, 2004) as well as the oxidation of alkenes (Hughes et al., 2005) and alcohols (Prati & Rossi 1998), such as glycerol.

2.2 Synthesis of Bimetallic Systems

Materials which improve the catalytic performance of a catalyst can be regarded as catalyst promoters. Promoters do not have to possess a high catalytic activity by themselves, but they improve the catalytic performance with regards to activity, selectivity and stability. Two types of promoters can be defined: chemical and structural. Chemical promoters affect the chemical nature of catalyst's surface thereby influencing the active sites and consequently increasing the activity of the catalyst (Gates, 2001). A structural promoter offers stability to the catalyst by minimising contact between the surface metal atoms (Gates, 2001). This reduces the loss in surface area of the catalytically active phase by sintering and thereby, deactivation.

Bimetallic catalysts offer the possibility of improved activity and selectivity when compared to monometallic catalysts. These improvements in the catalysts have been related to a change in the electronic and chemical structure of the catalyst in comparison to the parent metal, if an alloy is formed.

Transition metals, especially those in group 8, are catalytically active for a range of reactions (Sinfelt, 1977). A metal such as nickel or platinum in group 8 is characterised by having an incompletely filled d-band, whereas metals such as copper or gold in group 1B have a filled d-band (Sinfelt, 1977). It has been proposed (Mott & Jones, 1936) that an alloy of a group 8 and group 1B metal has a d-band that is filled to a greater degree than that of the pure group 8 metal. For example, when looking at a nickel-copper alloy, substituting copper atoms for nickel atoms in the metal lattice adds extra electrons to the lattice. These extra electrons

from the copper enter the d-band of the alloy until it is filled. The activity of the bimetallic system has been seen to depend on the ratio in which the 2 metals are present (Schwank, 1985; Luo et al., 2005a; Bond et al., 2006). Thus, by varying the composition of the alloy a change in the catalytic activity can be observed since the extent to which the d-band is filled is varied (Sinfelt, 1977).

Surface science studies have been performed to account for the differences observed between mono- and bimetallic catalysts (Kitchin et al., 2004). Two primary mechanisms have been proposed to be responsible for the differences in surface chemical properties, the first being the strain effect, where the average bond length between metal atoms in the monolayer surface is different to that in the parent metals. Secondly, heterometallic bonding interactions, commonly known as the "ligand effect", between the surface atoms and the substrate cause a change in the surface electronic structure which changes the surface chemical properties. One cannot separate the strain and ligand effects experimentally since they occur together and what is observed is the combined effect of both phenomena (Kitchin et al., 2004). The ligand effect may occur when the promoter is on the surface of the other metal, whereas the strain effect requires alloy formation. A study by Mihut et al. (2002) showed that bimetallic catalysts impregnated with individual Au and Pt precursors (tetrachloroauric and hexachloroplatinic acid) displayed similar behaviour to a monometallic Pt catalyst. Monometallic Pt/SiO_2 (1 or 0.15 wt%) and Au/SiO_2 (2 or 0.3 wt%) were prepared by incipient wetness impregnation. Two bimetallic catalysts were also prepared by co-impregnation on SiO_2 support with 1-wt% Pt 2-wt% Au and 0.15-wt% Pt 0.3-wt% Au. The lack of improvement in catalytic activity with the addition of Au was thought to be the result of phase segregation of the two metals due to their miscibility gap (Ponec et al., 1995). It was later shown (Luo et al., 2005b; Mott et al., 2007) that bimetallic AuPt nanoparticles display alloy properties, which is in sharp contrast to the bimetallic miscibility gap known for bulk bimetallic AuPt metals (Ponec et al., 1995). The Au-Pt system can form alloys at temperatures larger than 0K (Xu et al., 2009). Xu et al. (2009) estimates that the Au-Pt system can have at 400K a gold-rich phase (containing up to 10 mol-% Pt) and a platinum-rich phase (containing at least 6 mol-% Pt). Of further interest, is the meta-stable region as described by the chemical spinodal, which shows a meta-stable gold-rich phase at 400K (containing up to 32 mol-% Pt) and a meta-stable platinum-rich phase (containing at least 90 mol-% Pt). The meta-stable state is more predominant, when the number of vacancies in the crystal is lower. It has been deduced that the energy for the reaction of a vacancy increases with decreasing diameter (Ruffino et al., 2008), however the number of vacancies is still very low at 400K, which may result in a stabilisation of the meta-stable state.

2.3 Alcohol oxidation

Selective alcohol oxidation is an important industrial process used in the production of fine chemicals. Recently, there has been a focus on employing aerobic oxidations, using air or pure oxygen as the oxidant rather than stoichiometric reagents, such as $K_2Cr_2O_7$. Oxygen is a low-cost oxidant which leaves water as the only by-product, making this approach more environmentally friendly than the classic metal oxide method, if the selectivity to the desired product compounds is maintained.

2.3.1 Alcohol oxidation over supported gold catalysts

Supported Pt and Pd catalysts are commonly used for polyol oxidation. It was found that the main disadvantage of these catalysts is their deactivation with increasing reaction time (Van Dam et al., 1987; Prati & Rossi, 1997; Villa et al., 2010a). Various studies (Mallat & Baiker, 2004; Boronat et al., 2011) are in agreement that the mechanism for aerobic alcohol oxidation on metal catalysts, such as Pt-group metals (PGM), proceeds with the formation of a metal-alkoxy species which undergoes a hydride elimination resulting in a compound containing a carbonylic group and a metal-hydride intermediate. Improvements in the activity, selectivity and stability of the catalyst can be achieved by adding a second metal or changing the nature of the individual metal. In the latter case, supported Au nanoparticles on activated carbon or oxides have been used for the oxidation of alcohols and aldehydes (Demirel-Gülen et al., 2005).

In contrast to the PGM, gold cannot catalyse alcohol dehydrogenation in the absence of a base. A detailed mechanism of alcohol oxidation on supported Au nanoparticles has not yet been established. Due to the poor activity of Au in the absence of a base, it was proposed that the rate-limiting step is the H^+ abstraction from a primary OH group. Another opinion (Mallat & Baiker, 2004) is that the rate-limiting step is the cleavage of the C-H bond at the α-carbon atom, similar to the mechanism accepted for Au-electrodes (Betowska-Brzezinska et al., 1997).

In comparing alcohol oxidation over supported Au, Pt and Pd catalysts, Au was more selective and least prone to metal leaching, over oxidation by oxygen and self poisoning by strongly adsorbed by-products (Prati & Rossi, 1997; Prati & Rossi, 1998; Bianchi et al., 2000; Carrettin et al., 2002). A review of supported metal catalysts for the oxidation of ethylene glycol and glycerol to monocarboxylates with air or oxygen (Mallat & Baiker, 2004) showed that supported Au nanoparticles are better catalysts than PGM-based catalysts in terms of activity and more so, in terms of selectivity.

2.3.2 Alcohol oxidation over supported bimetallic catalysts

A study of the oxidation of alcohols on carbon (AC) supported Au, Pd and AuPd catalysts was conducted in order to compare the activity of monometallic and bimetallic catalysts (Villa et al., 2009). It should be noted that the Au-Pd system differs significantly from the Au-Pt system, since different intermediate compounds (alloys) can be expected, i.e. Au_3Pd, AuPd and $AuPd_3$ (Sluiter et al., 2006). Bimetallic AuPd catalysts were prepared in Au/Pd ratios ranging from 90/10 to 20/80. The bimetallic catalysts were prepared by firstly immobilising a gold sol (using $NaAuCl_4{\cdot}2H_2O$ as a precursor) on activated carbon. The preformed Au particles act as nucleation centres for the subsequent immobilisation of Pd (from Na_2PdCl_4) thus forming a bimetallic system (Wang et al., 2008; Villa et al., 2009). These catalysts were tested and compared to their monometallic catalysts in the oxidations of benzyl alcohol and cinnamyl alcohol (see Figure 2.1). The turnover frequency for the oxidation of benzyl alcohol, which has been assumed to be defined as the moles of alcohol converted per mole of metal loaded in the reactor at 15 minutes, for the bimetallic AuPd with $Au_{80}Pd_{20}$/AC (when compared monometallic Au) to has an activity 15 times greater than Au/AC. The activity of $Au_{80}Pd_{20}$/AC is nearly double that of Au/AC in the oxidation of cinnamyl alcohol. For both benzyl alcohol and cinnamyl alcohol a maximum in activity is seen at a Pd mol fraction of 20%.

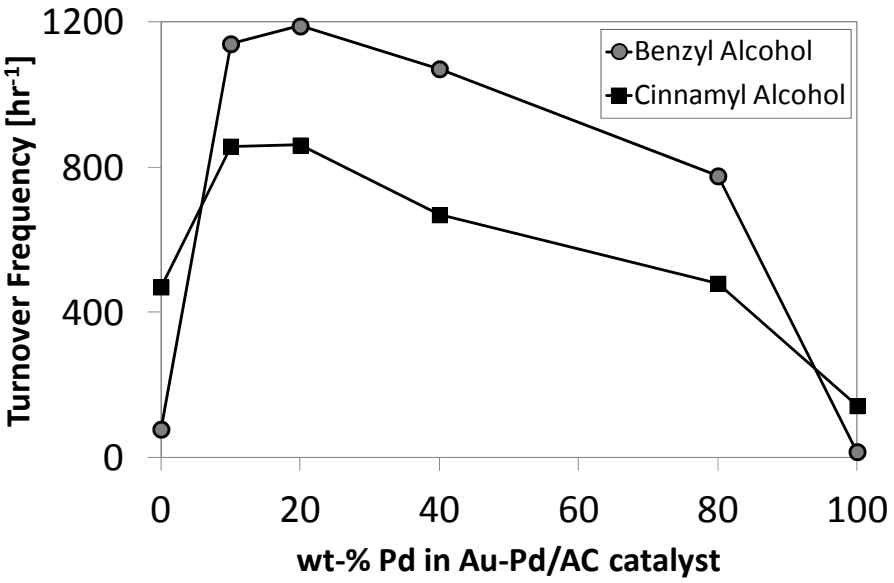

Figure 2.1: Activity[1] of carbon supported Au, Pd and AuPd catalysts in alcohol oxidation[2]

(adapted from Villa et al., 2009)

1. TOF: calculated after 15 min of reaction
2. Catalyst testing: [alcohol] = 0.3M; alcohol/metal = 1/500 mol/mol; T = 60°C; pO_2 = 1.5 atm; stirrer rate = 1250 rpm, alcohol/$NaOH_{initial}$ = 1 mol/mol

Characterisation of these catalysts (Wang et al., 2008; Villa et al., 2009) showed that the first 3 bimetallic catalysts with Au/Pd ratios of 90/10, 80/20 and 60/40 formed metal alloys

whereas $Au_{20}Pd_{80}$/AC showed inhomogeneity and Pd segregation was detected. This could possibly explain the significantly lower activity observed for this catalyst. All these reactions proceeded under basic conditions. Interestingly, in the absence of a base, the activity of all catalysts was lower and a difference in selectivity was also observed (see Table 2.1). In the oxidation of benzyl alcohol the selectivity to benzaldehyde in the presence of a base decreases with the formation of benzoic acid. It is possible that the base promotes the further oxidation of the aldehyde to the carboxylic acid. It should also be noted that the effect of the base on activity and selectivity is dependent on the Au/Pd ratio. The bimetallic catalyst with the highest Au content (Au/AC and $Au_{90}Pd_{10}$/AC) displayed the largest increase in activity and a greater oxidation of the aldehyde, similar to that of pure gold (Au/AC). Villa et al. (2009) proposed that in a Au-rich bimetallic catalyst, a Au-type mechanism prevails where the rate determining step is assumed to be the hydride abstraction from the alcohol group since the presence of a base has the highest effect. In a Pd-rich catalyst the rate determining step is the H transfer from Pd-H species since the effect of the base is negligible on the activity. The effect of the base on selectivity is still large.

Table 2.1: Oxidation of benzyl alcohol - TOF and Selectivity with or without base

(adapted from Villa et al., 2009)

Catalyst (1 wt%)	TOF in the presence of base [h^{-1}]	TOF in the absence of base [h^{-1}]	Selectivity at 90% conversion [%]					
			Benzaldehyde		Benzoic acid		Benzyl benzoate	
			Base	No base	Base	No base	Base	No base
Au/AC	78	2	26 [a]	>99 [a]	41	-	33	-
$Au_{90}Pd_{10}$/AC	1140	780	28	>99	40	-	32	-
$Au_{80}Pd_{20}$/AC	1189	1021	46	>99	32	-	22	-
$Au_{60}Pd_{40}$/AC	1071	985	45	>99	31	-	24	-
$Au_{20}Pd_{80}$/AC	776	716	50	>99	26	-	24	-
Pd/AC	16	15	58 [a]	>99 [a]	28	-	18	-

a. Selectivity at 50% conversion

Further useful work in the oxidation of hydrocarbons, namely glucose, has been performed. When glucose is placed in water, it is similar to glycerol in that it has a hydroxyl group attached to each carbon in the chain (see Figure 2.2). Unlike glycerol, the functional group of the glucose molecule is the aldehyde group at the start of the chain. The aldehyde group in glucose will be oxidised preferentially (Biella at al., 2002) whereas oxidation will occur at the primary alcohol group in glycerol. When glycerol is oxidised, it is proposed to form an aldehyde, glyceraldehydes, which is then further oxidised to various organic acids (Ketchie et al., 2007a). It is therefore useful to consider the oxidation of glucose in the present study since the aldeyhde oxidation (glyceraldehyde) will undergo a similar mechanism as glucose.

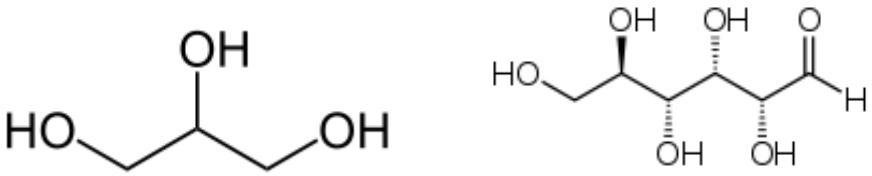

(a) (b)

Figure 2.2: (a) Glycerol and (b) Glucose chemical structures

Glucose oxidation was performed on carbon supported mono- and bimetallic catalysts of Au, Pt, Pd and Rh (Comotti et al., 2006). Monometallic gold, platinum, rhodium and palladium catalysts on carbon were prepared by immobilizing the corresponding metal sol on carbon. Aqueous solutions of $HAuCl_4$, K_2PtCl_4, $RhCl_3$ or $PdCl_2$ were used as precursors. Bimetallic catalysts were also prepared by immobilizing the preformed metal sols. Mixtures of $HAuCl_4$+K_2PtCl_4, $HAuCl_4$+$PdCl_2$, $HAuCl_4$+$RhCl_3$ were used as metal precursors of gold–platinum, gold–palladium and gold–rhodium catalysts, respectively. Catalytic testing was performed at conditions of controlled and uncontrolled pH. (see Table 2.2)

Table 2.2: Catalytic activity of mono- and bimetallic catalysts for glucose oxidation

(adapted from Comotti et al., 2006)

Catalyst	Conversion [%]		TOF [h^{-1}]	
	Uncontrolled pH [a]	Controlled pH [c]	Uncontrolled pH [a]	Controlled pH [c]
Au	11	43	51	17200
Pt	13	-	60	-
Pd	<2	-	<2	-
Rh	<2	-	<2	-
AuPt, 1:1	64	-	295	-
AuPt, 2:1	77 [b]	44	924 [b]	17600
AuPd, 1:1	20	-	92	-
AuRh, 1:1	<2	-	<2	-

a. 1 wt% metal on carbon; T = 343K; P_{O_2} = 300kPa; **glucose/Au = 3000; reaction time = 6.5h; pH_{start} = 6 pH_{end} = ca. 2.6**
b. 1 wt% metal on carbon; T = 343K; P_{O_2} = 300kPa; **glucose/Au = 3000; reaction time = 2.5h; pH_{start} = 6 pH_{end} = ca. 2.6**
c. 1 wt% metal on carbon; T = 343K; **P_{O_2} = atmospheric; glucose/Au = 20 000; reaction time = 2.5h; pH = 9.5**

Oxidation reactions at uncontrolled pH renders bimetallic AuPt (1:1), AuPt (2:1) and AuPd superior in terms of activity compared to all 4 monometallic catalysts. In fact, AuPt (2:1) reaches a higher conversion after a much shorter reaction time – under the same conditions, the conversion increases 7 fold in less than half the reaction time relative to monometallic Au. Rh and Pd are similarly as inactive at these conditions, whilst there bimetallic counterparts behave much differently. Whilst Pd by itself is not as active for glucose oxidation, bimetallic AuPd does show a considerable activity at uncontrolled pH whereas not much difference in activity is observed for Rh and AuRh. Since monometallic gold is not inactive, this could indicate that Au particles are covered by Rh particles on the catalyst

surface. Interestingly, is the choice of Rh as a promoter for Au bimetallic catalysts in comparison to Pd and Pt. One would expect the authors to use Ni to compare with Pd and Pt since they are all from Group 10, whereas Rh is a Group 9 metal. When comparing monometallic Au with bimetallic AuPt (2:1), there appears to be a marked increase in activity at conditions of uncontrolled pH. However, there doesn't appear to be any difference in activity when comparing the 2 catalysts at controlled pH. If gold is the source of the catalytic activity, AuPt (2:1) only has two thirds the gold content that monometallic Au has, so whilst its effect is less pronounced Pt still promotes the gold catalyst at controlled pH. Looking closely at the reaction conditions, we see that they are different when moving from controlled pH to uncontrolled pH, so one cannot make a true comparison across those results. When comparing catalytic activity across catalysts, it is important to use the same reaction conditions to draw fruitful conclusions.

2.4 Glycerol Oxidation

In recent years there has been a drive toward the use of cleaner fuels as a result of the growing concern about global warming. Biodiesel has emerged as one such fuel since it uses a renewable feedstock. Biodiesel is obtained by the transesterification with alcohol of triglycerides, which can be obtained from various plant and seed oils. The major by-product of this process is glycerol. Approximately 100kg of glycerol is obtained per ton of biodiesel produced (Kenar, 2007). There has been an increase in the market for biodiesel over the last few years and this trend is expected to remain. The commercial viability of biodiesel production depends on, amongst other factors, the availability of a suitable market for the by-product, glycerol.

One possible route is the consumption of glycerol, which yields a range of products that can be used in the production of fine chemicals and pharmaceuticals. Presently, these oxidation reactions are carried out using expensive enzymatic pathways or stoichiometric oxidants which involves the production of large amounts of undesired side products (Carrettin et al., 2004) that are harmful to the environment. A vast scope thus exists for the development of the catalytic oxidation of glycerol which will yield environmental and economic benefits.

2.4.1 Glycerol oxidation over supported Au catalysts

Due to its high boiling point (290^{o}C), the selective oxidation of glycerol with air or oxygen is carried out in the liquid phase (Porta & Prati 2004). Supported gold catalysts have been investigated (Ketchie at al., 2007a; Porta & Prati, 2004) for their suitability in oxidising alcohols and polyols in the presence of oxygen. Glycerol oxidation experiments over supported gold catalysts in the presence of a base are performed to achieve a high

selectivity toward glyceric acid. This requires the formation of the aldehyde, glyceraldehyde, which is then further oxidised to glyceric acid. However, a complex reaction pathway exists, as can be seen in Figure 2.3, making it difficult to achieve high selectivity to the desired product. Glycerol is converted to an intermediate compound, glycerolate, in the presence of a base which is further oxidised to the aldehyde, glyceraldehyde, in the presence of a gold catalyst and oxygen. A rapid interconversion of glyceraldehyde to dihydroxyacetone (DHA) occurs which is catalysed by OH^- ions in solution, provided by the base, e.g. NaOH. Glyceraldehyde and DHA can react with the base to form lactic acid or formic acid and acetic acid. Further oxidation of glyceraldehyde and DHA can occur in the presence of oxygen, a base and the gold catalyst to form glyceric acid which can consecutively be oxised to tartronic acid. It has also been suggested that hydrogen peroxide forms in the oxidation of glycerol (Ketchie et al., 2007a), this will also be discussed in Section 2.4.4. Hydrogen peroxide, in the presence of a gold catalyst is said to be responsible for the formation of the C-C cleavage product, glycolic acid and carbon dioxide. Glycolic acid can then be further oxidised to oxalic acid in the presence of oxygen, a base and the gold catalyst.

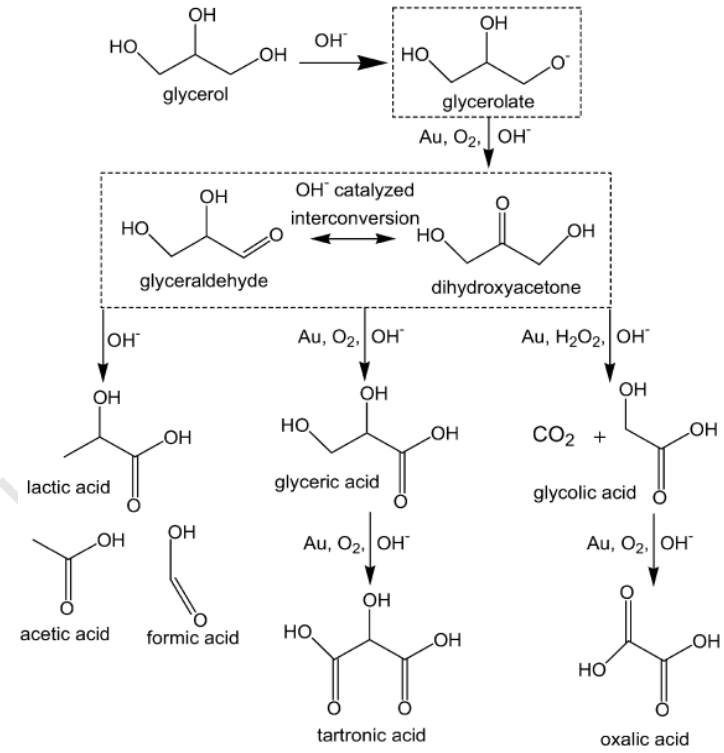

Figure 2.3: Proposed reaction pathway for oxidation of glycerol

(Ketchie et al., 2007a)

As previously discussed, catalytic oxidation of polyols such as glycerol requires the presence of a base, which suggests hydroxyl ions offer a promotional affect in the reaction (Carrettin et al., 2002; Porta & Prati, 2004; Demirel-Gülen et al., 2005). HPLC analysis of glycerol oxidation over carbon supported gold catalysts (Ketchie et al., 2007a) showed that the main

products (at T = 35°C) from the reaction are glyceric acid, glycolic acid, tartronic acid and oxalic acid (see Figure 2.4). Figure 2.4 shows the selectivity to the main products as well as the change in glycerol concentration over the course of the reaction. These products are in their salt form at the elevated pH of the reaction. At 60°C lactic acid, formic acid and acetic acid were also observed in small amounts. Their carbon balance of C_3 and C_2 products closed within 3%. The authors report that glyceric acid and glycolic acid account for 90 mol% of the C_3 and C_2 products (see Figure 2.4). Over the course of the reaction there is a slight increase in glyceric acid selectivity and a slight increase in glycolic acid selectivity.

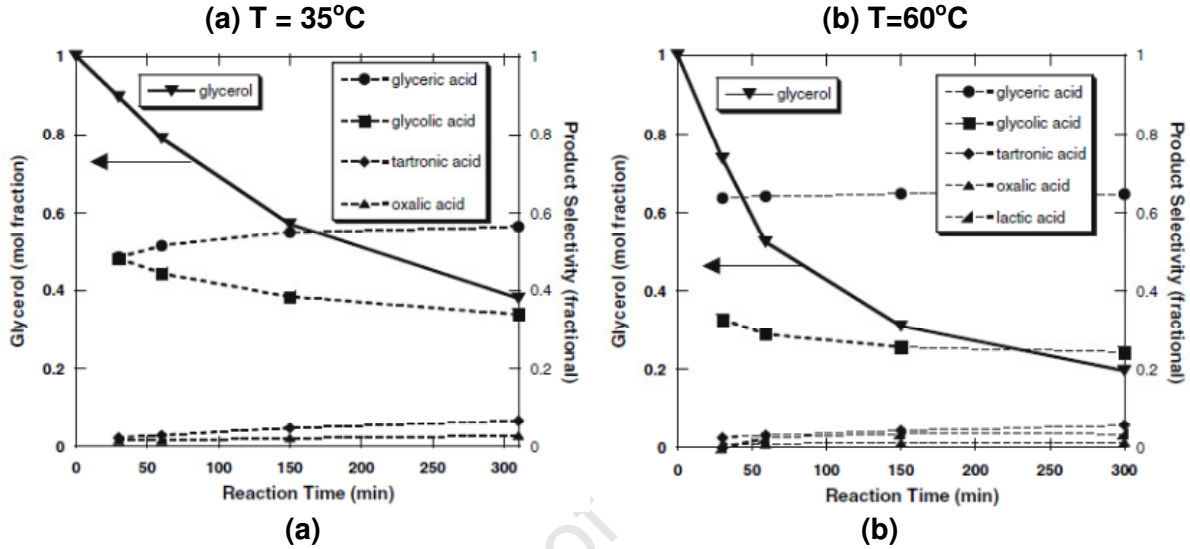

Figure 2.4: Reaction selectivity - Glycerol oxidation[a] over Au/C

(Ketchie et al., 2007a)

a. 0.3M glycerol; 0.6M NaOH; glycerol/Au = 16 000; P_{O_2} = 10 atm; (a) T = 35°C; (b) T = 60°C

Another study into the selectivity of the reaction on carbon supported gold catalysts was performed by Porta & Prati (2004). Two catalysts were tested in this study – (a) 1% Au on activated carbon and (b) 1% Au on graphite. Figure 2.5 shows the product distribution obtained. The main products were identified to be glyceric acid, glycolic acid and tatronic acid. The product distribution shows that with an increase in glycerol conversion, there is an increase in glyceric acid concentration, an increase in tartronic acid concentration and an increase in glycolic acid concentration. The total amount of glyceric acid and tatronic acid was however calculated to be constant over the course of the reaction. This indicates that glycolic acid is not formed from further oxidation of glyceric acid. In agreement with the previous study (Ketchie et al., 2007a), tartronic acid is formed by the oxidation of glyceric acid.

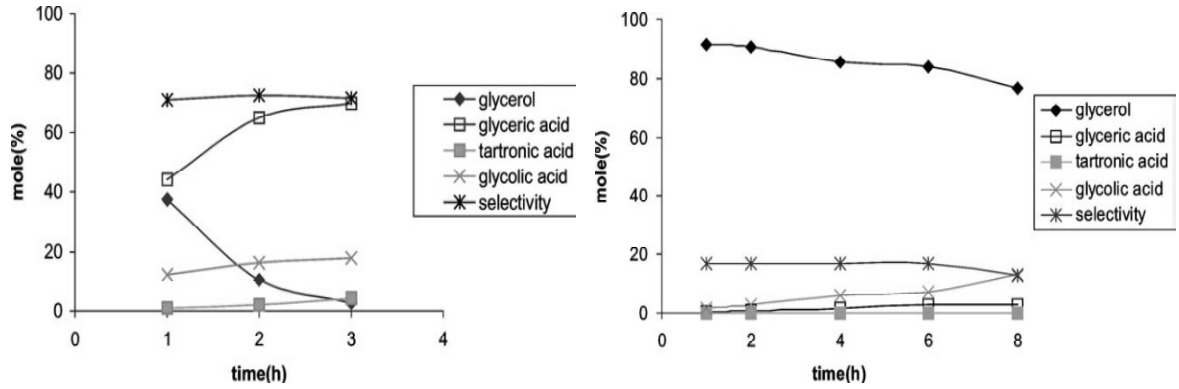

(a) (b)

Figure 2.5: Oxidation of glycerol[a] over Au nanoparticles supported on (a) active carbon and (b) graphite

(Porta & Prati, 2004)

a. Glycerol 10 wt%; glycerol/Au = 500; glycerol/NaOH = 1; T = 60°C; P_{O_2} = 3 atm

2.4.2 Glycerol oxidation conditions over supported Au-based catalysts

When performing an experiment, it is important to consider the reaction conditions which will affect the rate of the reaction. Various studies have been conducted to examine the influence of different reaction conditions on the oxidation of glycerol. The key conditions of concern for this study are initial glycerol concentration, temperature, pressure and pH.

Initial glycerol concentration

Across the literature concerning glycerol oxidation over gold catalysts, there appears to be a tendency to use similar initial glycerol concentrations. It was found that initial concentrations of 1.5 M (Demirel et al., 2007a; Demirel et al., 2007b; Demirel et al., 2007c; Wörz et al., 2010) and 0.3 M (Ketchie et al., 2007a; Prati et al., 2009; Demirel-Gülen et al., 2005; Dimitratos et al., 2009b; Dimitratos et al., 2005; Bianchi et al., 2005; Ketchie et al., 2007b; Ketchie et al. 2007c) are most often used.

No published research has been found concerning the effect of initial glycerol concentration on the rate of the reaction. However, the results of a study investigating reaction conditions for glucose oxidation over gold catalysts can be considered potentially relevant given the structural similarity of glucose and glycerol (Beltrame et al., 2006). In this study the effect of initial glucose concentration was examined, temperature and oxygen partial pressure on the rate of the oxidation reaction. Table 2.3. shows the initial reaction rates as a function of initial glucose concentration at 303.2K and 333.2K. Increasing the initial glucose concentration by a factor of 10 results in a rate that is approximately 1.5 times greater at both 303.2 K and 333.2 K. This behaviour is expectant of a Langmuir-Henshilwood type of reaction close to surface saturation. One may expect that glycerol will behave in a similar manner, i.e. an

increase in initial glycerol concentration will result in an initial increase in the initial rate of reaction.

Table 2.3: Initial reaction rate at different glucose concentration and temperature

(adapted from Beltrame et al., 2006)

$C^0_{glucose}$ [mol.L^{-1}]	r_0 [mol.L^{-1}.h^{-1}]	
	T = 303.2 K	T = 333.2 K
0.05	0.0959	0.4849
0.075	0.1083	0.5899
0.1	0.1165	0.6259
0.3	0.1320	0.7405
0.5	0.1425	0.7548

Reaction temperature

As with initial glycerol concentration, reaction temperatures used across literature are all very similar. It was found that most research groups conduct their experiments at 60°C (Carrettin et al., 2002; Carrettin et al., 2003; Carrettin et al., 2004; Porta & Prati, 2004; Hutchings et al., 2006; Demirel et al., 2007a; Demirel et al., 2007b; Demirel et al., 2007c; Ketchie et al., 2007a; Ketchie et al., 2007b; Ketchie et al., 2007c; Dimitratos et al., 2009a; Wörz et al., 2010) with some at lower temperatures of 50°C (Prati et al., 2007; Dimitratos et al., 2009b; Villa et al., 2010a; and Prati, 2010; Villa et al., 2010c) and 30°C (Bianchi et al., 2005; Dimitratos et al., 2005).

It is generally known that an increase in reaction temperature will result in an increase in reaction rate. An investigation into glycerol oxidation conditions was performed (Demirel-Gülen et al., 2005) in order to optimise reaction parameters. The influence of temperature on the reaction rate is demonstrated in Figure 2.6. The change in the glycerol concentration is shown as a function of reaction time at different temperatures varying from 25-100°C. The reaction rate constant was determined at the various temperatures and the activation energy of glycerol oxidation on Au/C was estimated to 50 ±5 kJ/mol (Demirel-Gülen et al., 2005). It is clearly seen that with an increase in reaction temperature, there is an increase the rate of the reaction. One can see that even at 40°C there is a considerable decrease in glycerol concentration so modest temperatures are required to achieve noticeable activity.

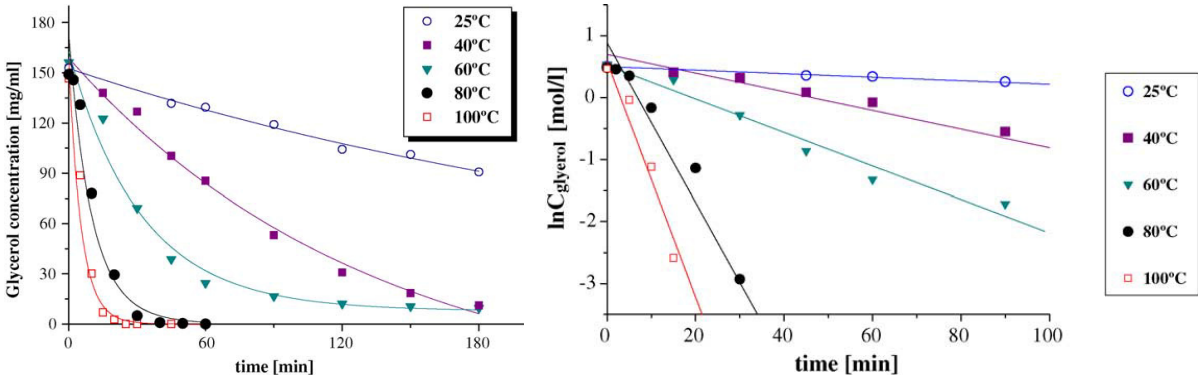

Figure 2.6: Glycerol conversion with 1% Au/C at different reaction temperatures [a]

(Demirel-Gülen et al., 2005)

a. 100 ml of a 1.5M glycerol solution, glycerol/ Au = 3500 mol/mol, NaOH/glycerol = 2 mol/mol, P_{O_2} = 10 bar, rpm = 1500.

Oxygen partial pressure

The effect of oxygen pressure has also been investigated to verify the dependency of the reaction rate and selectivity on this parameter (Demirel-Gülen et al., 2005). The effect of oxygen pressure was compared at 6 and 10 bar. Glycerol concentration as a function of reaction time is given at different 6 and 10 bar, both at 60°C and 40°C (see Figure 2.7). Under the described conditions, the oxygen pressure hardly influences the reaction rates of the glycerol oxidation. No result for the effect on selectivity was reported for this study.

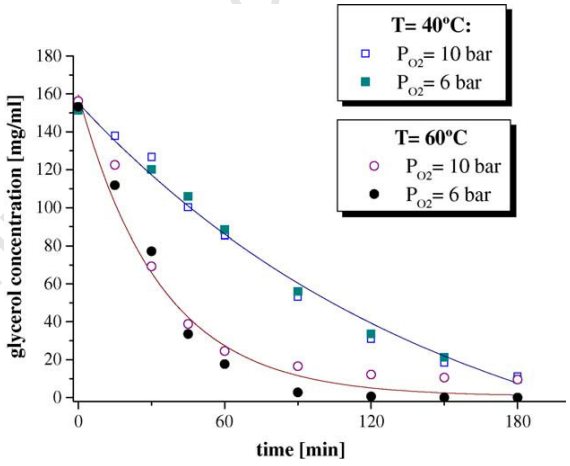

Figure 2.7: Oxygen pressure dependent glycerol conversion with 1% Au/C at different temperatures [a]

(Demirel-Gülen et al., 2005)

a. 100 ml of a 1.5M glycerol solution, glycerol/Au = 3500 [mol/mol], NaOH/glycerol = 2 [mol/mol], rpm = 1500.

Dimitratos et al. (2009b) investigated the effect of oxygen pressure on activity and selectivity at 1, 3 and 6 bar (see Table 2.4). The turnover frequency at 30 minutes, based on the total metal loaded in the reactor, is given as a function of oxygen partial pressure. The main products were found to be glyceric acid, glycolic acid and tartronic acid. The selectivity to these products, calculated at 40% glycerol conversion, is also given as a function of oxygen

partial pressure. The catalytic activity increased slightly from 1 to 3 bar of oxygen pressure (based on TOFs) and remained nearly constant from 3 to 6 bar. In the previous study by Demirel-Gülen et al. (2005) it was seen that oxygen partial pressured between 6 and 10 bar do not affect the reaction rate. However, from this study it is seen that lower partial pressures (below 6 bar) do have an effect on the reaction rate with there being an increase in the rate with an increase in oxygen pressure. In terms of selectivity, an increase in the oxygen pressure led to a progressive increase in the selectivity to glyceric acid at the expense of tartronic and glycolic acid. This phenomenon will be further discussed in Section 2.4.4. These results may then be interpreted in terms of a higher oxygen pressure minimizes the hydrogen peroxide formation resulting in a decrease in glycolic acid. With an increase in reaction rate one expects to see an increase in the selectivity to all consecutive products such as tartronic acid and glycolic acid. However in this case, only the glyceric acid selectivity increases whilst that of tartronic acid and glycolic acid remains the same.

Table 2.4: Liquid phase oxidation of glycerol using Au–Pd/C at different oxygen pressure [a]

(Adapted from Dimitratos et al., 2009b)

Catalyst (1 wt%)	pO_2 [bar]	TOF [h^{-1}] [b]	Selectivity at 40% conversion [%]		
			Glyceric acid	Tartronic acid	Glycolic acid
Au-Pd/C	1	1352	72	6.5	19
	3	1891	77	5.7	14
	6	1661	80	5.8	12

a. 0.3 M glycerol, glycerol/metal = 3,400 mol/mol, NaOH/glycerol ratio = 4 mol/mol, T = 50°C, rpm = 1500

b. TOF at 0.5h reaction time. TOF based on total metal loading.

pH

Glycerol oxidation reactions were performed using Pd, Pt and Au supported catalysts (Carrettin et al., 2003). In this study, the oxidation reaction was monitored in the absence and presence of different bases. The reactions were performed at 60°C, 3 bar oxygen pressure, a glycerol/metal molar ratio = 500, a base/glycerol molar ratio = 1 and a stirrer rate = 1500 rpm. The catalysts tested had loadings of 5-wt% Pt/C, 5-wt% Pd/C and 1-wt% Au/C. The results show that the highest glycerol conversion and highest selectivity to glyceric acid was observed in the presence of NaOH. It is noted that, for supported Pd and Pt catalysts, the addition of OH^-, as NaOH, increases the conversion of glycerol. However, for Au/C catalysts, the presence of OH^- is essential to observe any glycerol oxidation. Carrettin et al. (2003) propose that in the absence of a base the initial dehydrogenation of glycerol via H-abstraction (the first step in the oxidation process) is not possible for the Au/C catalyst and is slow for the Pd/C and Pt/C catalysts. In the presence of a base, the H^+ is readily abstracted from one of the primary hydroxyl groups of glycerol to form glyceric acid, thereby facilitating

the rate limiting step. Therefore, in agreement with what has been previously observed (Mallat & Baiker, 1994; Prati & Rossi, 1998), it is proposed that the oxidation mechanism of glycerol with Au catalysts proceeds via an initial deprotonation pathway which is only possible in the presence of a base (Carrettin et al., 2003). Other studies have also confirmed this observation (Porta & Prati, 2004; Ketchie et al., 2007a).

Not much research in the gold catalysed oxidation of glycerol has been performed using an alumina support. However, γ-Al_2O_3 is commonly used as a support in heterogeneous catalysis due to its thermal stability and high surface area (up to 300 m^2 g^{-1}) which allows for the dispersion of active phases (Euzen et al., 2002). In a very basic or acidic environment, alumina dissolution will occur and this will change the pH of the solution. The rate of dissolution of alumina in aqueous solutions is said to be minimum at the point of zero charge (PZC) and increase on either side of the point of zero charge, where pH at the point of zero charge of alumina is 8 (Carrier et al., 2007).

The speciation diagram of aluminium ions in sodium hydroxide solution has been developed (Panias et al., 2001) and is shown in Figure 2.8. The figure shows the concentration of aluminium ions of boehmite in an aqueous solution as a function of pH at 25°C and 1 atm. Different aluminium species are formed at different pH. According to the diagram, the lowest rate of dissolution occurs in a pH range of ca. 5.5 and 8.

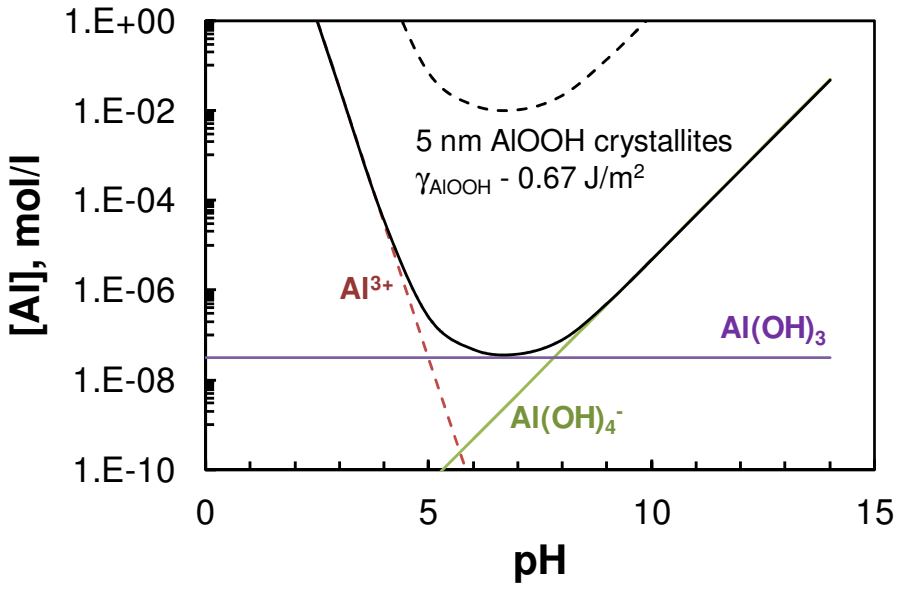

Figure 2.8: Boehmite dissolution in sodium hydroxide solution

Since alumina dissolution will cause the pH of the solution to drop unfavourably, it is important that precise control of the solution is maintained between these limits. This can be achieved by the addition of base (NaOH) during the course of the reaction.

2.4.3 Glycerol oxidation over supported Au-metal bimetallic catalysts

As previously mentioned, one of the greatest challenges associated with the catalytic oxidation of glycerol is to direct the reaction pathway to the desired product. Supported Au-based catalysts have been studied (Bianchi et al., 2005) to compare the behaviour of monometallic Au catalysts to that of bimetallic Au-Pt and Au-Pd catalysts in the oxidation of glycerol. The monometallic Au, Pd and Pt catalysts were obtained by preparing monometallic sols from the respective precursor materials (Solid $NaAuCl_4 \cdot 2H_2O$ and K_2PtCl_4 and an aqueous solution of Na_2PdCl_4). Bimetallic sols were obtained by firstly preparing a gold sol (from solid $NaAuCl_4 \cdot 2H_2O$) and subsequently adding the aqueous MCl_4^{2-} (M = Pd or Pt) solution. After a few minutes of sol generation, the colloid was immobilised by adding activated carbon under vigorous stirring. Glycerol oxidation experiments were performed at 30 and 50^{o}C and an oxygen pressure of 3atm. The pH in the reactor was not maintained at a constant value. The results are shown in Table 2.5. The turnover frequency calculated after 15 minutes, based on the total metal loaded in the reactor, is shown as a function of the two reaction temperatures for each of the catalysts tested. The main products identified from the oxidation of glycerol were glyceric acid, glycolic acid and tartronic acid. The selectivity to these products at 50% conversion of glycerol for each of the catalysts tested is also shown in Table 2.5. The bimetallic catalysts were more active than the monometallic catalysts at both 30 and 50^{o}C. At a temperature of 50^{o}C the AuPt/C catalyst displayed an increase in activity by a factor of 1.8 (TOF) compared to the Au catalyst. At the same reaction temperature and 50% conversion of glycerol the glyceric acid selectivity was 8% higher with the AuPt/C catalyst than with the Au-catalyst. However, it was also reported that at 90% conversion of glycerol the glyceric acid selectivity decreased by 3% with the AuPt/C catalyst (not shown in Table 2.5). It is possible that at higher conversions of glycerol, glyceric acid is further oxidised to tartronic acid (see Figure 2.3). Interestingly, at both temperatures the Pd/C catalyst displayed the highest selectivity to glyceric acid and the lowest selectivity to the C_2 product, glycolic acid. Its bimetallic counterpart, AuPd/C, displayed similar results when compared to AuPt/C. In fact, AuPt/C, whilst being the most active, gave the highest selectivity to glycolic acid at both reaction temperatures.

Table 2.5: Oxidation of glycerol using carbon supported Au, Pd, Pt, AuPd and AuPt catalysts a

(Adapted from Bianchi et al., 2005)

Catalyst (1 wt%)	T [°C]	TOF [h^{-1}] [b]	Selectivity at 50% conversion [%]		
			Glyceric acid	Glycolic acid	Tartronic acid
Au/C	30	779	62	10	21
	50	1090	65	12	9.2
Pt/C	30	-	-	-	-
	50	532	42	31	5.9
Pd/C	30	514	88	0.4	11
	50	1151	80	2.7	14
AuPd/C	30	1234	68	4.7	26
	50	1775	77	4.5	18
AuPt/C	30	1435	58	35	2.7
	50	1953	73	23	2.9

a. 10 ml water, 0.3M glycerol, glycerol/M= 500 mol/mol, NaOH/glycerol = 4 mol/mol, T = 30, 50°C, P_{O_2} = 3 atm

b. Calculation of TOF (h^{-1}) after 0.25h of reaction. TOF based on total metal loading.

A similar study also comparing an Au catalyst to a bimetallic AuPt catalyst was performed (Demirel et al., 2007b). Unlike most glycerol oxidation studies, the study was carried out at atmospheric pressure and pH controlled conditions. Different Pt mol fractions (0, 0.2, 0.25, 0.33, 0.5 and 1) were investigated to observe the behaviour of Pt in the Au catalyst. The catalyst activity was measured as the time taken to reach 50% conversion of glycerol. The highest activity was observed at platinum mol fraction between 0.2 and 0.4. The selectivity to glyceric acid decreased by 10-14% at 50% conversion of glycerol with the bimetallic catalyst. There was however an increase in the selectivity to dihydroxyacetone of 10% with the same catalyst.

2.4.4 The Formation and Effects of H_2O_2 in Glycerol Oxidation

A by-product in glycerol oxidation is glycolic acid (see Figure 2.3), a C_2 product formed by further oxidation of glyceraldehyde (Ketchie et al., 2007a). Hydrogen peroxide formation has been investigated during glycerol oxidation over supported gold catalysts. An increase in the observed rate of formation of hydrogen peroxide has been related to an increase in concentration of the C_2-product, glycolic acid (Prati et al., 2009).

Monometallic Gold Catalysts

To test whether H_2O_2 is the cause of the C-C scission product, a known peroxide decomposer, MnO_2, was added to the glycerol oxidation reaction, at 333K and 10 atm oxygen (Ketchie et al., 2007c). The concentration of H_2O_2 was observed to decrease from 1.7mM to 0.12mM upon addition of the MnO_2. This correlated to a change in glyceric acid

selectivity from 64 to 78%. This result suggests that the selectivity toward glyceric acid can be increased by minimising the formation of H_2O_2.

Bimetallic Gold Catalysts

Different AuPd bimetallic catalysts were studied for the oxidation of glycerol (Ketchie et al., 2007b). Results showed an increased selectivity toward glyceric acid in the presence of bimetallic AuPd catalysts. A decrease in the observed rate of formation of H_2O_2 was observed as well. Tests were performed in order to determine if the Pd is responsible for the decomposition of H_2O_2. A mixture of supported monometallic Au and Pd catalysts was added to a glycerol oxidation reaction. In the presence of Pd, the observed rate of formation of H_2O_2 was lower and the glyceric acid selectivity saw a 20% increase. The results suggest that H_2O_2 formed in-situ over Au-catalysts is decomposed by Pd which leads to the increased selectivity to glyceric acid. Platinum, also a Group 10 element, may therefore behave similarly to Pd when added as a promoter in the oxidation of glycerol over supported Au catalysts.

Thermodynamic Analysis

The formation of H_2O_2 from H_2O and O_2 was considered a possible reaction pathway, however a thermodynamic analysis for this pathway indicates the reaction is improbable:

$$\Delta G^{rxn}(298K) = 123 \text{ kJ/mol and } K = 3 \cdot 10^{-22} \text{ (Stull et al., 1969)}$$

An alternative reaction pathway should thus be considered.

In the oxidation of glucose to gluconate over supported gold catalysts, hydrogen peroxide is said to form as a co-product (Beltrame et al., 2004). A thermodynamic analysis was thus performed for the formation of H_2O_2 as a co-product in the oxidation of ethanol to acetaldehyde. This was done to deduce whether H_2O_2 formation is thermodynamically possible in the oxidation of alcohols. The following results were obtained:

$$\Delta G^{rxn}(298K) = -70.5 \text{ kJ/mol and } K = 2.3 \cdot 10^{12} \text{ (Stull et al., 1969)}$$

indicating that the reaction is thermodynamically feasible.

Two different reaction pathways can be considered for the oxidation of alcohols, which produces peroxides:

Path 1: $Alcohol + \frac{1}{2}O_2 \rightarrow Organic\ Peroxide \rightarrow Aldehyde + H_2O$

Path 2: $Alcohol + O_2 \rightarrow Aldehyde + H_2O_2 \rightarrow Aldehyde + H_2O + \frac{1}{2}O_2$

The first is the oxidation of the alcohol to the corresponding aldehyde and H_2O_2 which is then further decomposed to H_2O and O_2. The second is the oxidation of the alcohol to the corresponding organic peroxide which decomposes to the aldehyde and H_2O (van Steen, 2010). Based on Density Functional Theory (DFT) calculations (T=298K) for the two reaction pathways, the formation of H_2O_2 is thermodynamically favoured over the formation of the organic peroxide (van Steen, 2010). For oxidation of glycerol, the energies for organic peroxide and H_2O_2 formation are 113.5 kJ/mol and -59 kJ/mol, with respect to the energy of the starting alcohol and O_2, respectively (see Figure 2.9). The top path shows the formation of the organic peroxide (path 1) and the bottom path shows the formation of the aldehyde and H_2O_2 (path 2).

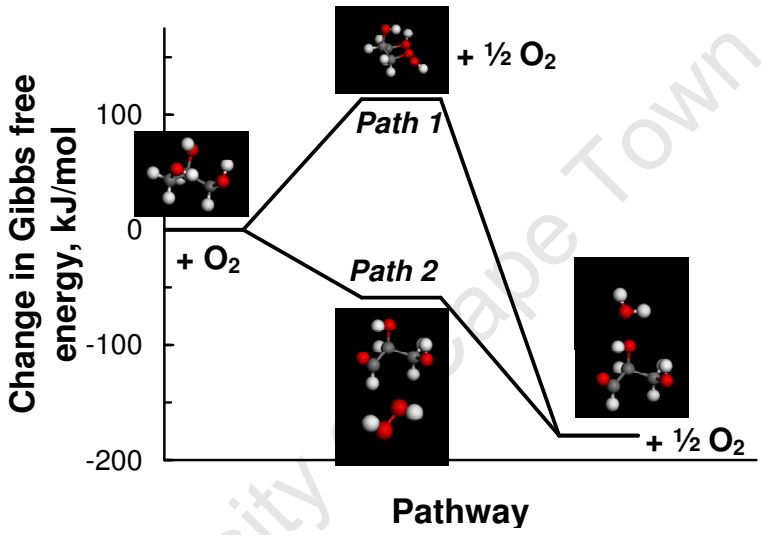

Figure 2.9: Change in Gibbs free energy for oxidation of glycerol

(van Steen, 2010)

Chapter 3. Objectives & Hypothesis

3.1 Aims and Objectives

Bimetallic catalysts have been shown to perform better when compared to its monometallic counterparts in the oxidation of glycerol in terms of activity and selectivity to glyceric acid (Bianchi et al., 2005; Demirel et al., 2007b). The pressure of oxygen has an effect on the activity and selectivity specifically at low oxygen partial pressures (Dimitratos et al., 2009b). The use of air as an oxidant is economically favourable but this will lower the partial pressure of oxygen. In this study we investigate the oxidation of glycerol with a bimetallic AuPt catalyst and using oxygen at atmospheric pressure.

The main focus of this study was to determine the effect of platinum in a bimetallic AuPt catalyst compared to a monometallic Au catalyst. This was done by preparing two AuPt catalysts with different Au/Pt ratios. These catalysts were characterised and tested in the oxidation of glycerol with oxygen in a semi-batch reactor. The activity of the catalyst was monitored and comparisons were made with a monometallic Au catalyst. It was also determined whether the presence of platinum has any effect on the selectivity to glyceric acid.

3.2 Hypothesis

The experimental program was set up such that it tests the following hypothesis:

> *In the catalytic oxidation of glycerol, despite operating with oxygen as an oxidant at atmospheric pressure the positive effects of platinum in the bimetallic catalyst is still observed.*

3.3 Key Questions

The following key questions were addressed:

1. How do the physical characteristics of the bimetallic catalyst compare to the monometallic Au catalyst?
2. What effect does the Au/Pt ratio have on the activity?
3. What effect does the Au/Pt ratio have on the selectivity?
4. Does the presence of platinum have any effect on the deactivation of the catalyst?

Chapter 4. Experimental Methods

4.1 Catalyst Preparation

A monometallic gold catalyst and 2 bimetallic gold-platinum catalysts were prepared for the purpose of this study. It was ensured that all catalysts had the same total metal loading by mass ($g_{metal}/g_{catalyst}$).

4.1.1 Preparation Methods

Supported metals are most commonly prepared from metal salts and porous supports such as metal oxides. Different methods of catalyst preparation can be used. These include deposition-precipitation, co-precipitation and impregnation (Knowles et al., 2007) as well as ion-exchange (Ivanova et al., 2004), with the latter not widely considered in gold catalyst preparation.

Ion exchange was used to prepare the Au catalyst. The Au catalyst was then used as a support for the bimetallic AuPt catalyst by impregnation. With both ion exchange and impregnation the support material is suspended in a metal precursor solution. In impregnation, the support is added to the metal precursor solution with the solvent removed by evaporation (Bond & Thompson, 1999). Impregnation can theoretically result in 100% of metal loaded on the catalyst since there is no filtration step in which any metal not attached to the support is discarded in the filtrate. Impregnation is a useful method of preparation in that the desired metal loading of the catalyst can be achieved, which is much harder to do with the ion exchange method (Knowles et al., 2007). Impregnation and ion exchange are widely used in the preparation of other metal catalysts but are less commonly used in gold catalyst preparation. Gold impregnation on carbon supports have been shown to yield large crystallite sizes of greater than 200nm (Prati & Martra, 1999). With ion exchange there is an exchange between ions in solution and ions on the surface of the support followed by removal of the excess solution through filtration. There is theoretically the possibility of achieving highly dispersed catalysts since the deposition of unattached gold is avoided. Brunelle (1978) showed that this is possible in the case of platinum on silica. Agglomeration of small particles is typically seen in the precipitation step of most preparation methods whereas this is avoided when using ion exchange.

Ion exchange

Metal ion complexes in solution exchange with species on the surface of the support during ion exchange. Supports are typically metal oxides. Both cationic and anionic ion exchange is possible. The iso-electric point (IEP) of a support refers to the pH at which the support has a neutral charge. When the support is placed in a solution at a pH lower than its IEP, the surface tends to contain an excess of positive charge which results in an electrostatic attraction between the metal anions in solution and the surface of the support; this is anionic ion exchange. Cationic exchange occurs when the support is placed in a solution with a pH higher than its IEP; the surface becomes negatively charged and is electrostatically attracted to cations in solution. (Brunelle, 1978) The IEP of alumina is approximately 8, so anions will exchange at a precursor solution pH below 8 whereas cations will exchange at a pH above 8.

Direct anionic ion exchange (DAE) has been proposed for the preparation of supported gold catalysts (Ivanova et al., 2004) using $HAuCl_4$ ($H^+ + AuCl_4^-$) precursor solution. A cause for concern is the presence of Cl^- ions in the precursor solution since Au-Cl bridges are thought to form on the catalyst (Ivanova et al., 2004). These bridges are thought to promote the process of sintering during calcination leading to the agglomeration of Au particles (Oh et al., 2002). This problem may be avoided by washing the Au catalyst with ammonia solution prior to the calcinations step. This allows for the removal of chlorine ligands which are replaced with hydroxyl groups on the alumina surface. (Ivanova et al., 2004) An important safety note is the possible formation of ammonia gold complexes, which poses the risk of explosions (Ivanova et al., 2006). It is therefore of utmost importance that all of the gold in solution is removed from the catalyst before the ammonia wash.

In other catalyst preparation methods (deposition precipitation, impregnation), agglomeration of small particles is typically seen during the precipitation step. Direct anionic exchange (DAE) reduces agglomeration by eliminating this step (Ivanova et al., 2006). Any gold not attached to the surface of the catalyst is removed in the washing steps, preventing the additional deposition of gold (Case, 2009) so a catalyst with a high degree of gold dispersion can be obtained.

Impregnation

Impregnation is another method of depositing the active material onto catalyst supports. This method involves placing the support in contact with a solution that contains the precursors of the active phases (Hutchings & Vedrine, 2004; Rodriguez-Reinoso & Sepulveda-Escribano, 2009). Two different methods of impregnation are identified: incipient-wetness impregnation and slurry impregnation (Rodriguez-Reinoso & Sepulveda-Escribano, 2009). During incipient-wetness impregnation, the support is wetted with the precursor solution to just fill

the pore volume with the solution. The solvent is subsequently removed resulting in the active phase being deposited on the pore walls. In the second method, the support is placed in a volume of precursor solution much larger than the pore volume. The excess solvent is then removed from the slurry by evaporation and the active phase is left on the pore walls.

4.1.2 Preparation of Anionic Precursor Solution

The direct anionic exchange preparation method was used to prepare the Au catalysts. The respective volume of aurochloric acid ($HAuCl_4$) solution (see Table 4.1) at a concentration of 250 gAu/l was added to an Erlenmeyer flask filled with approximately 800ml deionised water. NaOH at a concentration of 0.2M was added to the solution to ensure a pH between 4 and 5. The entire solution ($HAuCl_4$, H_2O & NaOH) was made up to a volume of 1L in a volumetric flask. Table 4.1 below summarises the various precursor solutions.

Table 4.1: Preparation of gold precursor solutions

Catalyst Code	$HAuCl_4$ added [ml]	NaOH added [ml]	Initial pH	Au concentration [mmol/L]
Au_{100}	2	40	4.84	2.54
$Au_{63}Pt_{37}$	0.8	20	4.98	1.02
$Au_{28}Pt_{72}$	0.4	10	4.21	0.51

4.1.3 Loading and Ageing of Au catalyst

γ-Alumina (Puralox SCCa 5-150, Sasol Germany, Batch# 9574, S_{BET} = 162 m^2/g) was used as a support for the catalysts. The support was sieved to recover particles smaller than 250 µm. 10g of the sieved support was weighed out and added to the 1L anionic precursor solution. The mixture was stirred at a rate of 700rpm and allowed to age for approximately 22 hours. 10ml samples of the precursor solution were taken before and after the ageing process. These samples were analysed by Atomic Absorption Spectroscopy (AAS) to determine the concentration of gold in the solutions and deduce the gold uptake.

4.1.4 Washing and Calcining of Au catalyst

The Au catalyst precursor was subsequently filtered and washed with 1L of cold deionised water. The filtrate from this filtering step, termed the water wash filtrate (WWF), was made up to a volume of 2L for the determination of gold loss during the washing step using AAS analysis. The filtered catalyst was then suspended in 250ml concentrated ammonia (32 wt%) solution for 20 minutes whilst stirring at a rate of 700rpm. This was followed by another filtration and washing step with 1L of deionised water. This filtrate, termed the ammonia wash filtrate (AWF), was made up to a volume of 1L with deionised water for the determination of gold loss during the NH_3 washing step using AAS. The washed catalyst was

dried in an oven at 120°C for approximately 10 minutes. The dried catalyst was then calcined in pure hydrogen in a fluidized bed. The temperature was ramped to 200°C for 2 hours, where it remained at 200°C for a further 2 hours, followed by a 2 hour cooling period to room temperature.

4.1.5 Preparation of the AuPt & Pt catalysts

The bimetallic catalysts were prepared using a one step impregnation process (slurry impregnation). Tetraamine platinum(II)chloride monohydrate ($(NH_3)_4PtCl_2 \cdot H_2O$) (STREM CHEMICALS, CAS# 13933-32-9, LOT# 133630-S) was used as the platinum precursor. $(NH_3)_4PtCl_2$ salt (3.92g) was dissolved in deionised water and made up to a volume of 25ml in a volumetric flask. The monometallic gold catalyst was used as the support material for the platinum impregnation. The respective volume of the platinum solution added to the support was calculated by ensuring that the total metal (Au+Pt) loading on all the catalysts was maintained at 2.2 wt%. A monometallic Pt catalyst was also prepared using a single step impregnation process to achieve a loading of 2.2 wt% Pt (see Appendix II for calculation of loading).

Platinum solution was added to a round bottom flask together with the support and approximately 50ml of deionised water. The solution was removed in a rotary evaporator operating at 80°C and 250mbar. The solvent was allowed to evaporate for approximately 1 hour or until the catalyst particles were dry. The catalyst was then calcined in hydrogen in the same manner as the monometallic gold catalysts.

4.2 Catalyst Characterisation

4.2.1 Loading

Digestion of catalysts

The gold catalyst was digested using concentrated acids and analysed by AAS to determine the mass composition. Acid digestion of the catalyst was performed as follows. The catalyst (0.1g) was weighed out into a 250ml wide-mouthed Erlenmeyer flask. To this, 10ml of a HCl/HF mixture ([HCl] = 30 wt%, [HF] = 40 wt%) in the ratio 4:1 per volume was added and the contents heated to boiling. Upon boiling, 10ml of HNO_3 (60 wt%) was added to the flask and boiled until approximately 2ml of the volume remained. Following this, 5ml of concentrated $HClO_4$ was added to the flask and once again boiled until the sample volume was reduced to approximately 2ml. This is noted by the formation of a white cloud which rises once the reaction takes place. The solution was then diluted with deionised water and made up to a volume of 100ml. This solution was then analysed by AAS. The filtrate and was solutions were also analysed by AAS to determine the gold content.

Atomic Absorption Spectroscopy (AAS)

The gold concentration in the various solutions was determined by AAS. The atomic absorption spectrophotometer was calibrated with standards of known concentrations. A calibration curve was then plotted which aided in determining the concentration of gold in the liquid samples.

4.2.2 Particle Size

Transmission Electron Microscopy (TEM)

The size and shape of the gold crystallites was determined from TEM images. A small mass of catalyst was suspended in a methanol solution and dropped onto a carbon coated copper grid. These samples were then placed in the microscope for analysis. Electron beams are emitted which travels through an ultra thin specimen of the catalyst. As a result of interactions between the specimen and the electron beams, an image is formed which is magnified onto a fluorescent screen. At least 2 images were taken of each sample. The size of the identified gold crystallites was determined by using ImageJ © software with the images obtained from the TEM.

High resolution transmission electron microscopy was also performed. The HRTEM samples were prepared in a similar manner with the exception of the grid used. A holey carbon coated copper grid was used, which is more suitable for HRTEM analysis.

Energy dispersive X-ray spectroscopy (EDX or EDS) is a technique used to analyse the chemical or elemental composition of a sample. An EDX spectrum is obtained which provides information on the elemental composition of the sample. Energy dispersive spectroscopy together with elemental mapping was used to distinguish between platinum and gold in the bimetallic samples. From elemental mapping, images were created that create a colour contrast between gold and platinum particles on the sample. EDS analysis was performed to specifically identify the position of platinum crystallites in relation to the gold crystallites and also so that the average particle sizes.

Hydrogen Chemisorption

The catalysts were characterized using H_2-chemisorption. The H_2 chemisorption was carried out in an adsorption apparatus Micrometrics ASAP 2020C. The hydrogen uptake was measured at various temperatures ranging from 50-150^{o}C after a treatment of the catalyst in hydrogen at 200^{o}C for 4hrs (after heating it up from room temperature with 10^{o}C/min). The catalysts were subsequently evacuated for 2 hrs at 200^{o}C followed by cooling down to the analysis temperature, at which temperature the sample was further evacuated for 2 hrs. The

H_2-uptake was repeated after evacuation for 12 hrs, in order to determine the amount of strongly adsorbed and weakly adsorbed hydrogen.

4.3 Catalyst Testing

4.3.1 Glycerol Oxidation

The gold catalysed liquid phase oxidation of glycerol was used to tests the catalysts. Glycerol reacts with oxygen in the presence of hydroxyl ions to form a range of organic acids in a complex reaction pathway as discussed in Section 2.4.

The gold catalysed liquid phase reaction took place in a 500 ml three-necked round bottom flask in a semi-batch operation while controlling temperature and pH. For each run, the respective mass of catalyst was added to 200ml of deionised water and 4ml of 0.3M NaOH in the round bottom flask. The flask was placed in a water bath over a heating plate and magnetic stirrer. The solution was continuously stirred at a rate of 350rpm while maintaining a temperature of 60^{o}C. A glass-fritted sparger was used to sparge oxygen at 5ml/s into the solution and a pH probe was used to monitor the pH. Since no vapours should leave the reactor vessel an overhead condenser is used. The experimental setup is illustrated in Figure 4.1.

The solution was stirred for approximately 2 hours so that the temperature and pH could stabilise before the reaction was started. After 2 hours, 1ml of a 6.84M glycerol solution was added to the reactor, which represents the start of the reaction. Organic acids formed during the reaction lowers the pH of the reaction mixture. To control the pH to a desired pH of 10 the reaction mixture was titrated by adding 0.3M NaOH solution. Titration was performed by an auto-titrator (Titroline Alpha plus). The reaction was allowed to run for 1 hour during which 1ml samples were taken every 10 minutes. These samples were immediately filtered to remove any catalyst that came with the sample. Table 4.2 summarises the different experimental conditions carried out with each set of runs.

Table 4.2: Experimental conditions for glycerol oxidation runs

Experiment #	Catalyst	Mass [g]	Glycerol/Au [mol/mol]
1a, 1b, 1c [a]	Au_{100}	0.2	2686
2a, 2b, 2c [a]	$Au_{63}Pt_{37}$	0.2	4263
3a, 3b, 3c [a]	$Au_{28}Pt_{72}$	0.2	9593
4a, 4b, 4c. 4d [b]	Au_{100}	0.2	Varied
5a, 5b, 5c, 5d [c]	Au_{100}	0.2	2686

a. T = 60 ^{o}C; atmospheric pressure; pH = 10; VO_2 = 300 ml(NTP)/min; $[Glycerol]_{initial}$=0.03 M

b. T = 60 ^{o}C; atmospheric pressure; pH = 10; VO_2 = 300 ml(NTP)/min; $[Glycerol]_{initial}$ = 0.003M / 0.03M / 0.16M / 0.6M

c. T = 60 ^{o}C; atmospheric pressure; pH = 7 / 8 / 9 / 10; VO_2 = 300 ml(NTP)/min; $[Glycerol]_{initial}$=0.03 M

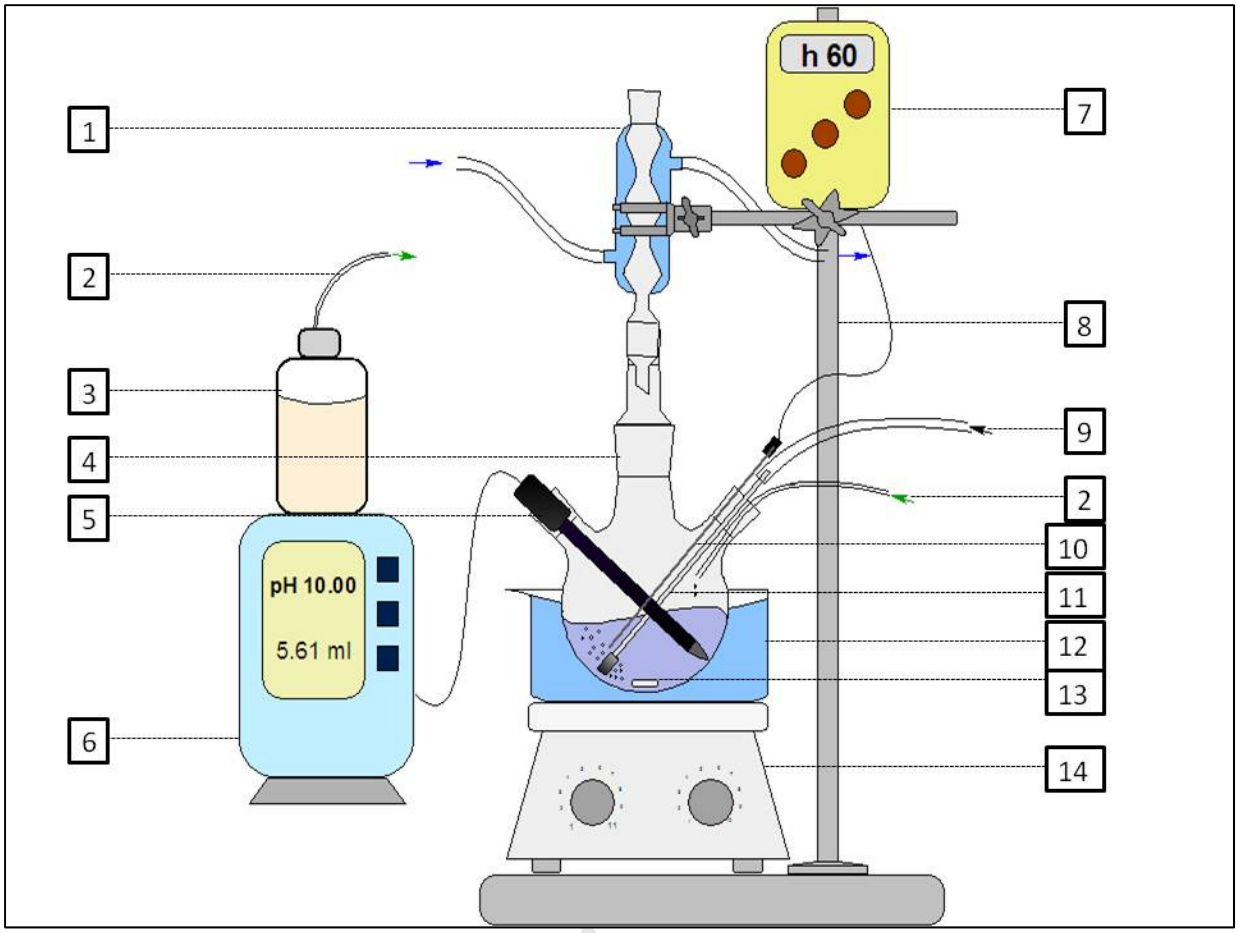

Figure 4.1: Experimental setup for oxidation of glycerol

1. *Overhead condenser & Cooling water*
2. *Sodium hydroxide addition*
3. *Sodium hydroxide storage*
4. *Reactor (three-necked round bottom flask)*
5. *pH probe*
6. *Auto-titrator*
7. *Temperature controller*
8. *Retort stand*
9. *Oxygen*
10. *Temperature probe*
11. *Oxygen sparger*
12. *Water bath*
13. *Magnetic stirrer*
14. *Hot plate*

4.3.2 High Performance Liquid Chromatography (HPLC)

Samples were taken every 10 minutes during the glycerol oxidation reaction and these were used for analysis on a Waters HPLC apparatus. The apparatus is equipped with a UV (210nm) and an RI detector and all products were separated at room temperature and a pressure of 1000 psi using a BioRad column (BioRad Aminex HPX-87-H 300mm x 7.8mm). A 0.01M H_2SO_4 solution was used as the mobile phase at a flow rate of 0.6 ml/min.

Possible products formed as a result of the oxidation of glycerol were identified and purchased. Standard solutions with different concentrations of glycerol and the identified organic products were prepared and analysed by HPLC. From this analysis retention times and response factors were obtained. Every product has a specific time/time range in which it will elute from the column. The concentrations of these products correspond to a certain peak area which was calculated by integrating peaks (using Breeze © software) obtained for the organic products using a UV detector. A calibration curve of concentration as a function of peak area was then generated for glycerol and each of the possible products formed (see Appendix). The gradient of the linear calibration curve is used as the response factor when analysing a reaction sample. By using the peak at a certain retention time, a certain product can be identified from the standard solutions tested and the product of that peak area and the corresponding response factor gives the concentration of that compound in the sample. Figure 4.2 demonstrates how the response factor for glyceric acid was determined, where the slope of the curve is the response factor.

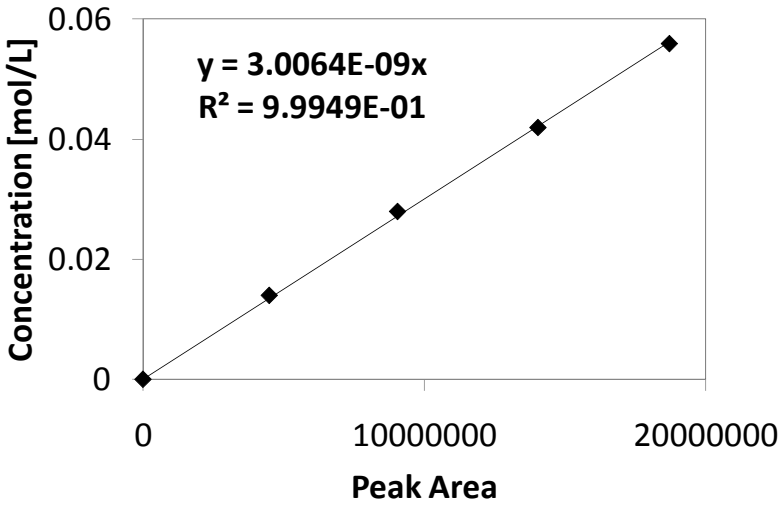

Figure 4.2: Determination of response factor for glyceric acid

Table 4.3 shows the retention times and response factors for all possible organic products. There are slight shifts in the retention time which is possibly as a result of changes in room

temperature since the column was not heated, fluctuations in system pressure and minor differences in mobile phase composition. The response factor for carbonic acid was determined slightly differently since the relationship between concentration and peak area was not linear. It is speculated that due to the acidic medium of the column, carbonic acid (at high concentrations) is converted to carbon dioxide in the detector due to a reduction in pressure once the stream leaves the column. The response factor for carbonic acid was therefore taken as the gradient of the line from the origin to the lowest concentration.

Table 4.3: HPLC retention times and responce factors for possible products

Compound	Retention time [min]	Response factor [$mol.L^{-1}.Peak\ area^{-1}$]
Glycerol	13.25 – 13.35	1.02×10^{-7}
Dihydroxyacetone (DHA)	13.62 – 13.70	1.35×10^{-8}
Glyceric acid (GA)	10.98 – 11.18	3.01×10^{-9}
Glycolic acid (GlyA)	12.60 – 12.81	1.11×10^{-8}
Tartronic acid (TA)	8.45 – 8.74	1.80×10^{-9}
Glyceraldehyde	10.80 – 10.90	9.63×10^{-9}
Oxalic acid	8.23 – 8.40	7.34×10^{-8}
Acetic acid	15.06 – 16.10	1.56×10^{-8}
Formic Acid	13.10 – 13.15	1.04×10^{-8}
Lactic acid	14.60 – 14.63	7.73×10^{-9}
Carbonic acid	6.30 – 6.35	1.21×10^{-8}

Figure 4.3 shows an example of a HPLC trace for an analysed sample taken 10 minutes from the start of the reaction. The signals obtained are the absorbance by the UV detector given as a function of retention time. Products were identified based on the retention times determined when analysing standard solutions. The four main products identified were DHA, glyceric acid, glycolic acid and tartronic acid. Traces of other organic products were also found but these four were found to be the main products as will be confirmed later by a carbon balance. It can be seen that peak separation is not very clear so careful identification and integration of peaks was necessary in order to obtain the correct concentrations of compounds in the sample. External standards were used during HPLC analysis to note any shifts in the retention times of products. Breeze © software integrates the peaks and provides the peak area as a function of retention time (see example Table 4.4). The product of the peak area and corresponding response factor gives concentration of a specific compound. The glycerol conversion is determined by using the initial concentration of glycerol at t = 0 min and the concentration determined by HPLC at each 10 min time interval. The increase in the liquid volume is noted by observing the amount of base added to control the pH. From the HPLC determined concentration and the volume, a yield can be calculated at each 10 minute interval, with yield being defined as the moles of carbon contributed by

glycerol and each of the product compounds. Selectivity can then be determined by normalising all products. An example is provided in Table 4.5 which uses the HPLC results obtained from a sample taken at 10 minutes when testing $Au_{63}Pt_{37}$.

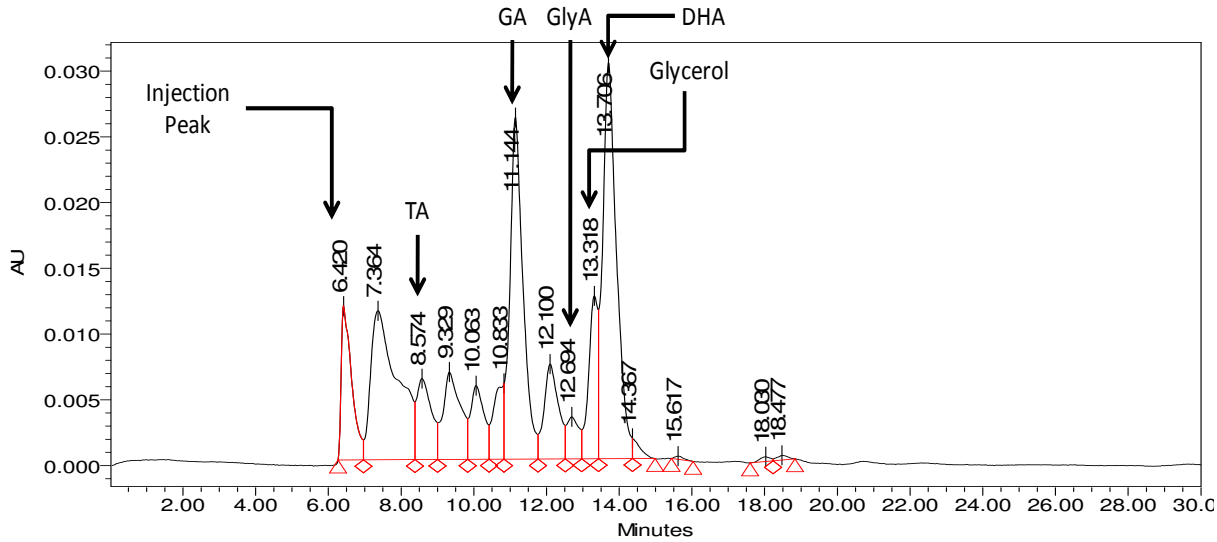

Figure 4.3: HPLC trace for glycerol oxidation (Catalyst: $Au_{63}Pt_{37}$)

T = 60 °C; atmospheric pressure; pH = 10; VO_2 = 300 ml(NTP)/min; $[Glycerol]_{initial}$=0.03 M)

Table 4.4: Peak area and retention times for HPLC trace shown in Figure 4.3

Retention time [min]	Peak Area	% Area	Product identification
6.420098206	**233758.394**	**6.89**	**Injection peak**
7.36410123	581520.9403	17.13	
8.574082314	**172342.6744**	**5.08**	**Tartronic acid**
9.329084603	223878.4002	6.60	
10.06333212	143996.9059	4.24	
10.83333333	112976.5274	3.33	
11.14397251	**653409.1403**	**19.25**	**Glyceric acid**
12.10006055	199362.7058	5.87	
12.69410393	**73985.68315**	**2.18**	**Glycolic acid**
13.31774519	**160790.670**	**4.74**	**Glycerol**
13.70566961	**797584.8223**	**23.50**	**Dihydroxyacetone**
14.36666667	21948.76175	0.65	
15.6168125	4147.600568	0.12	
18.02954854	7194.809746	0.21	
18.47748209	7309.68277	0.22	

Table 4.5: Sample calculation of conversion, yield and selectivity obtained from HPLC results

Compound	Peak Area	Response factor	Concentration [mol/L]	Conversion [%]	Volume $_{t=10min}$ [L]	Yield [mol-C]	Selectivity [C-%]
Glycerol	160790.670	1.02×10^{-7}	1.64×10^{-2}	50.94	0.209	1.03×10^{-2}	-
Tartronic acid	172342.6744	1.80×10^{-9}	3.10×10^{-4}	-	0.209	1.95×10^{-4}	2.03
Glyceric acid	653409.1403	3.01×10^{-9}	1.96×10^{-3}	-	0.209	1.23×10^{-3}	12.9
Glycolic acid	73985.68315	1.11×10^{-8}	8.25×10^{-4}	-	0.209	3.45×10^{-4}	3.61
Dihydroxyacetone	797584.8223	1.35×10^{-8}	1.08×10^{-2}	-	0.209	6.77×10^{-3}	70.7
Missing	-	-	-	-	0.209	1.03×10^{-3}	10.7

Chapter 5. Results

5.1 Catalyst characterization

In this study, the two key parameters for characterising alumina supported gold and gold-platinum catalysts are gold loading and gold crystallite size. The gold loading was measured by atomic absorption spectroscopy (AAS) and the crystallite size was determined from TEM images.

5.1.1 Gold loading from atomic absorption spectroscopy (AAS)

Table 5.1 shows the metal loading of the catalysts used in this study obtained from AAS (actual loading) as well as the theoretical loading. The total metal loading in the supported catalysts was kept constant at 2.2 wt.-%. Hence, the gold content in the bimetallic catalyst was reduced by 37 and 72% respectively.

Table 5.1: Theoretical and actual loading of metals on catalysts

Catalyst	W_{Au} [wt-%] Theoretical	W_{Au} [wt-%] Actual	W_{Pt} [wt-%]
Au_{100}	5	2.2	0
$Au_{63}Pt_{37}$	2	1.4	0.8
$Au_{28}Pt_{72}$	1	0.6	1.6

Figure 5.1 shows a gold mass balance obtained from the AAS analysis of the precursor solutions, water wash filtrates (WWF), ammonia wash filtrates (AWF) and digestion of solid catalysts. The difference in the Au input and Au output in catalyst preparation is represented by the “missing” fractions. At higher gold loadings, it is seen that most of the gold is removed during the water washing process, except for $Au_{28}Pt_{72}$ where most of the gold is removed during the ammonia washing step. In the WWF there is a decrease in the gold content with a decrease in gold loading. The gold in the WWF is simply the excess gold that has not been attached to the support, so the decrease could simply be due to the fact that there is a lower concentration of gold at start of the ion exchange process as the loading decreases. The purpose of the ammonia wash is to remove any chlorine bridges that is said to form between Au particles on the catalyst (Ivanova et al., 2004). However, during the ammonia wash some gold is also removed and it appears that there is an increase in the gold removed as the initial gold concentration decreases. However, when looking at it in absolute terms, the

amount of gold removed with the AWF is approximately constant with an increase/decrease in the initial gold concentration.

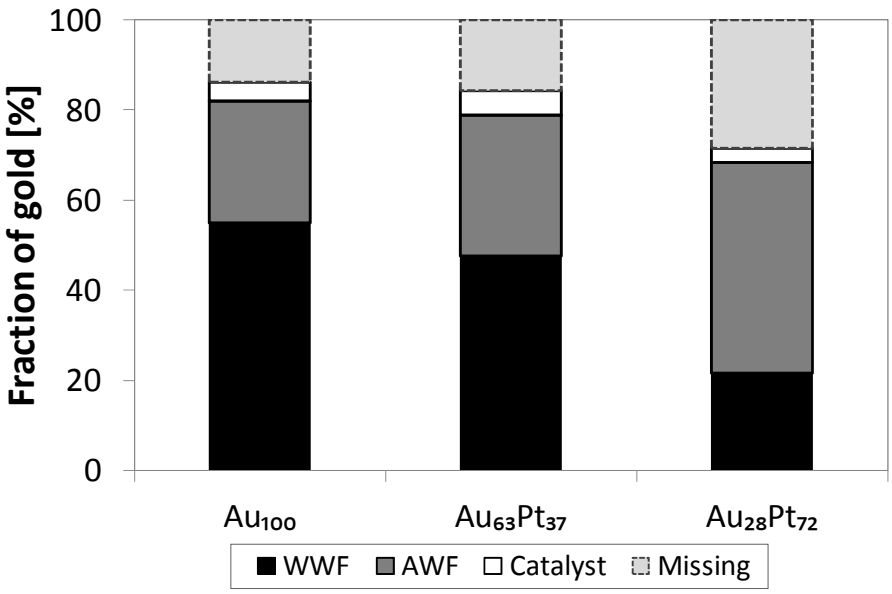

Figure 5.1: Gold balance based on AAS analysis of precursor solutions, filtrates and solid catalysts; WWF = Water wash filtrate, AWF = Ammonia wash filtrate

5.1.2 Determination of crystallite size

Transmission electron microscopy (TEM)

A sample of TEM images for Au and AuPt catalysts supported on γ-Al_2O_3 is shown below. The γ-Al_2O_3 is seen as grey spherical and cylindrical shapes with the metal particles having a darker circular form to to a higher electron density. The images shown are of the better images received from the TEM analysis. The catalyst was suspended in methanol and treated with ultrasound before being spread on the carbon grid. This breaks up the agglomeration of catalyst particles and allows for a better distribution on the grid so that clearer images are obtained.

A narrow metal crystallite size distribution is obtained via direct anionic exchange of aurochloric acid on to γ-Al_2O_3 (see Figure 5.2 and Table 5.2). It is interesting to note that the average gold crystallite size in the monometallic gold catalysts is ca. 50% larger than the metal crystallites in the bimetallic gold-platinum catalysts.

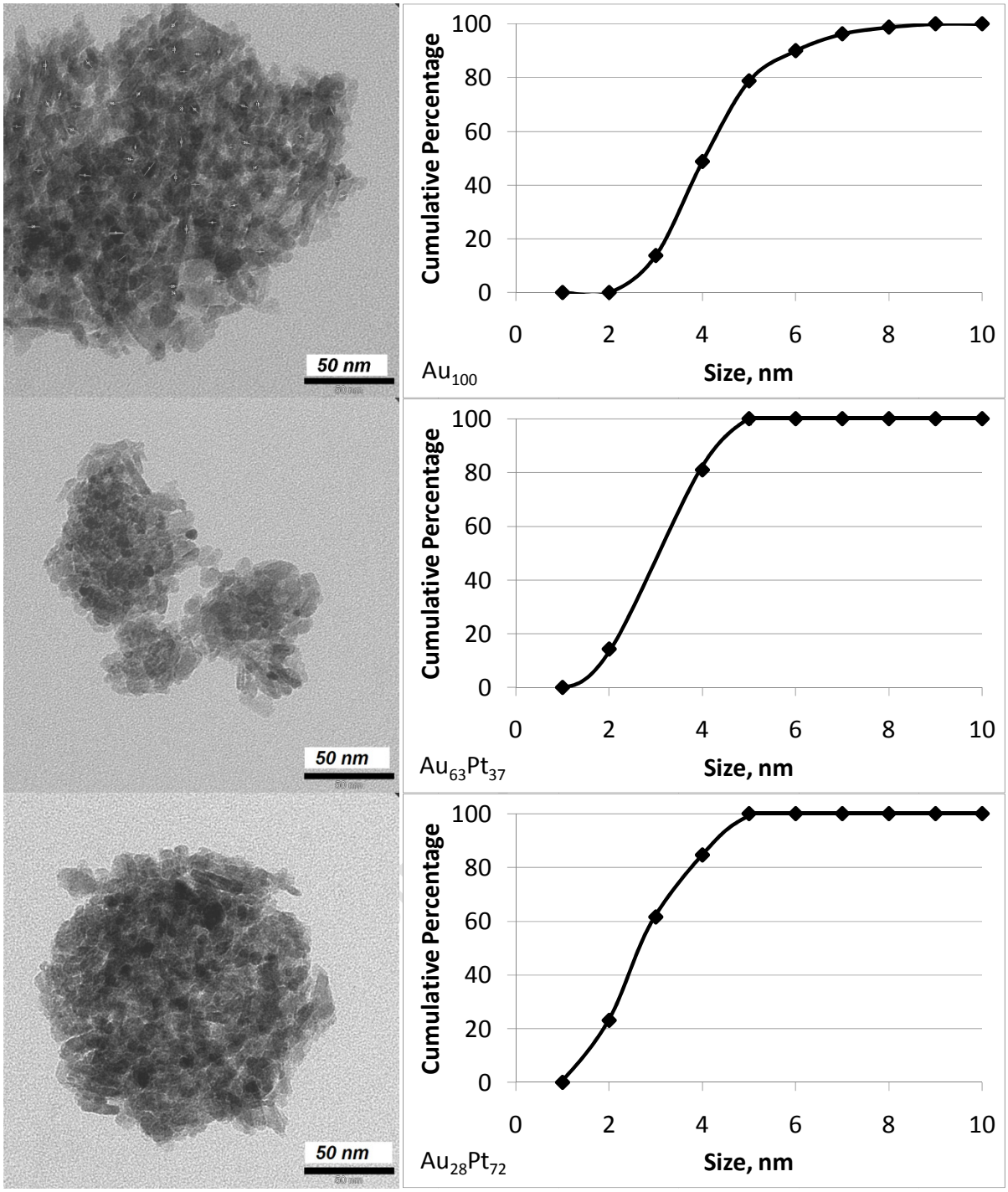

Figure 5.2: TEM-images and crystallite size distribution of Au_{100} (top), $Au_{68}Pt_{32}$ (middle) and $Au_{28}Pt_{72}$ (bottom)

Table 5.2: Average metal crystallite size obtained from TEM images

Catalyst	d_{metal} [nm]	n
Au_{100}	4.2 ± 1.3	80
$Au_{63}Pt_{37}$	2.9 ± 1.0	21
$Au_{28}Pt_{72}$	2.8 ± 1.1	13

Figure 5.3 shows images obtained from elemental mapping of the bimetallic catalysts. This technique creates a contrast in colour between different elements on the sample allowing one, in this case, to identify the position of the platinum crystallites in relation to the gold containing crystallites. The light grey cylindrical shapes are the alumina support whilst the circular black shapes are the gold containing crystallites. The red regions show the presence and position of platinum on the catalyst. Not much red can be seen in image (a) which is expected since this is the catalyst with the lower Pt loading, $Au_{63}Pt_{37}$. It was not possible to obtain a crystallite size distribution for the platinum crystallites from the TEM images since the crystals appeared to be very small and were hard to measure. Zooming in to get a closer view of the crystallites would only distort the resolution and not give a true account of the crystallite size.

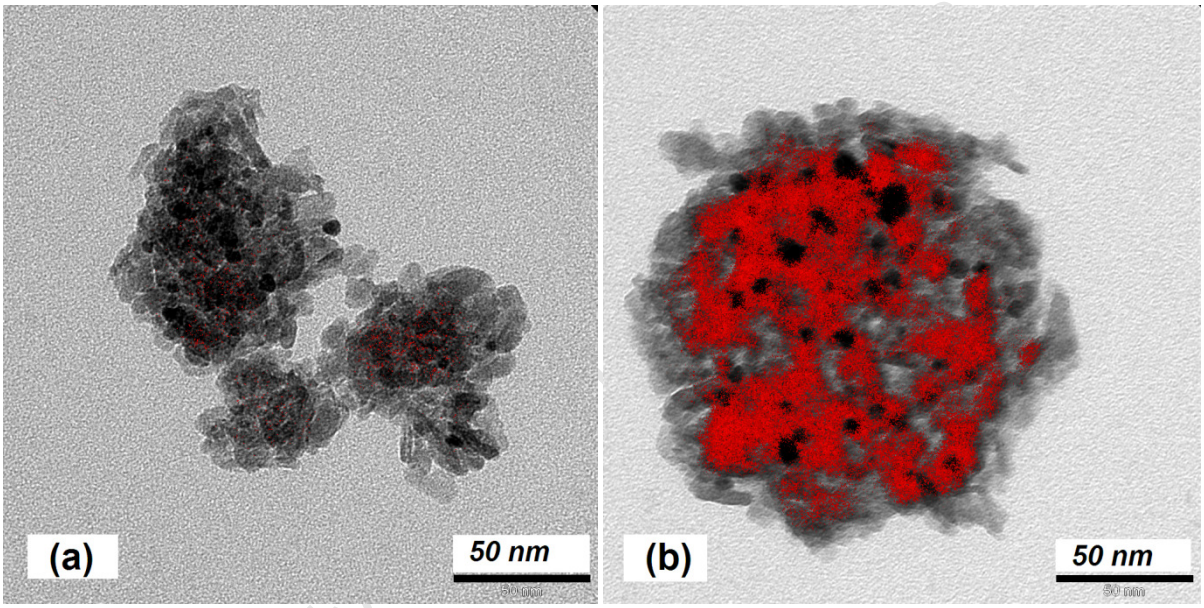

Figure 5.3: Elemental mapping of bimetallic catalysts (a) $Au_{63}Pt_{27}$ and (b) $Au_{28}Pt_{72}$

High resolution transmission electron microscopy was then performed in an attempt to obtain a size distribution and average crystallite size of the platinum particles. The best HRTEM images obtained are shown (see Figure 5.4.) for each of the 3 catalysts prepared. Two images are given for each catalyst at different magnifications. For Au_{100} (image a) the darker circular shapes are the gold containing crystallites. For the bimetallic catalysts (images b & c) the darker circular shapes are also thought to be the gold containing crystallites since there appearance against the alumina support is very similar to the monometallic catalyst. This was also confirmed by performing EDX analysis. For the monometallic Au_{100} catalyst, EDX analysis of the sample revealed the elements Al, O, C, Cu and Au. EDX analysis over the darker circular shapes on the bimetallic catalysts revealed the same elements but also traces of Pt, which is expected. Interestingly, the average metal crystallite size obtained from analysis of the HRTEM images gives larger metal crystallites for the bimetallic catalysts as

compared to TEM. Metal crystallite size for all catalysts is very similar according to HRTEM analysis. With HRTEM analysis twice the number of particles was counted with bimetallic catalyst $Au_{63}Pt_{37}$ compared to that of TEM analysis. A similar number of particles were counted for TEM and HRTEM analysis with Au_{100} and $Au_{28}Pt_{72}$. Since the platinum crystallite size was not identified from TEM and HRTEM images, a different method for obtaining this size was therefore used.

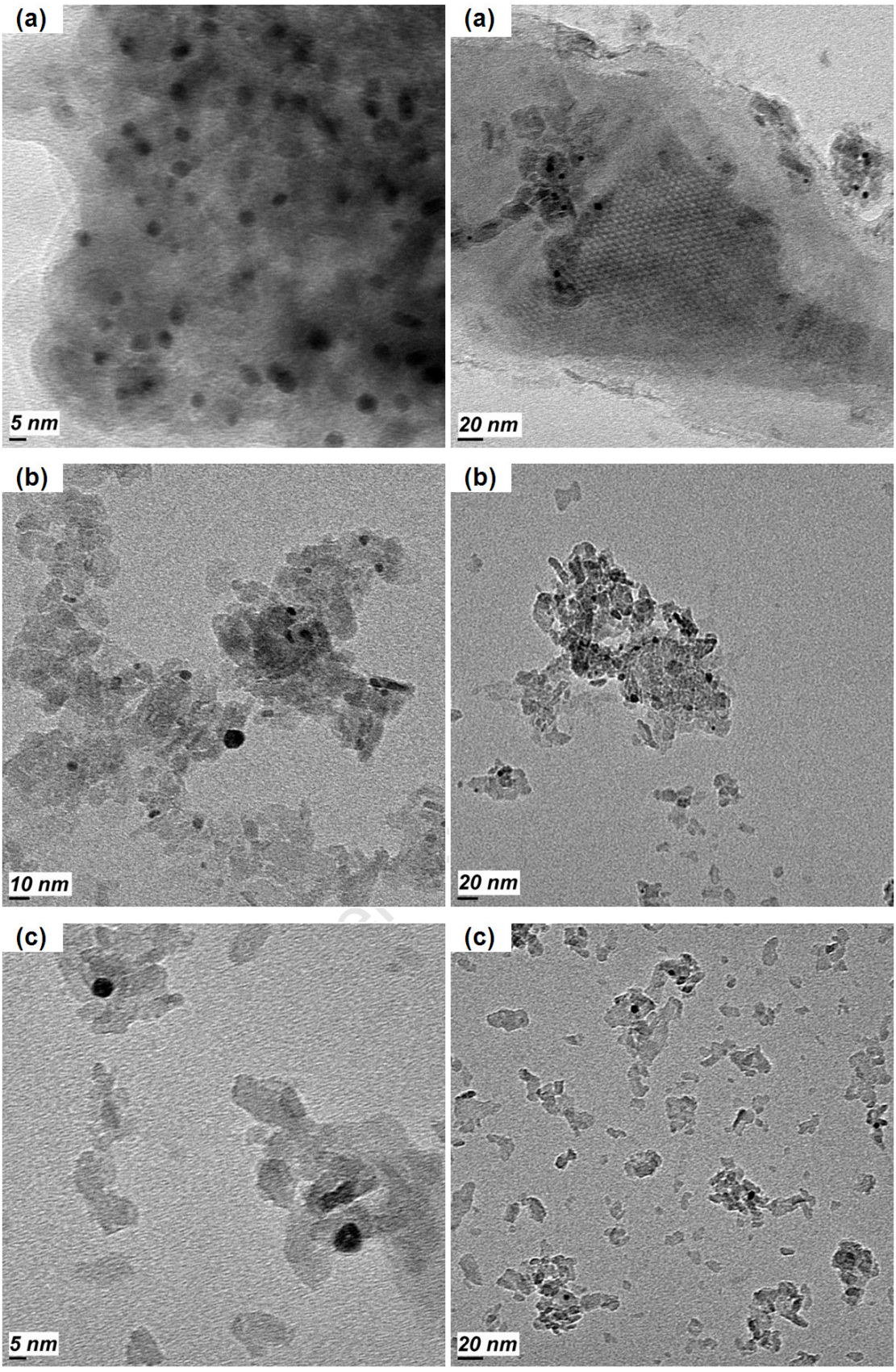

Figure 5.4: HRTEM images and average gold crystallite sizeof alumina supported Au and AuPt catalysts: (a) Au100, (b) Au63Pt72 and (c) Au28Pt72

Evaluation of H_2-chemisorption

The catalysts were characterized using H_2-chemisorption. The H_2 chemisorption was carried out in an adsorption apparatus Micrometrics ASAP 2020C. The hydrogen uptake was measured at various temperatures ranging from 50-150^{o}C after a treatment of the catalyst in hydrogen at 200^{o}C for 4hrs (after heating it up from room temperature with 10^{o}C/min). The catalysts were subsequently evacuated for 2 hrs at 200^{o}C followed by cooling down to the analysis temperature, at which temperature the sample was further evacuated for 2 hrs. The H_2-uptake was repeated after evacuation for 12 hrs, in order to determine the amount of strongly adsorbed and weakly adsorbed hydrogen.

i. Alumina

Figure 5.5 shows the hydrogen uptake on the alumina support at 150^{o}C. Some hydrogen uptake was observed on the bare alumina support. With increasing hydrogen pressure the amount adsorbed onto the support seems to increase linearly. A linear increase would imply a molecular adsorption of hydrogen onto the support surface. Dissociative adsorption of hydrogen on the surface would yield a correlation of the adsorbed volume of hydrogen with the square root of the hydrogen pressure. This correlation yielded a much lower regression coefficient of 0.86. Hence, based on the data obtained here it might be concluded that hydrogen adsorbs associatively on the alumina surface.

The adsorption on the alumina surface is rather weak, since evacuation at 150^{o}C for 12 hrs removes most of the adsorbed hydrogen as evidenced by the repeat analysis. The strength of adsorption cannot be directly determined from these isotherms, since the slope of the isotherms is the product of the strength of adsorption and the amount of hydrogen adsorbed to form a monolayer (assuming that the isotherm can be described by a Langmuir-isotherm).

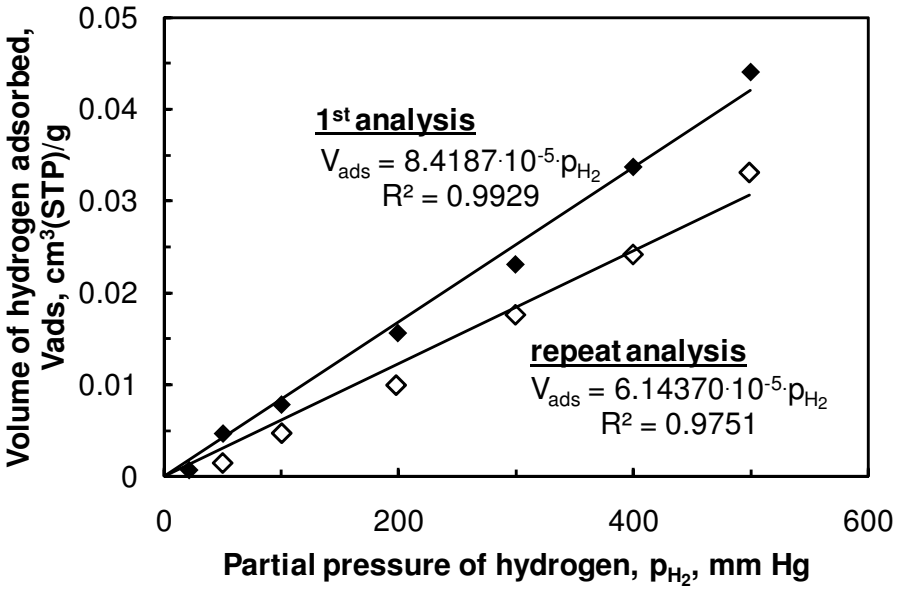

Figure 5.5: H_2-uptake on alumina at 150°C as a function of the hydrogen pressure

ii. Au/Al_2O_3

Hydrogen does adsorb on supported gold on alumina catalysts as was previously shown by Bus et al., (2005) and Bus and van Bokhoven (2007). The hydrogen uptake on the Au/Al_2O_3 catalyst was performed at 50, 100 and 150°C (see Figure 5.6). The hydrogen uptake can be described in terms of a rapid uptake at low pressure and an almost linear increase in the uptake with increasing pressure for hydrogen partial pressures larger than 50 mm Hg. The latter is typically weakly adsorbed and can be removed during the evacuation step at the analysis temperature. This may be (partly) attributed to adsorption onto the support (see above). The difference analysis shows the expected adsorption behavior for the isotherms at 50°C and 100°C, whereas the difference adsorption isotherm at 150°C is less representative of a typical adsorption isotherm. Furthermore, it should be noted that the limiting value (which is typically interpreted as the amount adsorbed to form a monolayer on the metal) increases with increasing temperature. This has previously been interpreted as an increase in the H/Au-ratio with increasing temperature (Bus & van Bokhoven, 2007) due to the activation barrier for H_2-dissociation on gold surfaces (Barrio et al., 2006).

During the evacuation step, all weakly adsorbed hydrogen can be removed, irrespective on its location on the catalyst. Hence, some hydrogen adsorbed on the metal may be removed as well. Hydrogen chemisorption on gold is expected to be endothermic on extended surfaces (Barrio et al., 2006), whereas on small clusters the adsorption of hydrogen can be endo- or exothermic (Phala, 2004). Thus, for large clusters and extended surfaces the strength of adsorption is expected to increase with increasing temperature. Hence, some of

the hydrogen adsorbed at 50°C may have been removed during the evacuation step. Hence, the 1st analysis was modeled as a dual Langmuir-isotherm in order to estimate the amount of hydrogen adsorbed onto the gold.

$$V_{H_2,ads} = V_{m,1} \cdot \frac{K_1 \cdot p_{H_2}^n}{1 + K_1 \cdot p_{H_2}^n} + V_{m,2} \cdot \frac{K_2 \cdot p_{H_2}^m}{1 + K_2 \cdot p_{H_2}^m}$$

Where V_m = monolayer volume [cm^3(STP)/g]

$V_{H2, ads}$ = volume of adsorbed hydrogen [cm^3(STP)/g]

K = adsorption constant [mm Hg^{-1}]

The high pressure range of the isotherm shows an almost linear increase in the amount of hydrogen adsorbed with increasing pressure indicating that the inhibition term can be neglected and the isotherm becomes:

$$V_{H_2,ads} = V_{m,1} \cdot \frac{K_1 \cdot p_{H_2}^n}{1 + K_1 \cdot p_{H_2}^n} + b \cdot p_{H_2}$$

The parameters of in the hydrogen adsorption isotherm were determined using non-linear regression (see Table 5.3). The data is well described by the isotherm as shown by the high regression coefficients and the low variance obtained. However, the parameters of the fit show a large variation. In particular the reaction order with respect to hydrogen shows a large variation at 50 and 100°C. The indicated reaction order of hydrogen at these temperatures may indicate the presence of dissociated hydrogen (for which a reaction order of 0.5 was expected). The very small value at 150°C represents a physically unrealistic value if the adsorption process follows a Langmuir mechanism.

Table 5.3: Fitting parameters to the hydrogen adsorption isotherm on Au/Al_2O_3 with the 95% confident interval assuming a variable reaction order with respect to hydrogen

$T_{analysis}$ [°C]	50	100	150
$V_{m,1}$, cm^3(STP)/g	0.017 ± 0.010	0.027 ± 0.042	0.225 ± 0.67
K_1, mm Hg^{-1}	0.81 ± 0.92	1.14 ± 3.70	0.08 ± 0.26
n	0.42 ± 0.50	0.24 ± 0.69	0.07 ± 0.05
b, cm^3(STP)/g/mm Hg	$1.13 \cdot 10^{-4} \pm 0.13 \cdot 10^{-4}$	$1.09 \cdot 10^{-4} \pm 0.19 \cdot 10^{-4}$	$1.43 \cdot 10^{-4} \pm 0.11 \cdot 10^{-4}$
R^2	0.996	0.996	0.998
variance	$2.95 \cdot 10^{-6}$	$2.01 \cdot 10^{-6}$	$1.83 \cdot 10^{-6}$

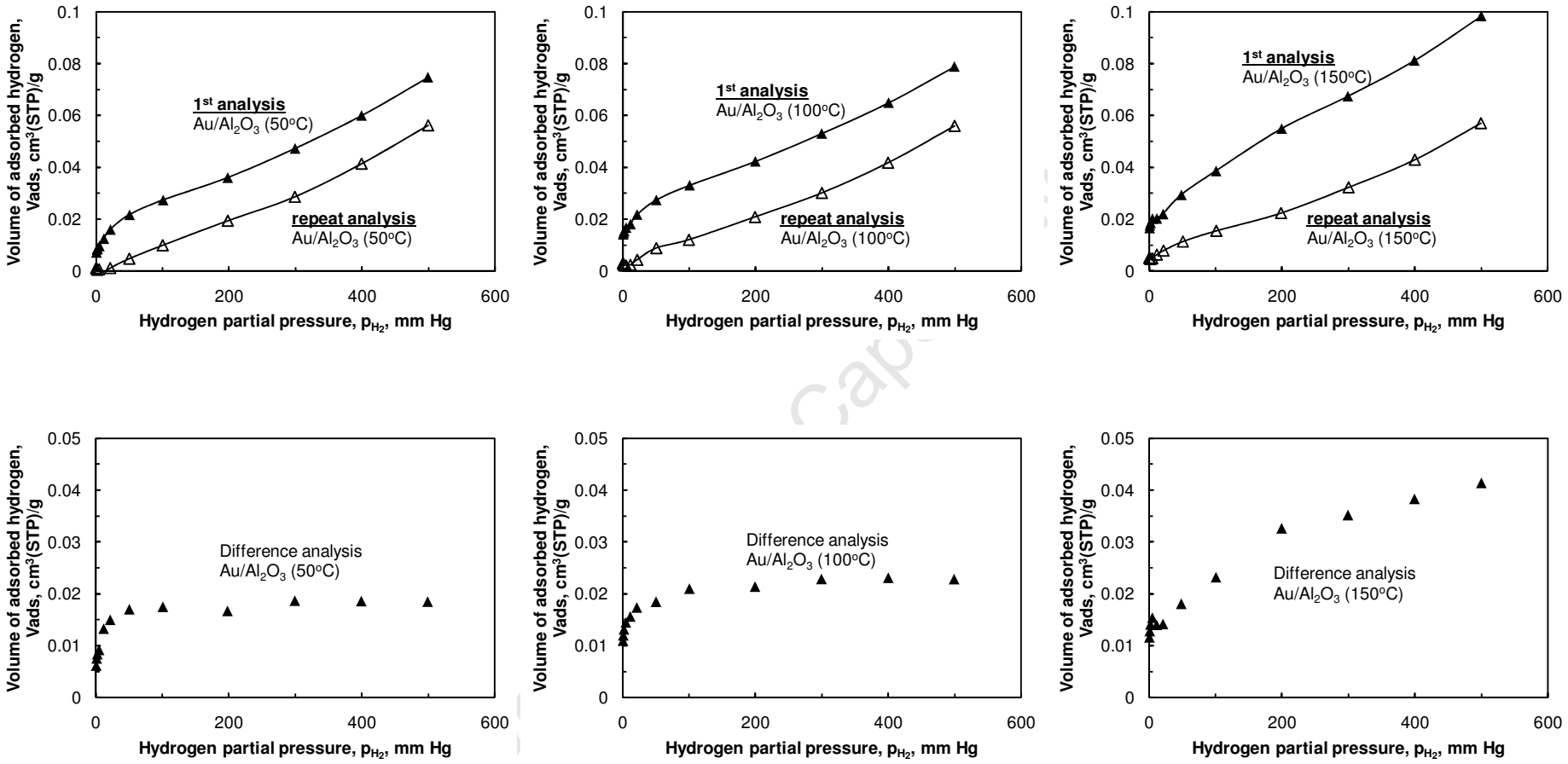

Figure 5.6: Hydrogen uptake on Au/Al$_2$O$_3$ at 50°C (left), 100°C (middle) and 150°C (right) as a function of the hydrogen partial pressure for the 1st and repeat analysis (top) and the difference analysis (bottom)

The large variation in the reaction order with respect to hydrogen results in a large uncertainty in the amount of strongly adsorbed hydrogen on the gold surface. Hence, the hydrogen uptake was modeled assuming the dissociative adsorption of hydrogen on gold:

$$V_{H_2,ads} = V_{m,1} \cdot \frac{K_1 \cdot p_{H_2}^{0.5}}{1 + K_1 \cdot p_{H_2}^{0.5}} + b \cdot p_{H_2}$$

The fitting parameters to this model describing the dissociative hydrogen chemisorption onto gold are given in Table 5.4. This model can describe the isotherm as well as the isotherm with a variable reaction order with respect to hydrogen with only the data obtained at 150°C showing a slightly larger variance. The data implies that the amount of strongly adsorbed hydrogen present on the gold surface amounts to 0.021 cm^3(STP)/g. The low amount of hydrogen taken up by the catalyst implies a low H/Au ratio. The total amount of atomic hydrogen relative to the total amount of metallic gold (2.2 wt.-%) amounts to 1.7%, which is lower than that reported previously for Au/Al_2O_3 catalysts (Bus et al., 2005). Assuming an average crystallite size of 4.2 nm and a surface gold density of 13.9 Au atoms per nm^2 (i.e. assuming a Au(111) surface), this would correspond to a $H/Au_{surface}$ of 0.05, which is similar to that reported by Bus et al. (2005) with Au/Al_2O_3 catalysts with a gold dispersion between 50 and 100% (based on EXAFS data).

The strength of adsorption (K_1) increases with increasing temperature, which is characteristic for an endothermic adsorption process. Despite the large variation in the adsorption constant at 50°C, a heat of adsorption for the dissociative adsorption of hydrogen of 28.4 ± 0.44 kJ/mol H_2 is estimated.

The product of the strength of adsorption of the weakly adsorbed hydrogen (represented by linear region of adsorption isotherm) and the amount of weakly adsorbed hydrogen does not seem to be a strong function of temperature. Furthermore, the constant b seems to be slightly larger than the value obtained on the bare alumina support implying that gold may facilitate the adsorption of weakly adsorbed hydrogen.

Table 5.4: Fitting parameters to the hydrogen adsorption isotherm on Au/Al_2O_3 with the 95% confident interval assuming dissociative adsorption of hydrogen onto gold

$T_{analysis}$ (°C)	50	100	150
$V_{m,1}$, cm^3(STP)/g	0.016 ± 0.004	$0.021 \pm 3.3 \cdot 10^{-7}$	$0.022 \pm 3.5 \cdot 10^{-7}$
K_1, mm Hg^{-1}	0.91 ± 0.78	$2.04 \pm 2.26 \cdot 10^{-4}$	$3.15 \pm 4.48 \cdot 10^{-5}$
b, cm^3(STP)/g/mm Hg	$1.15 \cdot 10^{-4} \pm 0.10 \cdot 10^{-4}$	$1.14 \cdot 10^{-4} \pm 1.36 \cdot 10^{-9}$	$1.52 \cdot 10^{-4} \pm 1.48 \cdot 10^{-9}$
R^2	0.996	0.997	0.997
Variance	$2.65 \cdot 10^{-6}$	$2.00 \cdot 10^{-6}$	$2.37 \cdot 10^{-6}$

iii. $Au_{63}Pt_{37}/Al_2O_3$

The hydrogen uptake on the bimetallic Au-Pt catalyst with a Au/Pt ratio of 63/37 as a function of the hydrogen partial pressure for the different adsorption temperatures ranging from 50-150°C is shown in Figure 5.7. Hydrogen does adsorb on supported gold on alumina catalysts as was previously shown. The hydrogen uptake on the bimeticallic catalyst is significantly larger than on the mono-metallic gold catalyst. Furthermore, it can be noted that the amount of hydrogen taken up at a given hydrogen pressure decreases with increasing temperature implying an exothermic adsorption process. Furthermore, it can be seen that the difference analysis shows a decrease in the amount of the so-called strongly adsorbed hydrogen with increasing temperature implying that with increasing temperature more hydrogen is removed from the surface by evacuation at the analysis temperature for 12 hrs.

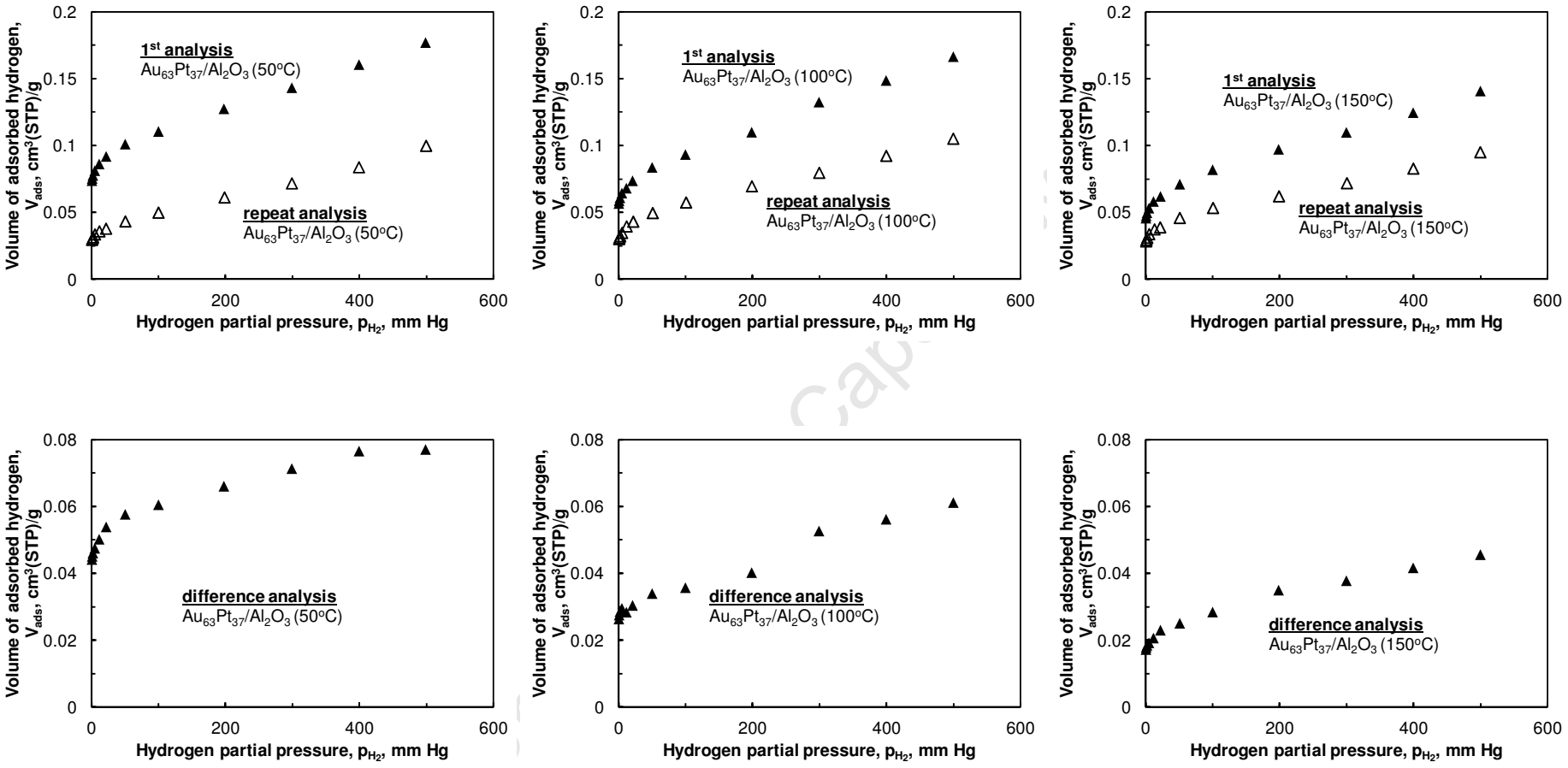

Figure 5.7: Hydrogen uptake on $Au_{63}Pt_{37}/Al_2O_3$ at 50°C (left), 100°C (middle) and 150°C (right) as a function of the hydrogen partial pressure for the 1st and repeat analysis (top) and the difference analysis (bottom)

The hydrogen uptake can be ascribed by a strong initial uptake followed by an almost linear increase in the uptake of hydrogen with pressure. Hence, the hydrogen uptake (1st analysis) was modeled by a Langmuir isotherm with a variable reaction order with respect to hydrogen and a weak adsorption (e.g. on the support):

$$V_{H_2,ads} = V_{m,1} \cdot \frac{K_1 \cdot p_{H_2}^n}{1 + K_1 \cdot p_{H_2}^n} + b \cdot p_{H_2}$$

The parameters of in the hydrogen adsorption isotherm were determined using non-linear regression (see Table 5.5). The data is well described by the isotherm as shown by the high regression coefficients and the low variance obtained. However, the parameters of the fit show a large variation. The reaction order with respect to hydrogen is extremely low (between 0.07 and 0.08). For molecular adsorption a reaction order of 1 is expected, and for dissociative adsorption of hydrogen a reaction order of 0.5 is expected. The low order with respect to hydrogen might imply the presence of very strongly adsorbed hydrogen.

Table 5.5: Fitting parameters to the hydrogen adsorption isotherm on $Au_{63}Pt_{37}/Al_2O_3$ with the 95% confident interval assuming a variable reaction order with respect to hydrogen

$T_{analysis}$ (°C)	50	100	150
$V_{m,1}$, cm^3(STP)/g	0.017 ± 0.010	0.28 ± 0.25	0.43 ± 0.40
K_1, mm Hg^{-1}	0.36 ± 0.79	0.27 ± 0.31	0.12 ± 0.13
n	0.07 ± 0.05	0.08 ± 0.03	0.09 ± 0.02
b, cm^3(STP)/g/mm Hg	$1.46 \cdot 10^{-4} \pm 0.09 \cdot 10^{-4}$	$1.66 \cdot 10^{-4} \pm 0.11 \cdot 10^{-4}$	$1.27 \cdot 10^{-4} \pm 0.10 \cdot 10^{-4}$
R^2	0.999	0.999	0.999

Hydrogen is known to adsorb strongly on platinum (Podkolzin et al., 2001) and platinum clusters (see e.g. Pistonesi et al., 2008). The presence of sites, which adsorb hydrogen strongly, can also be deduced from the experimentally obtained difference analysis (see Figure 5.7), which shows a significant presence of strongly adsorbed hydrogen at the lowest applied pressure. The presence of strongly adsorbed hydrogen, in addition to the presence of dissociatively adsorbed hydrogen on moderately strong adsorbing sites and the presence of sites adsorbing hydrogen weakly was modeled as:

$$V_{H_2,ads} = V_{strong} + V_{m,1} \cdot \frac{K_1 \cdot p_{H_2}^n}{1 + K_1 \cdot p_{H_2}^n} + b \cdot p_{H_2}$$

(It should be noted that the strongly adsorbed sites were assumed to be saturated at all measured pressures to minimize the number of fitting parameters).

With increasing analysis temperature, the amount of hydrogen adsorbed on the very strongly adsorbing sites decreases (see Table 5.6). This might indicate that at the higher adsorption

temperatures the strongly adsorbing hydrogen is better described by a Langmuir isotherm. However, attempting to include the strongly adsorbing site using a Langmuir isotherm for this site did not yield an improvement in the variance for the fit and the obtained equilibrium constant for the dissociative adsorption of hydrogen on these strongly adsorbing sites was large (ca. 500 $(mm\ Hg)^{-1}$) and almost invariant with temperature. If the catalyst is assumed to contain Pt-crystallites, which adsorb hydrogen very strongly and gold crystallites which adsorb hydrogen moderately strongly (i.e the possible presence of bimetallic crystallites is ignored, which can be justified partly based on the miscibility gap between Au and Pt (Ponec et al., 1995; Xu et al., 2009), although Bus et al. (2005) seem to indicate some Pt-Au nanoclusters in their catalysts), the average Pt-crystallite size can be estimated based on the amount of strongly adsorbed hydrogen at 50°C. A dispersion of the platinum of 14.7% can then be determined, which would correspond to platinum crystallites of ca. 9.3 nm. These large crystallites were not observed in the TEM-analysis. Platinum makes up ca. 37 wt-% of the 2.2 wt-% metal in the catalyst and should have been detected in the TEM-analysis. Hence, it might be concluded that not all platinum is present as pure platinum crystallites, but some platinum may be associated with the gold crystallites. Bus and van Bokhoven (2007) stated (based on EXAFS measurements) that nano-crystallites with a bulk Au-Pt ratio of 2:1 will be formed in bimetallic platinum-gold crystallites. The excess platinum in the catalysts may then be present as pure platinum crystallites. If all gold is associated with the gold platinum alloy, the dispersion of the excess platinum can be estimated as 91% (corresponding to platinum crystallites for the excess platinum of ca. 1.5 nm).

The amount of hydrogen adsorbed dissociatively on the moderately strong sites is ca. 0.04 cm^3/g (see Table 5.6). This amount of hydrogen might be ascribed to the hydrogen adsorbed on the platinum-gold alloy crystallites. The H/M ratio for the bimetallic crystallites is estimated to be 0.06 for the bimetallic system. The strength of adsorption for the moderately strongly adsorbed hydrogen, as expressed by K_1, seems to be decreased due to the presence of platinum in the catalyst. A heat of adsorption of -8 ± 0.73 kJ/mol H_2 is estimated for the dissociative adsorption of hydrogen on this bimetallic catalyst.

Table 5.6: Fitting parameters to the hydrogen adsorption isotherm on $Au_{63}Pt_{37}/Al_2O_3$ with the 95% confident interval assuming dissociative adsorption of hydrogen onto the metal crystallites in addition to the presence of very strongly adsorbing sites and weakly adsorbing sites

$T_{analysis}$ (°C)	50	100	150
V_{strong}, cm^3(STP)/g	0.067 ± 0.003	0.051 ± $2.5 \cdot 10^{-4}$	0.041 ± 0.004
$V_{m,1}$, cm^3(STP)/g	0.039 ± 0.004	0.035 ± $4.3 \cdot 10^{-4}$	0.042 ± 0.011
K_1, mm Hg^{-1}	0.26 ± 0.10	0.25 ± 0.01	0.18 ± 0.14
b, cm^3(STP)/g/mm Hg	$1.52 \cdot 10^{-4}$ ± $6.8 \cdot 10^{-6}$	$1.72 \cdot 10^{-4}$ ± $1.2 \cdot 10^{-6}$	$1.30 \cdot 10^{-4}$ ± $1.48 \cdot 10^{-5}$
R^2	0.9995	0.9992	0.9990
Variance	$6.03 \cdot 10^{-7}$	$1.62 \cdot 10^{-6}$	$1.03 \cdot 10^{-6}$

iv. $Au_{28}Pt_{72}/Al_2O_3$

The hydrogen uptake on the bimetallic Au-Pt catalyst with a Au/Pt ratio of 28/72 as a function of the hydrogen partial pressure for the different adsorption temperatures ranging from 50-150°C is shown in Figure 5.8. The observed trends are similar to those observed for the bimetallic catalyst $Au_{63}Pt_{37}/Al_2O_3$. The bimetallic gold-platinum catalyst with a higher platinum content does show a higher hydrogen uptake than the bimetallic gold-platinum catalyst with the lower platinum content.

The hydrogen uptake is modeled in the bimetallic catalyst with a high platinum content with the same isotherm as the bimetallic catalyst with a low platinum content:

$$V_{H_2,ads} = V_{strong} + V_{m,1} \cdot \frac{K_1 \cdot p_{H_2}^n}{1 + K_1 \cdot p_{H_2}^n} + b \cdot p_{H_2}$$

The fitting parameters to this model are given in Table 5.7. The high regression coefficients and the low variance obtained indicates the data is well described by the isotherm. With increasing analysis temperature, the amount of hydrogen adsorbed on the very strongly adsorbing sites decreases, similar to the catalyst with a lower platinum content. If the presence of bimetallic crystallites is once again ignored, the amount of strongly adsorbed hydrogen at 50°C can be used to estimate the Pt-crystallite size. A crystallite size of 10.5 nm is estimated which corresponds to a dispersion of platinum of ca. 10.4%. As with the previous bimetallic catalyst ($Au_{63}Pt_{37}$), large platinum crystallites were not seen on TEM images and with a platinum content of ca. 72 wt-% in the metal, these crystallites should have been identified. If we now use the results presented by Bus & van Bokhoven (2007) and assume that all gold is associated with the gold-platinum alloy with a Au-Pt ratio of 2:1, a large Pt-crystallite size of ca. 8.7 nm is calculated with a dispersion of 13% for the excess platinum. There is a fluctuation in the strength of adsorption (K_1) which indicates that ΔH is approximately zero.

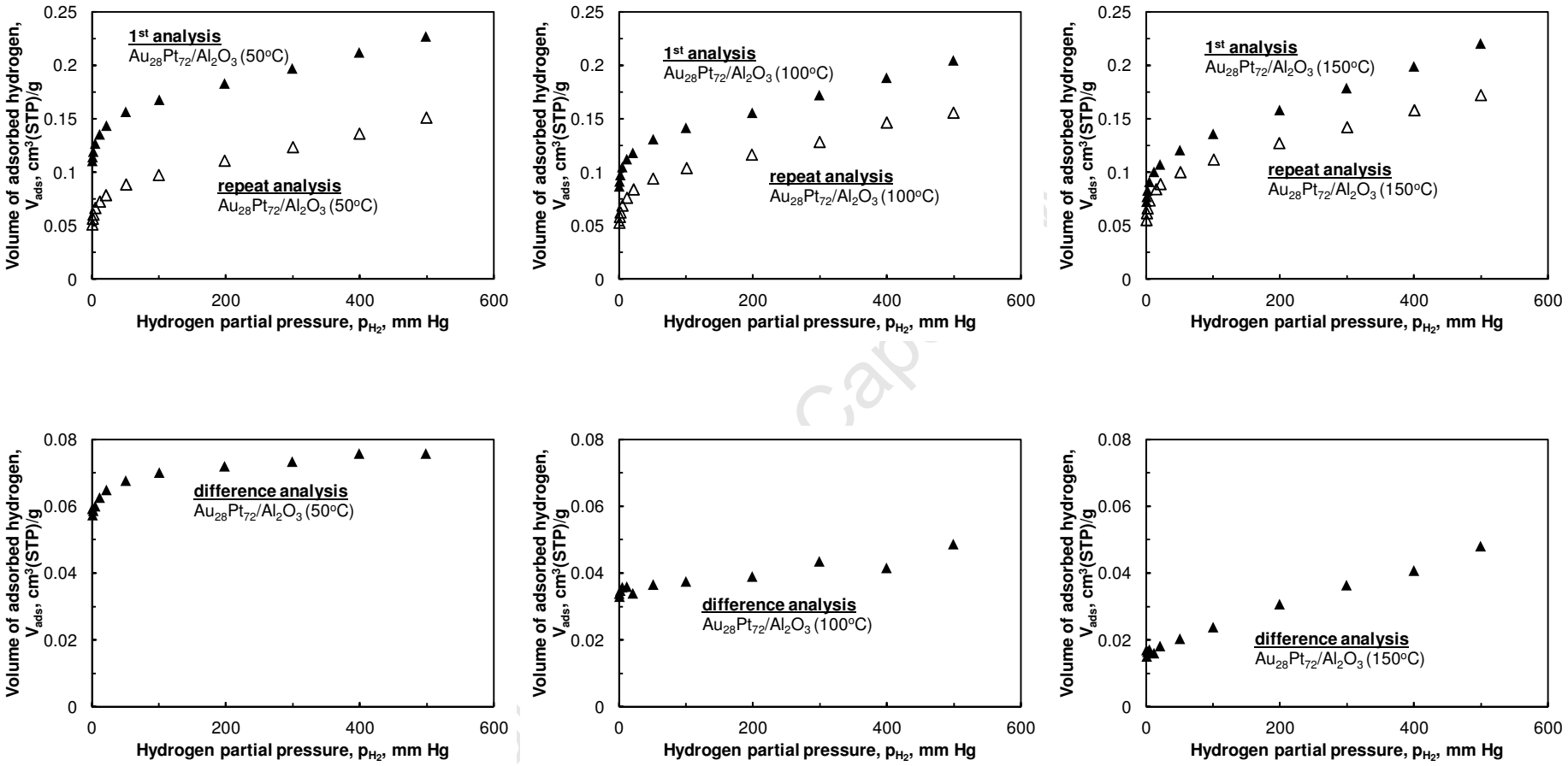

Figure 5.8: Hydrogen uptake on $Au_{28}Pt_{72}/Al_2O_3$ at 50°C (left), 100°C (middle) and 150°C (right) as a function of the hydrogen partial pressure for the 1st and repeat analysis (top) and the difference analysis (bottom)

Table 5.7: Fitting parameters to the hydrogen adsorption isotherm on $Au_{28}Pt_{72}/Al_2O_3$ with the 95% confident interval assuming dissociative adsorption of hydrogen onto the metal crystallites in addition to the presence of very strongly adsorbing sites and weakly adsorbing sites

$T_{analysis}$ (°C)	50	100	150
V_{strong}, cm^3(STP)/g	0.095 ± 0.005	0.070 ± 0.005	0.041 ± 0.004
$V_{m,1}$, cm^3(STP)/g	0.079 ± 0.005	0.068 ± 0.004	0.056 ± 0.003
K_1, mm Hg^{-1}	0.29 ± 0.10	0.46 ± 0.14	0.36 ± 0.07
b, cm^3(STP)/g/mm Hg	$1.24 \cdot 10^{-4} \pm 1.1 \cdot 10^{-5}$	$1.44 \cdot 10^{-4} \pm 9.2 \cdot 10^{-6}$	$1.91 \cdot 10^{-4} \pm 6.3 \cdot 10^{-6}$
R^2	0.9994	0.9991	0.9999
Variance	$9.75 \cdot 10^{-7}$	$1.43 \cdot 10^{-6}$	$3.39 \cdot 10^{-7}$

Table 5.8 summarises the findings of the H_2-chemisorption analysis, showing the heat of adsorption, dispersion of platinum on the catalyst and platinum crystallite size. The dispersion reported in the table refers to the dispersion of the pure platinum crystallites and not that associated with the gold in the bimetallic catalysts.

Table 5.8: Summary of findings of H2 chemisorption analysis

Catalyst	D_{Pt}	d_{Pt} [nm]	ΔH_{ads} [kJ/mol H_2]
$Au_{63}Pt_{37}$ / Al_2O_3	91%	1.5	-8.0 ± 0.73
$Au_{28}Pt_{72}$ / Al_2O_3	13%	8.5	≈ 0
Au / Al_2O_3	D_{Au} = 50-100%	d_{Au} = 4.2	28.4 ± 0.44

5.2 Catalyst testing

The prepared Au and AuPt catalysts were tested in the oxidation of glycerol. These reactions were performed in a semi-batch 500ml glass reactor. The reaction conditions are as follows:

Table 5.9: Catalyst testing protocol for the oxidation of glycerol using gold-based catalysts supported on γ-alumina

Variable	Value
Temperature	60°C
Pressure	Atmospheric
pH	10
Stirrer speed	400 rpm
O_2 flow rate	300 ml(NTP)/min
Mass of catalyst	0.2 g
Initial glycerol concentration	0.03 M

5.2.1 Reproducibility in runs

The pH of the reaction mixture was brought to pH 10 by the initial addition of NaOH before the start of the reaction. Organic acids formed during the course of the reaction (see Figure 2.3) lowers the pH of the reaction solution. The pH was carefully monitored and controlled by an auto-titrator which adds NaOH to the reaction vessel once the pH drops from the set point.

When comparing the properties of catalysts during a test reaction, it is important to maintain a good level of reproducibility. This was done by monitoring the addition of NaOH to the reaction vessel over the course of the reaction (see Figure 5.9). The figure below shows the addition of NaOH for the runs performed with two of the catalysts at the same reaction conditions. With Au_{100} one can see that runs 2 and 4 follow the same trend whilst runs 1 and 3 are out of the range. The differences in the NaOH addition could be attributed to the control mechanism of the instrument. Sometimes the auto-titrator displayed very precise control whilst other times it would over-compensate and add too much NaOH as can be see with Au100 run 1 at 20 minutes. When the system was disturbed, by aggressive sampling or instruments moving out of place, greater fluctuations was noted in the pH read by the auto-titrator causing the addition of more NaOH than was needed. These runs were discarded and not considered in the HPLC analysis. The disturbances came about during sampling, as the pipette had to be forced through the neck of the round bottom flask that was also the access point for the temperature controller and oxygen sparger. Te sparger lay very close to the magnetic stirrer which would cause major disruptions when knocked out of place and cause incorrect readings on the pH meter. By the repetition of runs and establishment of a simpler sampling method (by syringe rather than pipette), a better reproducibility was obtained as can be seen with the $Au_{63}Pt_{37}$ runs shown in Figure 5.9. When using the syringe instead, fewer disturbances were cause to the system as the syringe was smaller and shorter and therefore easier to handle and could fit through the neck of the flask with more ease.

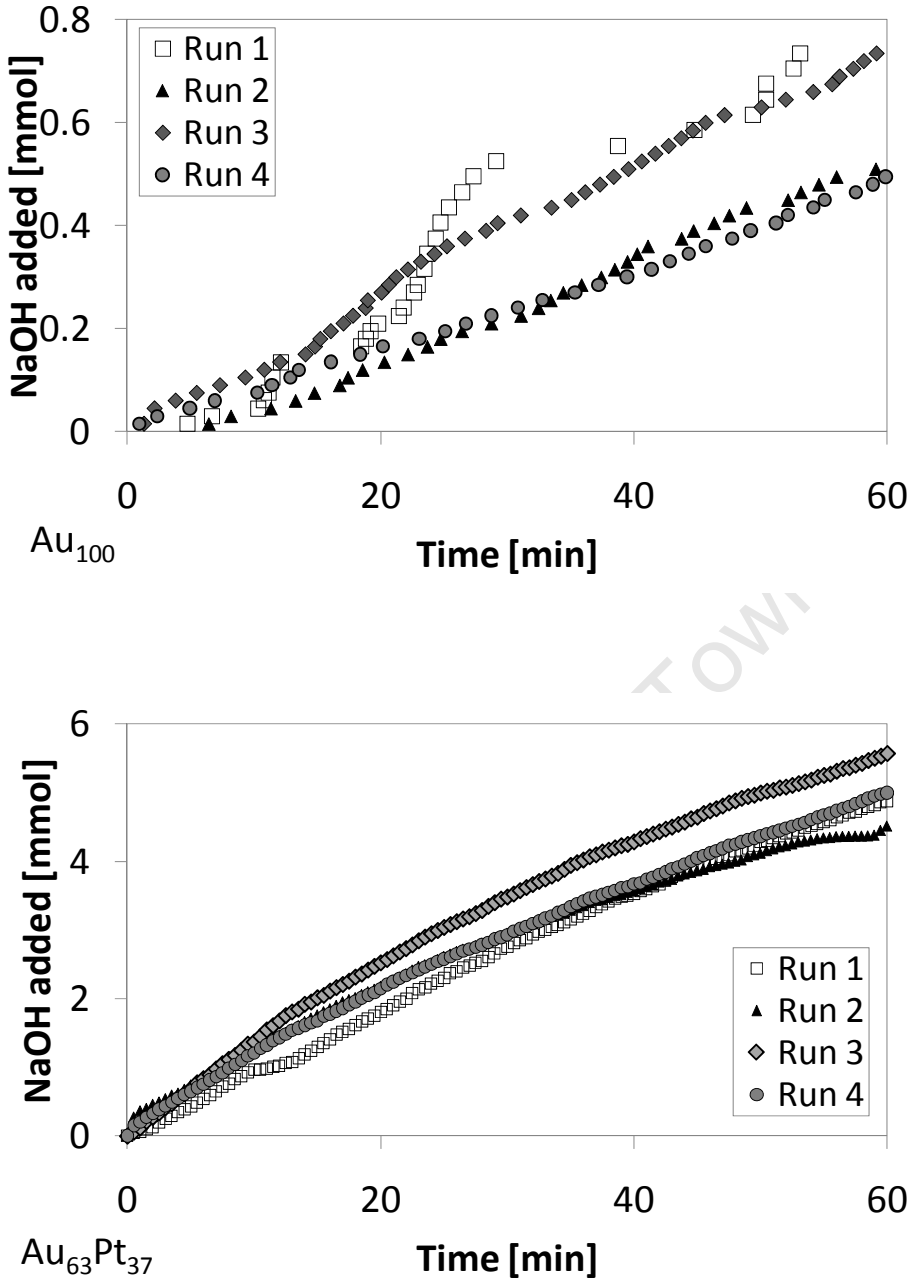

Figure 5.9: NaOH addition for testing catalysts in the oxidation of glycerol as a function of reaction time: Au_{100} (top) and $Au_{63}Pt_{37}$ (bottom)

(T = 60 °C; atmospheric pressure; pH = 10; V_{O_2} = 300 ml(NTP)/min; $[Glycerol]_{initial}$=0.03 M)

5.2.2 Glycerol oxidation over Au/γ-Al_2O_3 and AuPt/γ-Al_2O_3

Conversion

Glycerol conversion was obtained from the HPLC data. The concentration of glycerol and organic products in reaction samples could be calculated by multiplying peak areas by the calculated response factors. Figure 5.10 shows the glycerol conversion as a function of the

reaction time. The monometallic gold catalyst, Au_{100}, shows a conversion of ca. 34% after a reaction time of 10 minutes. The conversion of glycerol does not increase appreciably after this reaction time indicating severe and rapid deactivation of the catalyst. The bimetallic catalyst, $Au_{63}Pt_{37}$, shows after a reaction time of 10 minutes a slightly higher conversion of ca. 39 mol-%, which increases rather slowly to ca. 55 mol-% after 1 hr. The slow increase in the conversion followed by the initial high conversion indicates that this catalysts deactivated as well, but less severe than the monometallic gold catalyst. The bimetallic gold-platinum catalyst with the lowest gold loading, $Au_{28}Pt_{72}$, showed the lowest initial conversion of ca. 26 mol-% after a reaction time of 10 minutes. The conversion of glycerol increases steadily up to 30 minutes, after which the conversion only increases slightly, again indicating deactivation of the catalyst. It can also be seen that the 2 bimetallic catalysts reach final conversions that are very similar.

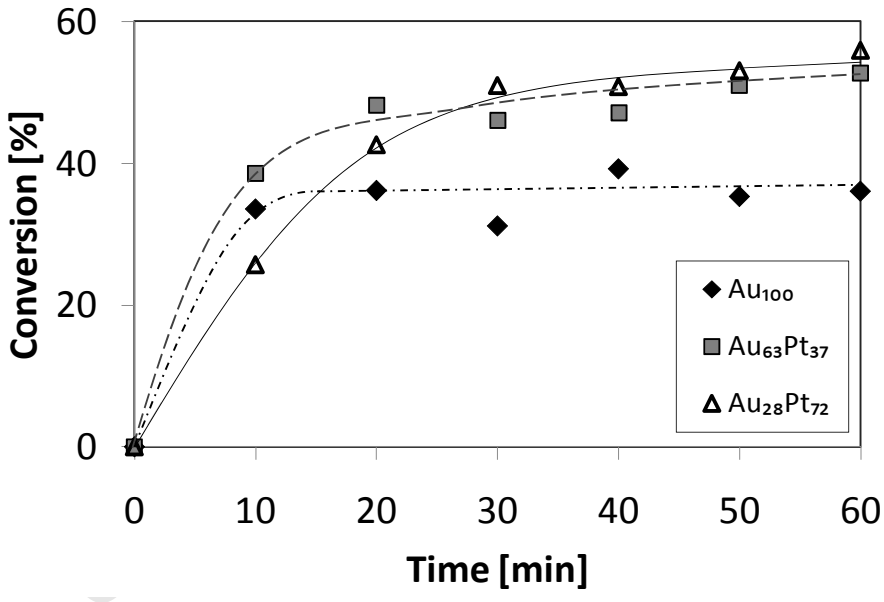

Figure 5.10: Conversion of glycerol as a function of reaction time

(T = 60°C; atmospheric pressure; pH = 10; V_{O_2} = 300 ml(NTP)/min; $[Glycerol]_{initial}$=0.03 M)

The deactivation behavior can be modeled by assuming a first order rate expression for the glycerol oxidation with respect to glycerol. This assumption is made based on the findings of Beltrame et al. (2006) where it was concluded that the oxidation of glucose in gold suspensions was first order with respect to glucose. The catalytic activity factor, a, can then be modeled as

$$\frac{da}{dt} = -k_d \cdot a^2$$

i.e

$$\frac{1-a}{a} = k_d \cdot t$$

And

$$-ln(1-X) = \frac{k}{k_d} \cdot ln(1 + k_d \cdot t)$$

The experimental date fit best to a second order deactivation model. It was shown by Fuentes & Gamas (1991) and Boskovic et al. (2004) that deactivation by sintering is represented by a first order process. A second order rate of deactivation is typical for deactivation by means of coking since certain areas of the catalyst is affected by the coking at a time. Pal et al. (1986) showed that the rate of deactivation of Pt-Re/Al_2O_3 catalysts by coking is best modeled by a second order rate law.

The data is not very well described as can be seen by the low regression coefficients (see Table 5.10). The fit is not great but if we plot the deactivation behavior of the bimetallic system as a function of the platinum content (see Figure 5.11), there appears to be a linear relationship between deactivation and the fraction of platinum in the catalyst. A higher platinum content relates to a slower rate of deactivation with a minimum deactivation at ca. 80 wt-% platinum (in the metal).

Table 5.10: Fitting parameters to the deactivation behaviour of catalysts with a 95% confidence interval as a function of platinum content

	Au_{100}	$Au_{63}Pt_{37}$	$Au_{28}Pt_{72}$
***k*, min^{-1}**	5.5 ± 0.18	0.7 ± 1.5	0.06 ± 0.04
***k_d*, min^{-1}**	102 ± 3.8	5.3 ± 14.3	0.15 ± 0.17
R^2	0.962	0.989	0.984
Variance	$8.3 \cdot 10^{-4}$	$4.1 \cdot 10^{-4}$	$7.6 \cdot 10^{-4}$

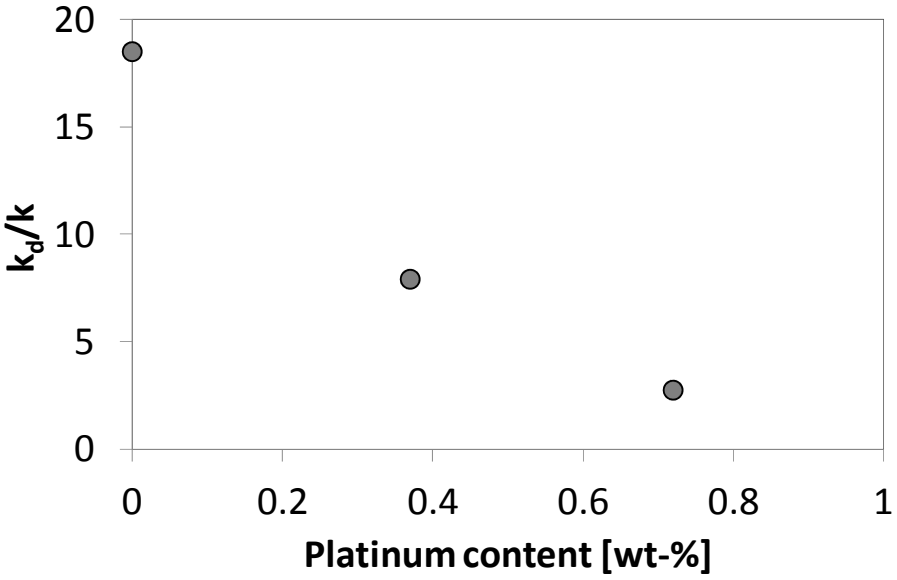

Figure 5.11: Deactivation behaviour of bimetallic Au-Pt catalysts as a function of platinum content

Selectivity

Four products were identified as the main products from the oxidation reaction over the AuPt catalysts. A carbon balance performed over the course of the reaction confirms this as can be seen in Figure 5.12. The missing carbon is less than 10% for both bimetallic catalysts. There is approximately 30% carbon unaccounted for with Au_{100}. Since no oxidation products could be identified from the HPLC analysis with standard solutions, the missing carbon is most likely coke. The bimetallic catalysts, having less gold and therefore a slower deactivation is not prone to the same degree of coke formation.

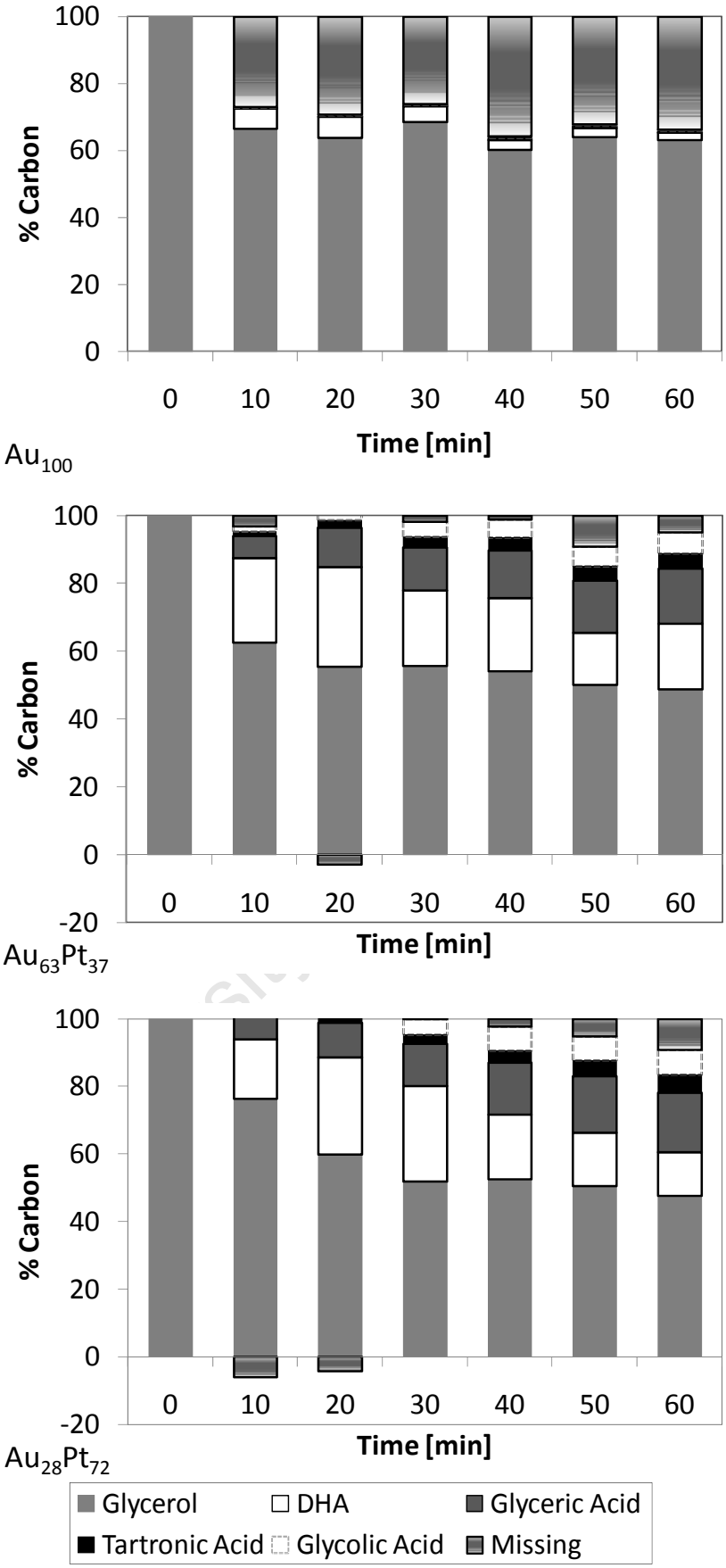

Figure 5.12: Carbon balance for Au_{100} (top), $Au_{63}Pt_{37}$ (middle) and $Au_{28}Pt_{72}$ (bottom) in the conversion of glycerol as a function of reaction time

(T = 60°C; atmospheric pressure; pH = 10; V_{O_2} = 300 ml(NTP)/min; $[Glycerol]_{initial}$=0.03 M)

The selectivity of a product was calculated as the moles of carbon that compound has relative to the total carbon of the products, including the missing carbon. Dihydroxyacetone was the main product observed in the oxidation of glycerol (see Figure 5.13). It should be noted that the low selectivity for dihydroxyacetone observed with the monometallic gold catalyst is caused by the large amount of coke obtained with this catalysts, thus substantiating the high rate of deactivation obtained with this catalyst (see above). The selectivity for dihydroxyacetone decreases gradually with time indicating the secondary conversion of dihydroxyacetone. Dihydroxyacetone is thought to form from the base catalysed tautomerisation of the primary oxidation product glyceraldehyde. However, it can be inferred by extrapolating the selectivity of dihydroxyacetone to a reaction time of 0 that other products (and in particular glyceric acid) is also formed as primary products in the oxidation of glycerol. This can be seen in Figure 5.14.

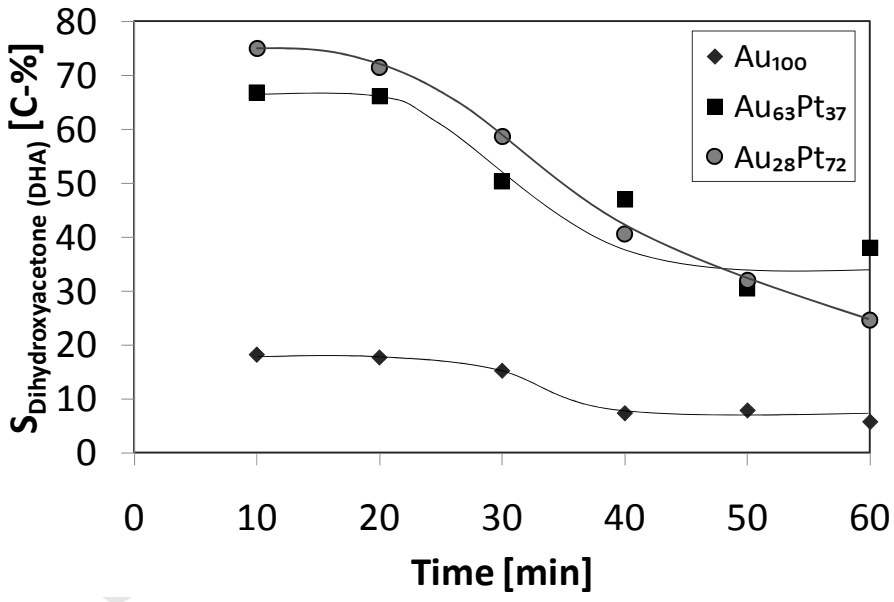

Figure 5.13: Selectivity to DHA in the oxidation of glycerol as a function of reaction time

(T = 60°C; atmospheric pressure; pH = 10; V_{O_2} = 300 ml(NTP)/min; $[Glycerol]_{initial}$=0.03 M)

Figure 5.14 shows the selectivity to glyceric acid (GA) and glycolic acid (GlyA). There appears to be a corresponding increase in glyceric acid with a decrease in DHA. Tartronic acid identified in the product samples was found to have a selectivity of less than 10% and is not shown in Figure 5.14. There is not much difference in the selectivity of these two products when comparing the bimetallic catalysts.

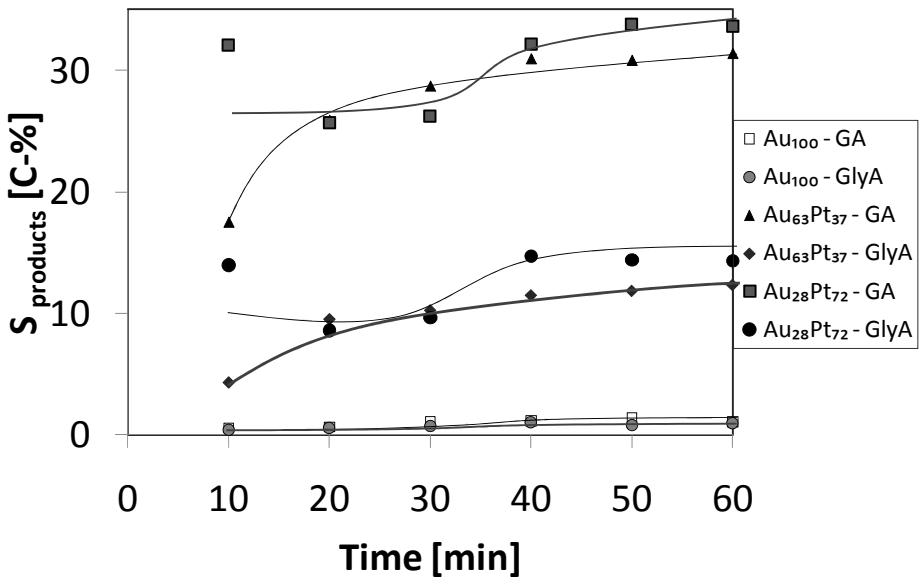

Figure 5.14: Selectivity to glyceric acid (GA) and glycolic acid (GlyA) in the oxidation of glycerol as a function of reaction time

(T = 60°C; atmospheric pressure; pH = 10; V_{O_2} = 300 ml(NTP)/min; $[Glycerol]_{initial}$=0.03 M)

5.2.3 Glycerol oxidation over Au/γ-Al_2O_3: Effect of initial glycerol concentration and pH

The results in this section were obtained from a study where the kinetics of the glycerol oxidation was investigated over γ-Al_2O_3 supported gold catalysts (data collected by Cheng et al., 2010). The catalyst used for the experiments was in fact Au_{100}, the same catalyst used in the current study.

Varying initial glycerol concentration

Experiments were performed with Au_{100} where the initial glycerol concentration in the system was varied. The other reaction parameters (temperature, pressure, oxygen flow and pH) were kept constant during these runs. Figure 5.15 shows the glycerol conversion as a function of reaction time at different initial glycerol concentrations.

With an increase in initial glycerol concentration there appears to be a decrease in the final conversion (after 1h) reached and also an increase in the rate of deactivation of the catalyst. At an initial glycerol concentration of 0.16 M a conversion of ca. 11% is reached after 10 minutes. There is a slow increase in conversion to ca. 27% after 1 hour. At the lowest initial glycerol concentration tested, 0.003M, a higher conversion of ca. 34% is reached after 10 minutes. With an increase in initial glycerol concentration there appears to be a decrease in the initial conversion after 10 minutes with a slow increase in conversion after 10 minutes. This slow decrease indicates deactivation of the catalyst after 10 minutes with a slower deactivation at lower initial glycerol concentrations.

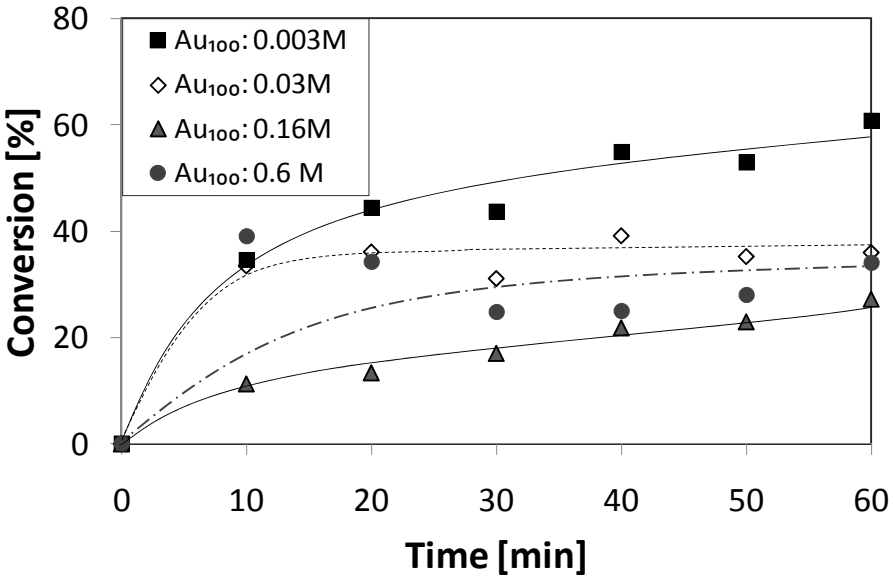

Figure 5.15: Conversion of glycerol as a function of reaction time, varying initial glycerol concentration

(Catalyst: Au_{100}; T = 60°C; atmospheric pressure; pH = 10; V_{O_2} = 300 ml(NTP)/min; $[Glycerol]_{initial}$=varied as shown in figure)

Figure 5.16 shows the selectivity to DHA and glyceric acid as a function of glycerol conversion when varying initial glycerol concentration. There is not much change in the DHA selectivity with respect to glycerol conversion. At an initial glycerol concentration of 0.6M there is no change in the DHA and glyceric acid selectivity with a change in glycerol conversion. The data point in the 0.6M data set that occurs at (25;41) can be considered an outlier since the increase in DHA selectivity from ca. 9% to ca. 41% at the same conversion of 25% and back down to ca. 7% is highly unlikely. Also, if DHA selectivity increases, glycerol conversion should increase (according to the reaction pathway) and this is not the case. At 0.16M initial glycerol concentration there appears to be a decrease in DHA selectivity from ca. 24% to ca. 10%. During this decrease the glycerol conversion only increases from ca. 11% to ca. 17%. This decrease in DHA selectivity is however not followed by an increase in glyceric acid selectivity, which remains the same at ca. 2% with the increase in glycerol conversion from ca. 11% to 27%. At the lowest initial glycerol concentration of 0.003M there is an increase in DHA selectivity from ca. 2% to 10% when the conversion increases from ca. 35% to 60%. Glyceric acid selectivity experiences a slight increase from ca. 2% to 5%. This initial glycerol concentration (0.003M) is the only one where a notable change in selectivity occurs as well as a significant change in glycerol conversion. This once again points toward rapid deactivation of the catalyst. It is seen that a higher rate of deactivation occurs at higher initial glycerol concentrations.

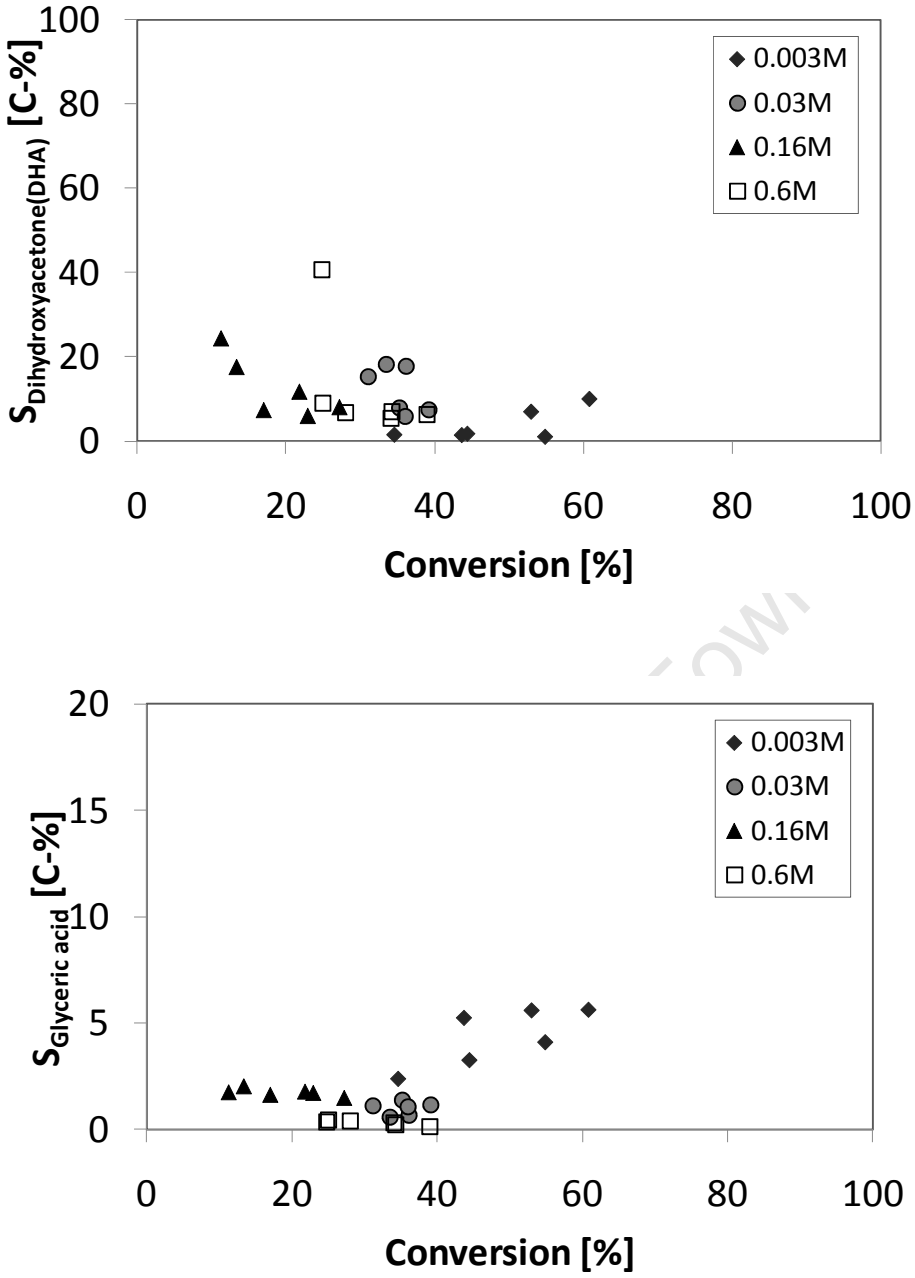

Figure 5.16: Selectivity to DHA (top) and Glyceric acid (bottom) in the conversion of glycerol as a function of glycerol conversion, varying initial glycerol concentration

(Catalyst: Au_{100}; T = 60°C; atmospheric pressure; pH = 10; VO_2 = 300 ml(NTP)/min; $[Glycerol]_{initial}$=varied as shown in figure)

We can also model the deactivation behaviour of the catalyst at the different initial glycerol concentrations by assuming a first order rate expression with respect to glycerol. The catalytic activity factor, a, can be modelled the same as was shown in Section 5.2.2.:

$$\frac{da}{dt} = -k_d \cdot a^2$$

i.e

$$\frac{1-a}{a} = k_d \cdot t$$

And

$$-ln(1-X) = \frac{k}{k_d} \cdot ln(1 + k_d \cdot t)$$

Table 5.11 shows the parameters obtained from non-linear regression of the data as a function of initial glycerol concentration. The data is not described very well by the data since the regression coefficients are not very large with a large negative value obtained at 0.16 M. A plot of the deactivation behaviour of the catalyst as a function of initial glycerol concentration is shown (see Figure 5.17). An initial glance at the data would lead to the conclusion that deactivation increases as the initial glycerol concentration increases. However, looking more carefully at the 95% confidence limits associated with the parameters, at 0.003 M the error is so large indicating a low reliability of that data point (for example, it is possible that k_d = 0.77 min^{-1} and k = 0.01 min^{-1} which would make k_d/k = 77). The error associated with the other points is fairly small so by excluding the data point at 0.003 M, it appears that the deactivation is constant over the range of concentrations. Deactivation is independent of the initial glycerol concentration. This implies that the deactivation behaviour does not depend on the concentration of glycerol in the bulk solution and that adsorption of glycerol on the catalyst surface is not a limiting factor.

Table 5.11: Fitting parameters to the deactivation behaviour of Au_{100} with a 95% confidence interval as a function of initial glycerol concentration

	0.003 M	0.03 M	0.16 M	0.6 M
***k*, min^{-1}**	0.09 ± 0.08	5.51 ± 0.18	0.05 ± 3.9·10^{-6}	4.65 ± 0.14
***k$_d$*, min^{-1}**	0.32 ± 0.45	102 ± 3.8	0.92 ± 9.1·10^{-5}	102 ± 3.5
R^2	0.979	0.962	-3.74	0.984
Variance	1.03·10^{-3}	8.3·10^{-4}	4.7·10^{-2}	7.6·10^{-4}

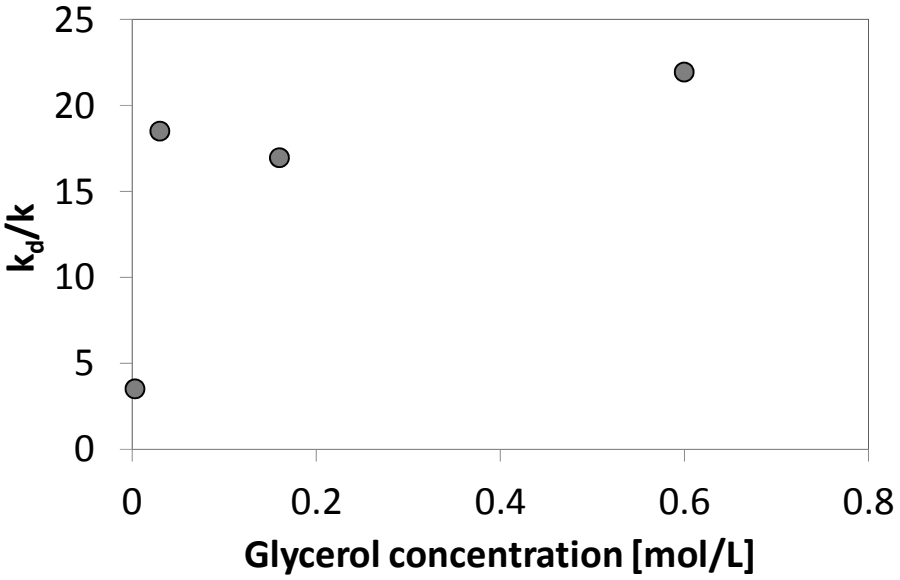

Figure 5.17: Deactivation behaviour of monometallic Au catalyst as a function of initial glycerol concentration

Varying pH

Glycerol oxidation experiments were performed with Au_{100} and the operating pH was varied with each run. Once again, deactivation of the catalyst is seen after ca. 10 minutes. After 10 minutes, for each of the runs performed at pH 7, 8, 9 and 10, the conversion remained fairly constant for the rest of the hour. The average conversion obtained is presented in Table 5.12. There is no significant effect on glycerol conversion with a change in operating pH. Table 5.12 also shows the selectivity to DHA and glyceric acid. The selectivity was taken as the average selectivity over the course of the reaction since there was no significant change in selectivity after 10 minutes. This can be seen in Figure 5.18 where the selectivity is given as a function of glycerol conversion. It is worth noting that whilst there is a strong deactivation of the catalyst after 10 minutes at each of the tested pH, the deactivation of the catalyst is not a strong function of the pH.

Table 5.12: Average glycerol conversion and selectivity to DHA and glyceric acid when varying operating pH [a]

pH	Average conversion [%]	DHA Selectivity [C-%]	Glyceric acid Selectivity [C-%]
7	43	33	1.45
8	45	33	0.36
9	43	23	1.27
10	35	12	0.98

a. Catalyst: Au_{100}; T = 60°C; atmospheric pressure; pH = varied as shown in table; V_{O_2} = 300 ml(NTP)/min; $[Glycerol]_{initial}$ = 0.03M; reaction time = 1 hour

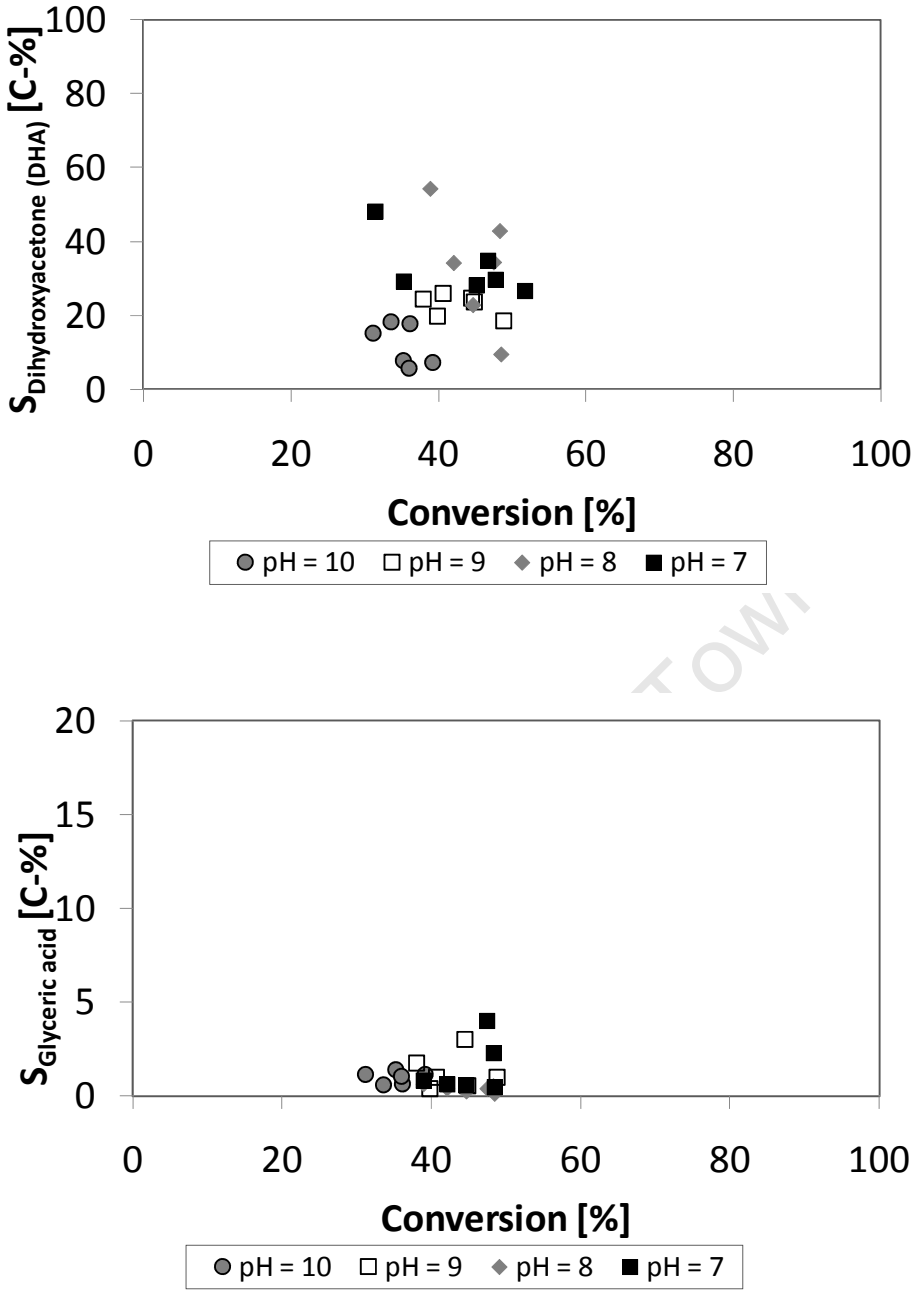

Figure 5.18: Selectivity to DHA (top) and Glyceric acid (bottom) in the conversion of glycerol as a function of glycerol conversion, varying operating pH

(Catalyst: Au_{100}; T = 60°C; atmospheric pressure; pH = varied as shown; V_{O_2} = 300 ml(NTP)/min; $[Glycerol]_{initial}$=0.03M)

Chapter 6. Discussion

6.1 Gold loading

The primary method used to determine Au loading on the prepared catalysts was AAS. Samples of the precursor solutions and filtrates were taken in order to determine the Au concentration. Acid digestion of the solid Au catalysts was performed to provide a gold solution which could be analysed by AAS to determine the Au concentration. It must be noted that these methods are subject to experimental error which is associated with the digestion and AAS analysis. These methods are subject to %RSD of 4-9%.

Gold was loaded on to the support via direct anionic exchange. The loading efficiency of gold on to alumina using direct anionic exchange from an aurochloric acid solution at pH of 5 ranged from 44-69%. The uptake of anionic gold complexes from the solution at pH of ca. 5 can be reasonable described using a Langmuir-isotherm (see Figure 6.1). The maximum amount of gold loaded on this support would then correspond to ca. 2.3 wt.-% corresponding to 0.54 Au atoms/nm^2, which is ca. 0.5 times the uptake reported for the uptake of $PtCl_6^{2-}$ on alumina (Regalbuto et al., 1999). This difference can be explained in terms of the differences in the geometry of the adsorbed complexes.

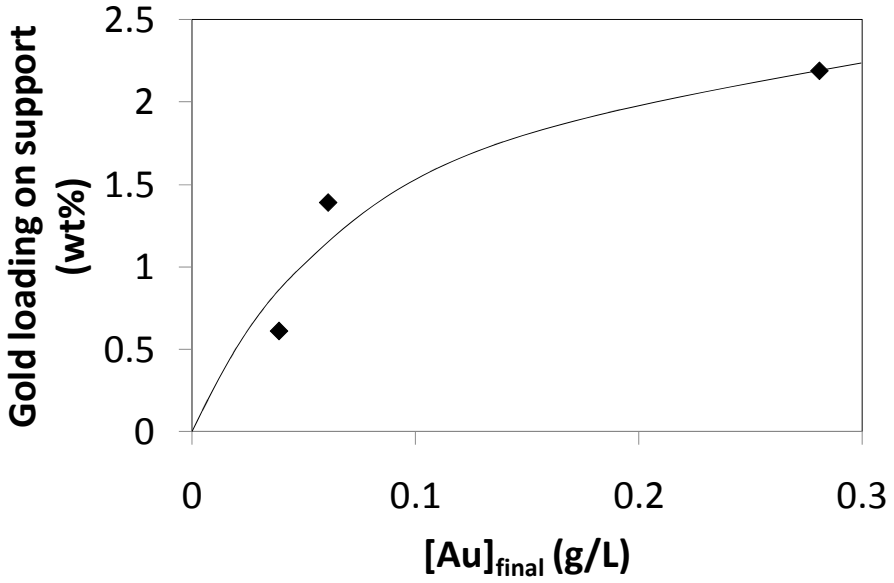

Figure 6.1: Uptake of gold from aurochloric acid solution by γ-Al_2O_3 at pH of 5 (solid line represents model fit to simple Langmuir isotherm)

6.2 Catalytic activity of monometallic and bimetallic catalysts

The oxidation of glycerol using oxygen was performed at a controlled temperature of 60°C and controlled pH of 10 at atmospheric pressure in a semi-batch glass reactor. Samples of the reaction mixture were taken every 10 minutes as the reaction was monitored for 1 hour. These samples were analysed by HPLC to determine the concentrations of glycerol and hence calculate conversion, as well as to identify and quantify the oxidation products and thereby determine selectivity. The concentration values obtained from HPLC data was used as the primary measurement of activity and selectivity of the catalysts. However, an initial measurement of activity was provided by the NaOH consumption data. If products are formed via the oxidation of glycerol\ according to the proposed reaction pathway (see Figure 2.3), the pH of the reaction solution will drop. Controlled pH was achieved with the use of an auto-titrator that measured the pH of the reaction solution and automatically added a corresponding amount of NaOH to bring the pH back up to the set point when the pH was recorded to have dropped, indicating the formation of organic acids. Figure 6.2 shows the consumption of NaOH for glycerol oxidation using the monometallic and bimetallic catalysts.

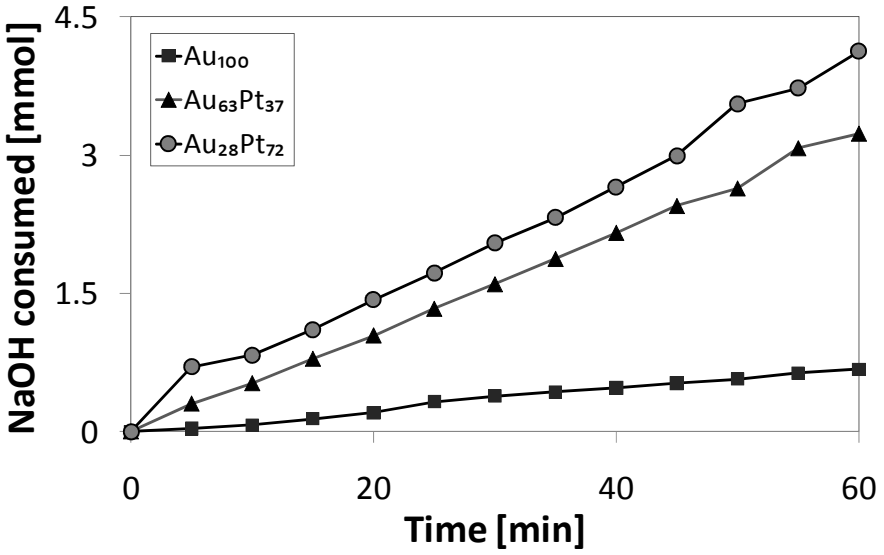

Figure 6.2: NaOH consumption for oxidatin of glycerol as a function of reaction time

(T = 60°C; atmospheric pressure; pH = 10; V_{O_2} = 300 ml(NTP)/min; $[Glycerol]_{initial}$=0.03M)

Each curve represents the average of three reproducible runs for each of the catalysts. A drop in pH was speculated to occur as a result of the formation of organic acids. So the consumption of NaOH could suggest which catalyst may be more active. In previous work (Case, 2009) the NaOH consumption data was the primary source of data to determine activity and selectivity in the oxidation of ethylene glycol with oxygen. In that case the

reaction pathway was straight forward with ethylene glycol forming glycolic acid upon oxidation. So, with every mole of NaOH consumed, 1 mol ethylene glycol is consumed and 1 mol sodium glycolate is formed (Case, 2009). In the present study however, the reaction pathway is not as simple since there is a possibility of parallel and series reactions occurring (see Figure 2.3). Therefore the NaOH consumption cannot be used as a reliable measure of activity and selectivity but only as an indication of reproducibility (see section 5.2.1) and as a check as to whether the catalyst is active or not.

Using the glycerol conversion (obtained from HPLC analysis) and loading data, the turnover frequency (TOF) can be calculated. The turnover frequency for the glycerol conversion (based on the total number of moles of metal in the reactor) of the alumina supported catalysts (see Table 6.1) are in the same range as those reported for Au supported on $MgAl_2O_4$ spinels (Villa et al., 2010), for Au-Pt on carbon (Dimitratos et al., 2006b), and for Au-Pd on carbon (Dimitratos et al., 2006a). It should further be noted that the average gold crystallite size in the monometallic gold catalyst was ca. 50% larger than that in the bimetallic gold-platinum catalysts. Hence, the turnover frequency expressed per surface gold atom decreases with increasing platinum content in the catalyst, if it can be assumed that the gold surface area is adequately represented by the average crystallite size of the gold crystallites detected by TEM.

Table 6.1: Average gold particle size and turnover frequency

Catalyst	d_{Au} [nm]	TOF [hr^{-1}] [a]
Au_{100}	4.2 ± 1.3	602
$Au_{63}Pt_{37}$	2.9 ± 1.0	685
$Au_{28}Pt_{72}$	2.8 ± 1.1	432

(T = 60°C; atmospheric pressure; pH = 10; V_{O_2} = 300 ml(NTP)/min; $[Glycerol]_{initial}$=0.03M)

a. Turn-over frequency based on the number of moles of glycerol converted after a reaction time of 10 min relative to the total number of moles of metal loaded in the reactor

Deactivation of the catalyst was noted after a reaction time of 10 minutes (see Figure 5.10). The deactivation in liquid phase reactions might be ascribed to sintering, leaching, metal oxidation, poisoning, or by formation of oligomeric/polymeric species (Besson et al., 2003). Leaching is typically observed via re-use of the spent catalyst and was observed for Au/CeO_2 (Demirel et al., 2007), although it is known that leaching from alumina support is more simplistic than from for example carbon support materials (Besson et al., 2000). Metal oxidation is not expected in noble metal catalysed oxidation reactions. Hence, possible mechanisms for catalyst deactivation are sintering, self-poisoning by product compounds and deposition of oligomeric species on the surface. The initially more active monometallic gold catalyst is more prone to deactivation than the bimetallic $Au_{63}Pt_{37}$-catalyst, which in turn deactivates faster than the bimetallic $Au_{28}Pt_{72}$-catalyst. The monometallic gold catalyst has

on average larger gold crystallites than the bimetallic Au-Pt catalysts. Hence, the monometallic gold catalyst is expected to deactivate least, if sintering (or leaching) is the dominant deactivation mechanism. Self-poisoning by product compounds due to "over-oxidation" (Besson et al., 2000) could be the cause of the observed deactivation order, since more active catalysts are then expected to deactivate faster. A carbon balance over the course of the reaction (see Figure 5.12) for each catalyst shows carbon unidentified by HPLC analysis, which is most likely coke. Self-poisoning of the catalyst due to the formation of coke explains why the initially more active monometallic catalyst is prone to a higher degree of deactivation than the bimetallic catalysts. The fact that the catalyst with a higher fraction of gold is subject to a greater degree of deactivation suggests that gold is predominantly responsible for the activity in the catalyst.

6.3 Selectivity

From the HPLC analysis of product samples, the selectivity to DHA, glyceric acid, tartronic acid and glycolic acid was determined. There appeared to be a greater selectivity to all the above mentioned products with the bimetallic catalyst as compared to monometallic gold. The lower selectivity of Au_{100} is related to the possibility of larger amounts of coke formed. Contrary to the literature presented (C. Bianchi et al., 2005; Demirel, Lehnert, et al., 2007), there is no significant difference between the observed conversion and selectivity when comparing the two bimetallic catalysts.

6.4 Initial glycerol concentration and pH

6.4.1 Initial glycerol concentration

No previous research has been performed regarding the initial concentration of glycerol in the oxidation of glycerol over supported Au catalysts. Glucose oxidation data shows that increasing the initial glucose concentration by a factor of 10 results in a rate ($mol.L^{-1}.h^{-1}$) that is approximately 1.5 times greater at both 30°C and 60°C (Beltrame et al., 2006). Using the HPLC data, we calculate the TOF at the different initial glycerol concentrations as shown in Table 6.2. The initial rate of reaction increases with an increase in initial glycerol concentration as can be seen from the table. An increase in concentration by a factor of 10 results in an initial rate ca. 13 times greater. This indicates that the initial rate of reaction is proportional to the initial glycerol concentration to the power 1. The TOF also increases by a factor of 10 when the initial glycerol concentration is increased by a factor of 10. This may indicate a reaction order of 1 but one has to be very careful since the glycerol concentration does not really change after 10 minutes and it is uncertain as to what happens in the first 10 minutes of the reaction.

Table 6.2: Turnover frequency at different initial glycerol concentrations

Initial glycerol concentration [mol/L]	TOF [hr^{-1}] [a]	r_0 [$mol.L^{-1}.h^{-1}$] [b]
0.003	59	0.01
0.03	598	0.13
0.16	970	0.87
0.6	6092	2.30

(T = 60°C; atmospheric pressure; pH = 10; V_{O_2} = 300 ml(NTP)/min; $[Glycerol]_{initial}$=varied as shown)

a. Turn-over frequency based on the number of moles of glycerol converted after a reaction time of 10 min relative to the total number of moles of gold loaded in the reactor

b. Initial rate calculated after 10 minutes

Whilst there is a larger initial rate at the higher initial glycerol concentrations there is an inverse relationship between conversion and initial glycerol concentration (see Figure 5.15). There is not much change in dihydroxyacetone selectivity with a change in initial glycerol concentration and the highest selectivity to glyceric acid is observed at the lowest initial glycerol concentration of 0.003 M (see Figure 5.16). Since selectivity is an important consideration it is better to run the reaction by starting with a lower initial glycerol concentration. This could also lower the rate of coke formation on the monometallic catalyst and subsequently, the rate of deactivation.

6.4.2 pH

The conversion of glycerol was not significantly affected by a change in operating pH. In fact, a higher average conversion was achieved at a pH of 7 than a pH of 10. According to HPLC analysis of product samples, the highest selectivity to glyceric acid was achieved at a pH of 7. This indicates that a high pH is not necessary for a reaction to occur. Since the presence of OH^- ions is necessary for the oxidation reaction to occur it is important that the reaction is not run at too low pH (i.e. below 7) and that careful control of the pH is maintained during the course of the reaction. Running the reaction at pH below 10 would also result in a lower rate of dissolution of the alumina support (see Figure 2.8, where a minimum rate of dissolution is found between pH 5.5 and 8) and therefore a longer catalyst life.

It is however interesting to note that the pH of the reaction mixture drops during the course of the reaction. This is assumed to be due to the formation of organic acids as the reaction proceeds. NaOH is added to the reactor vessel during the course of the reaction to control the pH of the reaction. From the addition of NaOH (see Figure 6.3) one would think that at a higher pH a higher glycerol conversion is achieved, since more NaOH is being added over the course of the reaction. However, as mentioned above, conversion of glycerol is independent of pH therefore the increase in NaOH consumption at higher pH is more likely

due to the fact that there is alumina dissolution occurring at higher pH (refer to Figure 2.8). The dissolution of alumina will cause a decrease in pH which is noted by the auto-titrator and thus more NaOH is added.

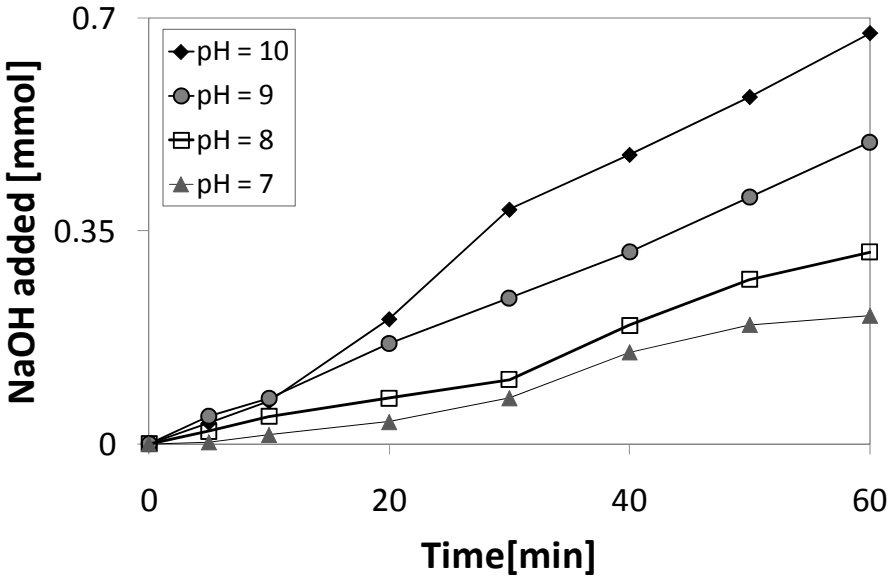

Figure 6.3: NaOH consumption in the conversion of glycerol as a function of reaction time

(Catalyst: Au_{100}; T = 60°C; atmospheric pressure; pH = varied as shown; V_{O_2} = 300 ml(NTP)/min; $[Glycerol]_{initial}$=0.03M)

Chapter 7. Conclusions

This study focuses on an alternative, environmentally friendly way of producing useful chemicals from a renewable source, i.e. the heterogeneously catalysed oxidation of glycerol performed under atmospheric pressure and mild temperature and controlled pH conditions with oxygen as the oxidising agent. Alumina supported gold catalysts were prepared by anionic ion exchange and some impregnated with platinum. The gold loading on the catalysts prepared by ion exchange was determined by atomic absorption spectroscopy. Platinum was then impregnated on the catalysts with a lower gold loading to achieve a total metal loading equal to the highest gold loading. TEM images were obtained and analysed to obtain average gold crystallite size. The activity and selectivity in the oxidation reaction of the monometallic gold catalyst was compared to that of the bimetallic gold-platinum catalysts by testing the catalysts in the liquid phase oxidation of glycerol.

The bimetallic catalysts achieve a 20% higher conversion in the oxidation reaction as compared to monometallic gold. The main products achieved with the bimetallic catalysts were dihydroxyacetone, glyceric acid, glycolic acid and tartronic acid. These products, together with the unconverted glycerol, make up 90% of the carbon in the system. For monometallic gold, the unconverted glycerol and the above four products identified make up only 70% of the total carbon in the system, indicating the possible formation of coke. The bimetallic catalysts displayed a greater selectivity to dihydroxyacetone, glyceric acid and glycolic acid as compared to monometallic gold. No significant activity was observed with the monometallic gold catalyst beyond 10 minutes and the glycerol conversion stayed constant, indicating deactivation of the catalyst. The bimetallic catalysts displayed a slower rate of deactivation and the carbon balance confirmed that it is likely that less coke was formed. In the catalysts investigated it was found that the fraction of platinum in the bimetallic catalyst has no significant effect on conversion and selectivity. However, the rate of deactivation of the catalyst decrease with an increase in platinum content with the lowest deactivation observed at ca. 80 wt-% platinum.

Increasing the pH of the reaction is not advantageous in terms of glycerol conversion, glyceric acid selectivity and catalyst life. Glycerol conversion and glyceric acid selectivity is seen to be greatest at a pH of between 7 and 8. Minimum support dissolution occurs at pH

of between 5.5 and 8, however the presence of a base is necessary for any reaction to occur so pH below 7 is not feasible.

For the different initial concentrations tested (0.003M, 0.03M, 0.16M, 0.6M), a greater conversion and selectivity to glyceric acid is achieved at the lowest initial glycerol concentration of 0.003 M. A larger initial rate and activity is observed at higher initial glycerol concentrations but this is to the detriment of the catalyst since this is also coupled with more coke formation and a higher rate of deactivation.

Reproducibility in catalytic testing was investigated by monitoring the addition of NaOH during the course of the reaction. A satisfactory level of reproducibility in the different runs was achieved. The auto-titrator used was very sensitive to mechanical disturbances in the system so reproducibility is still subject to operator influence.

Chapter 8. Bibliography

Beltrame, P., Comotti, M., Della, C. and Rossi, M. (2004), Aerobic oxidation of glucose I . Enzymatic catalysis. *Journal of Catalysis*, 228: 282-287.

Beltrame, P., Comotti, M., Della, M. and Rossi, M. (2006), Aerobic oxidation of glucose II . Catalysis by colloidal gold. , 297: 1-7.

Besson, M. and Gallezot, P. (2000), Selective oxidation of alcohols and aldehydes on metal catalysts. *Catalysis Today*, 57: 127-141.

Besson, M. and Gallezot, P. (2003), Deactivation of metal catalysts in liquid phase organic reactions. *Catalysis Today*, 81(4): 547-559.

Betowska-Brzezinska, M., Uczak, T. and Holze, R. (1997), Electrocatalytic oxidation of mono- and polyhydric alcohols on gold and platinum. *Journal of Applied Electrochemistry*, 27(46): 999-1011.

Bianchi, C., Porta, F., Prati, L. and Rossi, M. (2000), Selective liquid phase oxidation using gold catalysts. *Topics in Catalysis*, 13: 231-236.

Bianchi, C., Canton, P., Dimitratos, N., Porta, F. and Prati, L. (2005), Selective oxidation of glycerol with oxygen using mono and bimetallic catalysts based on Au , Pd and Pt metals. *Catalysis Today*, 103: 203-212.

Biella, S., Prati, L., Rossi, M. (2002), Selective oxidation of D-glucose on gold catalyst. *Journal of Catalysis*, 206: 242-247

Bond, G. C and Thompson, D. T. (1999), Catalysis by Gold. *Catalysis Reviews: Science and Engineering*, 41(3): 319-388.

Bond, G. C, Louis, C. and Thompson, D. T. (2006), *Catalysis by Gold* (G. J. Hutchings, Ed.). London: Imperial College Press.

Boronat, M., Corma, A., Illas, F., Radilla, J., Ródenas, T. and Sabater, M. J. (2011), Mechanism of selective alcohol oxidation to aldehydes on gold catalysts: Influence of surface roughness on reactivity. *Journal of Catalysis*, 278(1): 50-58.

Boskovic, G., Dropka, N., Wolf, D., Brükner, A., Baerns, M. (2004), Deactivation kinetics of Al/Al_2O_3 catalyst for ethylene epoxidation. *Journal of Catalysis*, 226: 334-342.

Brunelle, J. P. (1978), Preparation of catalysts by metallic complex adsorption on mineral oxides. *Pure and Applied Chemistry*, 50: 1211-1229.

Carrettin, S., Mcmorn, P., Johnston, P., Griffin, K. and Hutchings, G. J. (2002), Selective oxidation of glycerol to glyceric acid using a gold catalyst in aqueous sodium hydroxide. *Chemical Communication*: 696-697.

Carrettin, S., Mcmorn, P., Johnston, P., Griffin, K., Kiely, J. and Hutchings, G. J. (2003), Oxidation of glycerol using supported Pt , Pd and Au catalysts. *Physical Chemistry Chemical Physics*, 5: 1329-1336.

Carrettin, S., Mcmorn, P., Johnston, P., Griffin, K., Kiely, C. J., Attard, G. A. and Hutchings, G. J. (2004), Oxidation of glycerol using supported gold catalysts. *Topics in Catalysis*, 27(1-4): 131-136.

Carrier, X., Marceau, E., Lambert, J-F., Che, M. (2007), Transformations of □-alumina in aqueous suspensions 1. Alumina chemical weathering studied as a function of pH. *Journal of Colloid and Interface Science*, 308: 429-437.

Case, J. M. (2009), Gold catalysts prepared by ion exchange for use in ethylene glycol oxidation: An exploratory study, *Masters Thesis*. University of Cape Town: Department of Chemical Engineering, 1-70.

Cheng, Y. and O'Carroll, S. (2010), An investigation into the kinetics of glycerol oxidation over a supported gold catalysts, *BSc(Eng) Thesis*, University of Cape Town (unpublished), 1-80.

Comotti, M., Pina, C. D. and Rossi, M. (2006), Mono- and bimetallic catalysts for glucose oxidation. *Journal of Molecular Catalysis A: Chemical*, 251: 89-92.

Demirel, S., Kern, P., Lucas, M. and Claus, P. (2007a), Oxidation of mono- and polyalcohols with gold: Comparison of carbon and ceria supported catalysts. *Catalysis Today*, 122: 292-300.

Demirel, S., Lehnert, K., Lucas, M. and Claus, P. (2007b), Use of renewables for the production of chemicals: Glycerol oxidation over carbon supported gold catalysts. *Applied Catalysis*, 70: 637-643.

Demirel, S., Lucas, M., Wärnå, J., Salmi, T., Murzin, D. and Claus, P. (2007c), Reaction kinetics and modelling of the gold catalysed glycerol oxidation. *Topics in Catalysis*, 44: 1-7.

Demirel-Gülen, S., Lucas, M. and Claus, P. (2005), Liquid phase oxidation of glycerol over carbon supported gold catalysts. *Catalysis Today*, 103: 166-172.

Dimitratos, N., Porta, F. and Prati, L. (2005), Au , Pd (mono and bimetallic) catalysts supported on graphite using the immobilisation method synthesis and catalytic testing for liquid phase oxidation of glycerol. *Applied Catalysis*, 291: 210-214.

Dimitratos, N., Lopez-Sanchez, J. A., Lennon, D., Porta, F., Prati, L. and Villa, A. (2006a), Effect of particle size on monometallic and bimetallic (Au,Pd)/C on the liquid phase oxidation of glycerol. *Catalysis Letters*, 108(3-4): 147-153.

Dimitratos, N., Messi, C., Porta, F., Prati, L. and Villa, A. (2006b), Investigation on the behaviour of Pt(0)/carbon and Pt(0),Au(0)/carbon catalysts employed in the oxidation of glycerol with molecular oxygen in water. *Journal of Molecular Catalysis A: Chemical*, 256: 21-28.

Dimitratos, N., Lopez-Sanchez, J. A.,, Anthonykutty, M., Brett, G., Carley, A. F., Tiruvalam, C., Herzing, A. A., Kiely, C. J., Knight, W. and Hutchings, G. J. (2009a), Oxidation of glycerol

using gold – palladium alloy-supported nanocrystals. *Physical Chemistry Chemical Physics*, 11(25).

Dimitratos, N., Villa, A. and Prati, L. (2009b), Liquid phase oxidation of glycerol using a single phase (Au-Pd) alloy supported on activated carbon: effect of reaction conditions. *Catalysis Letters*, 133: 334-340.

Euzen, P., Raybaud, P., Krokidis, X., Toulhoat, H., Le Loarer, J-L., Jolivet, J-P. and Froidefond, C. (2000), 1591 (Schüth, F., Sing, K. S. W. and Weitkamp, J. (Eds.)), *Handbook of Porous Solids, Volume 3*. Weinheim: Wiley-VCH.

Fuentes, G. A., Gamas, E. D. (1991), Towards a better understanding of sintering phenomena in catalysis. *Studies in Surface Science and Catalysis*, 68: 637-644.

Gates, B. C. (2001), Catalysis, 2401 (Spencer, N. D. and Moore, J. H. (Eds.)), *Encyclopedia of Chemical Physics and Physical Chemistry, Volume 3*. London: The Institute of Physics.

Haruta, M., Kobayashi, T., Sano, H. and Yamada, N. (1987), Novel gold catalysts for the oxidation of carbon monoxide at a temperature far below 0°C. *Catalysis Letters*: 405-408.

Haruta, M., Yamada, N., Kobayashi, T. and Iijima, J. (1989), gold catalysts prepared by coprecipitation for low-temperature oxidation of hydrogen and of carbon monoxide. *Journal of Catalysis*, 115(2): 301-309.

Haruta, M. (2004), Gold as a novel catalyst in the 21st century: Preparation , working mechanism and applications. *Gold Bulletin*: 27-36.

Hughes, M. D., Xu, Y., Jenkins, P., Mcmorn, P., Landon, P., Enache, D. I., Carley, A. F., Attard, G. A., Hutchings, G. J., King, F., Stitt, E. H., Johnston, P., Griffin, K. and Kiely, C. J. (2005), Tunable gold catalysts for selective hydrocarbon oxidation under mild conditions. *Nature Letters*, 437: 1132-1135.

Hutchings, G. J. and Vedrine, J. C. (2004), Preparation of supported catalysts, 229-231, (Baerns, M. (Ed.)), *Basic Principles in Applied Catalysis*. Germany: Springer.

Hutchings, G. J., Carrettin, S., Landon, Philip, Edwards, Jennifer K, Enache, Dan, Knight, David W, Xu, Yi-jin and Carley, Albert F (2006), New approaches to designing selective oxidation catalysts: Au/C a versatile catalyst. *Topics in Catalysis*, 38(4): 0-7.

Ivanova, S., Petit, C. and Pitchon, V. (2004), A new preparation method for the formation of gold nanoparticles on an oxide support. *Applied Catalysis*, 267: 191-201.

Ivanova, S., Pitchon, V. and Petit, C. (2006), Application of the direct exchange method in the preparation of gold catalysts supported on different oxide materials. *Journal of Molecular Catalysis*, 256: 278-283.

Kenar, J. A. (2007), Glycerol as a platform chemical: Sweet opportunities on the horizon?*. *Lipid Technology*, 19(11): 249-253.

Ketchie, W. C., Murayama, M. and Davis, R. J. (2007a), promotional effect of hydroxyl on the aqueous phase oxidation of carbon monoxide and glycerol over supported Au catalysts. *Topics in Catalysis*, 44: 307-317.

Ketchie, W. C, Murayama, Mitsuhiro and Davis, R. J. (2007b), Selective oxidation of glycerol over carbon-supported AuPd catalysts. *Topics in Catalysis*, 250: 264-273.

Ketchie, W. C, Fang, Y., Wong, M. S., Murayama, M. and Davis, R. J. (2007c), Influence of gold particle size on the aqueous-phase oxidation of carbon monoxide and glycerol. *Journal of Catalysis*, 250: 94-101.

Kitchin, J., Nørskov, J., Barteau, M. and Chen, J. (2004), Role of strain and ligand effects in the modification of the electronic and chemical properties of bimetallic surfaces. *Physical Review Letters*, 93(15): 4-7.

Knowles, W. V., Nutt, M. O. and Wong, M. S. (2007), Supported metal oxides and the surface density metric, 251-254, (Regalbuto, John (Ed.)), *Catalyst Preparation: Science and Engineering*. Boca Raton: CRC Press.

Luo, J., Maye, M. M., Kariuki, N. N., Wang, L., Njoki, P., Lin, Y., Schadt, M., Naslund, H. R. and Zhong, C. (2005a), electrocatalytic oxidation of methanol: carbon-supported gold – platinum nanoparticle catalysts prepared by two-phase protocol. *New York*, 99: 291-297.

Luo, J, Maye, M. M, Petkov, V., Kariuki, N. N., Wang, L., Njoki, P., Mott, D., Lin, Y. and Zhong, C. (2005b), Phase properties of carbon-supported gold-platinum nanoparticles with different bimetallic compositions. *Chemistry of Materials*, (9): 3086-3091.

Ma, F., Hanna, M.A. (1999), Biodiesel production: a review. *Bioresource Technology*, 70: 1-15.

Mallat, T. and Baiker, A. (1994), Oxidation of alcohols with molecular oxygen on platinum metal catalysts in aqueous solutions. *Catalysis Today*, (19): 247-284.

Mallat, T. and Baiker, A. (2004), Oxidation of alcohols with molecular oxygen on solid catalysts. *Chemical Reviews*, 104: 3037-3058.

Mihut, C., Descorme, C., Duprez, D. and Amiridis, M. D. (2002), Kinetic and spectroscopic characterization of cluster-derived supported Pt – Au catalysts. *Journal of Catalysis*, 135: 125-135.

Morrison, L.R. (2000), Glycerol. in "Kirk Othmer Encyclopedia of Chemical Technology", Wiley & Sons, New York.

Mott, D., Luo, J., Njoki, P. N., Lin, Y., Wang, L. and Zhong, C. (2007), Synergistic activity of gold-platinum alloy nanoparticle catalysts. *Catalysis Today*, 122: 378-385.

Mott, N.F. and Jones, H. (1936), *Theories of the Properties of Metals and Alloys*. London: Oxford University Press.

Oh, H. S., Yang, J. H., Costello, C. K., Wang, Y. M., Bare, S. R., Kung, H. H. and Kung, M. C. (2002), Selective catalytic oxidation of CO: Effect of chloride on supported Au catalysts. *Journal of Catalysis*, 386(210): 375-386.

Pal, A. K., Bhowmick, M., Srivastava, R. D. (1986), Deactivation kinetics of platinum-rhenium reforming catalyst accompanying the dehydrogenation of methylcyclohexane. *Industrial & Engineering Chemistry Process Design and Development*, 25: 236-241.

Panias, D., Asimidis, P., Paspaliaris, I. (2007), Solubility of boehmite in concentrated sodium hydroxide solutions: model development and assessment. *Hydrometallurgy*, 59: 15-29

Phala, N. S., Klatt, G., van Steen E. (2004), A DFT study of hydrogen and carbon monoxide chemisorption onto small gold clusters. *Chemical Physics Letters*, 395: 33-37.

Ponec, V. and Bond, G. C. (1995), *Catalysis by Metals and Alloys*. Amsterdam: Elsevier.

Porta, F. and Prati, L. (2004), Selective oxidation of glycerol to sodium glycerate with gold-on-carbon catalyst: An insight into reaction selectivity. *Journal of Catalysis*, 224: 397-403.

Prati, L. and Martra, G. (1999), New gold catalysts for liquid phase oxidation. *Gold Bulletin (Switzerland),* 32: 96-101

Prati, L. and Rossi, M. (1997), Chemoselective catalytic oxidation of polyols with dioxygen on gold supported catalysts. *Studies in Surface Science and Catalysis*, 110: 509-516.

Prati, L. and Rossi, M. (1998), Gold on carbon as a new catalyst for selective liquid phase oxidation of diols. *Journal of Catalysis*, 560: 552-560.

Prati, L., Villa, A., Porta, F., Wang, D. and Su, D. (2007), Single-phase gold/palladium catalyst: The nature of synergistic effect. *Catalysis Today*, 122: 386-390.

Prati, Laura, Spontoni, Paolo and Gaiassi, Aureliano (2009), From renewable to fine chemicals through selective oxidation: The case of glycerol. *Topics in Catalysis*: 288-296.

Regalbuto, J., Navada, A., Shadid, S., Bricker, M.L. and Chen, Q. (1999), An experimental verification of the physical nature of Pt adsorption onto alumina. *Journal of Catalysis*, 184(2): 335-348.

Rodriguez-Reinoso, F. and Sepulveda-Escribano, A. (2009), Preparation of carbon supported catalysts, 137-139, (Serp, P. and Figueiredo, J. L. (Eds.)), *Carbon Materials for Catalysis*. Canada: John Wiley & Sons.

Ruffino, F., Grimaldi, M., Giannazzo, F., Roccaforte, F. and Raineri, V. (2008), Thermodynamic properties of supported and embedded metallic nanocrystals: Gold on/in SiO_2. *Nanoscale research letters*, 3(11): 454-460.

Schwank, J. (1985), Gold in Bimetallic Catalysts. *Gold Bulletin*, 18(1): 2-10.

Sinfelt, J. H. (1977), Catalysis by alloys and bimetallic clusters. *Accounts of Chemical Research*, 10(1): 15-20.

Sluiter, M., Colinet, C. and Pasturel, A. (2006), Ab Initio calculation of the phase stability in Au-Pd and Ag-Pt alloys. *Physical Review B*, 73(17): 1-17.

van Steen, Eric (2010), Thermodynamic analysis of peroxide formation in oxidation of organic alcohols. University of Cape Town: Department of Chemical Engineering.

Stull, D. R., Westrum, E. F. and Sinke, G. C. (1969), *The Chemical Thermodynamics of Organic Compounds*. New York: John Wiley & Sons.

Van Dam, H. E., Kieboom, A. P. G., Van Bekkum, H. (1987), Pt/C oxidation catalysts. Part 1. Effect of carrier structure on catalyst deactivation during the oxidation of glucose 1-phosphate into glucuronic acid 1-phosphate. *Applied Catalysis*, 33: 361-372.

Villa, A., Janjic, N., Spontoni, P., Wang, D., Sheng, D. and Prati, L. (2009), Au–Pd/AC as catalysts for alcohol oxidation: Effect of reaction parameters on catalytic activity and selectivity. *Applied Catalysis A: General*, 364: 221-228.

Villa, A., Chan-Thaw, C. E. and Prati, L. (2010a), Au NPs on anionic-exchange resin as catalyst for polyols oxidation in batch and fixed bed reactor. *Applied Catalysis B: Environmental*, 96(3-4): 541-547.

Villa, A., Gaiassi, A., Rossetti, I., Bianchi, C. L., van Benthem, K., Veith, G. M. and Prati, L. (2010b), Au on $MgAl_2O_4$ spinels: The effect of support surface properties in glycerol oxidation. *Journal of Catalysis*, 275(1): 108-116.

Villa, A., Wang, D., Su, D., Veith, M. and Prati, L. (2010c), Using supported Au nanoparticles as starting material for preparing uniform Au/Pd bimetallic catalysts. *Physical Chemistry Chemical Physics*, 12: 2183-2189.

Wang, D., Villa, A., Porta, F., Prati, L. and Su, D. (2008), Bimetallic gold / palladium catalysts: Correlation Between nanostructure and synergistic effects. *Journal of Physical Chemistry*, 112: 8617-8622.

Wörz, N., Brandner, A. and Claus, P. (2010), Platinum-Bismuth catalyzed oxidation of glycerol: Kinetics and the origin of selective deactivation. *Journal of Physical Chemistry*, 114: 1164-1172.

Xu, X.N., Qin, G.W., Ren, Y.P., Shen, B. and Pei, W.L. (2009), Experimental study of the miscibility gap and calculation of the spinodal curves of the Au–Pt system. *Scripta Materialia*, 61(9): 859-862.

Zhou, C. H., Beltramini, J. N., Fan, Y. X., Lu, G. Q. (2008), Chemoselective catalytic conversion of glycerol as a biorenewable source to valuable commodity chemicals. *Chemical Society Reviews*, 37: 527-549.

Zope, B. N., Hibbitts, D. D., Neurock, M., Davis, R. J. (2010), Reactivity of the gold/water interface during selective oxidation catalysis. *Science*, 330: 74-78.

Appendix I

HPLC Calibration Curves

I. Glycerol

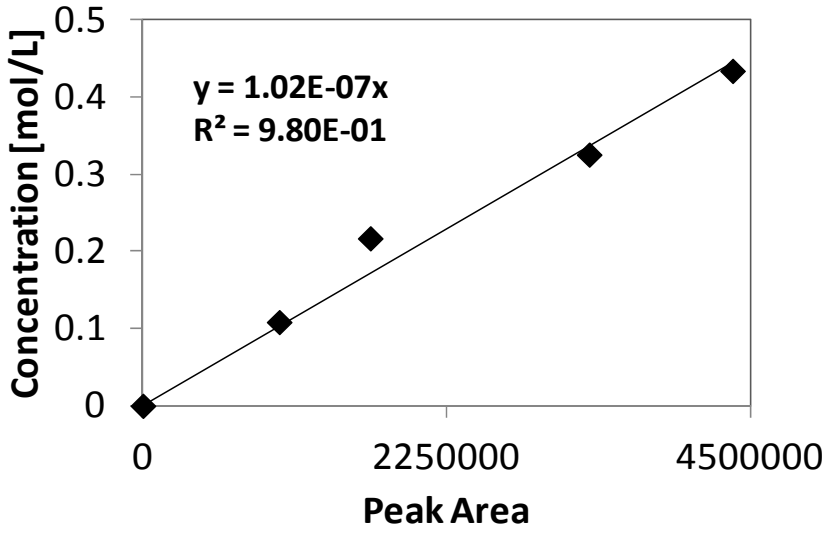

Figure 8.1: Glycerol calibration curve

II. Dihydroxyacetone

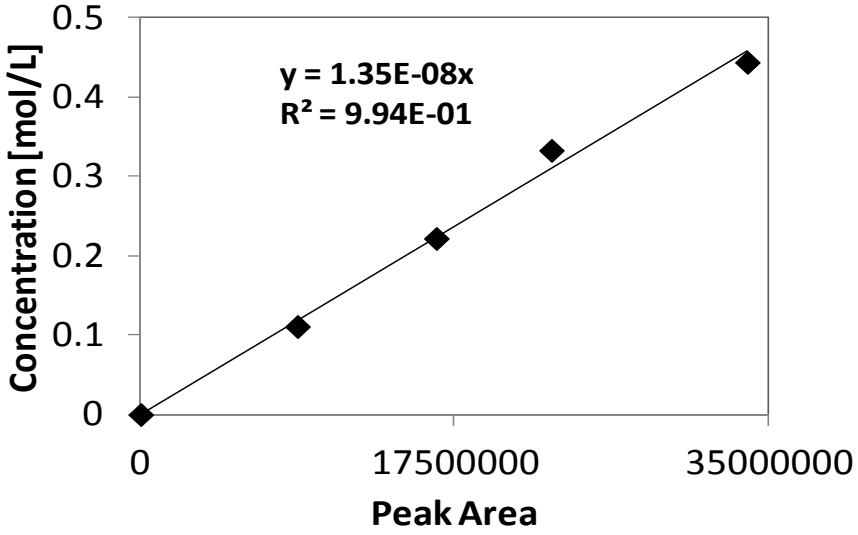

Figure 8.2: Dihydroxyacetone calibration curve

III. Glyceric acid

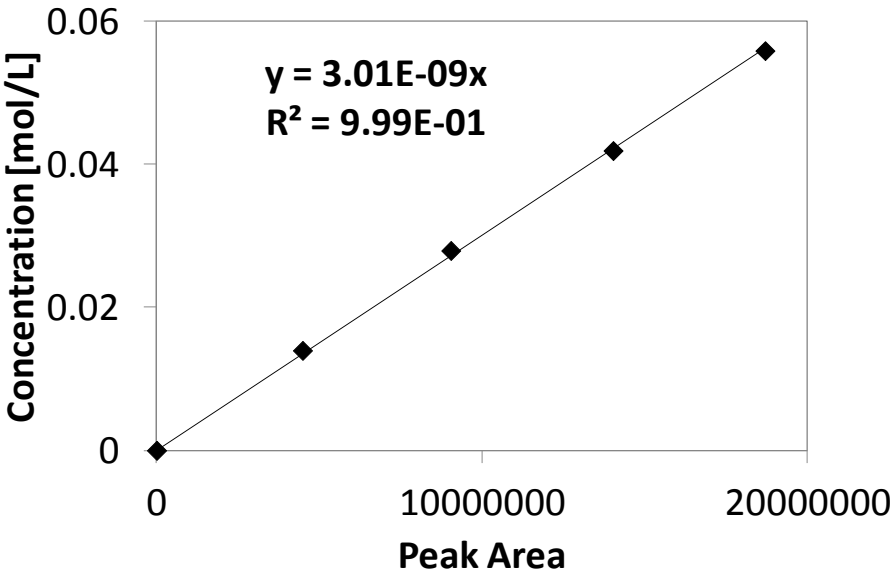

Figure 8.3: Glyceric acid calibration curve

IV. Glycolic acid

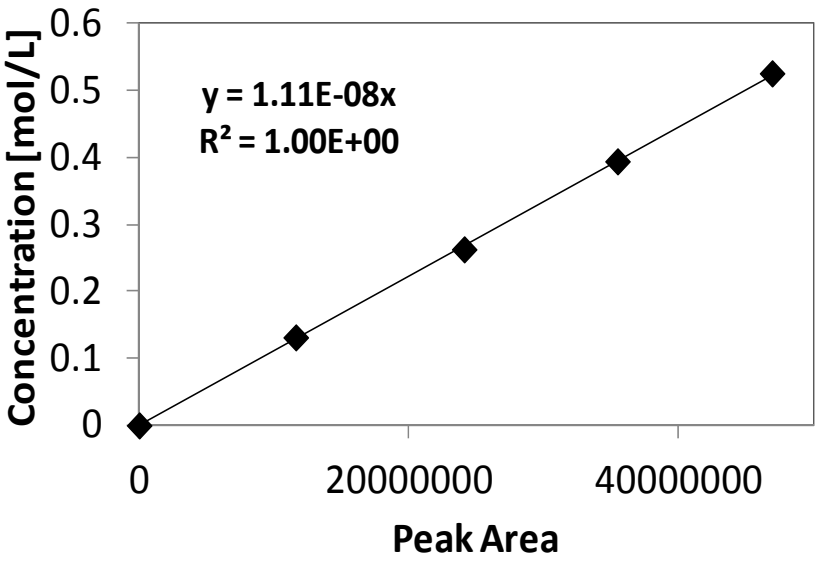

Figure 8.4: Glycolic acid calibration curve

V. Tartronic acid

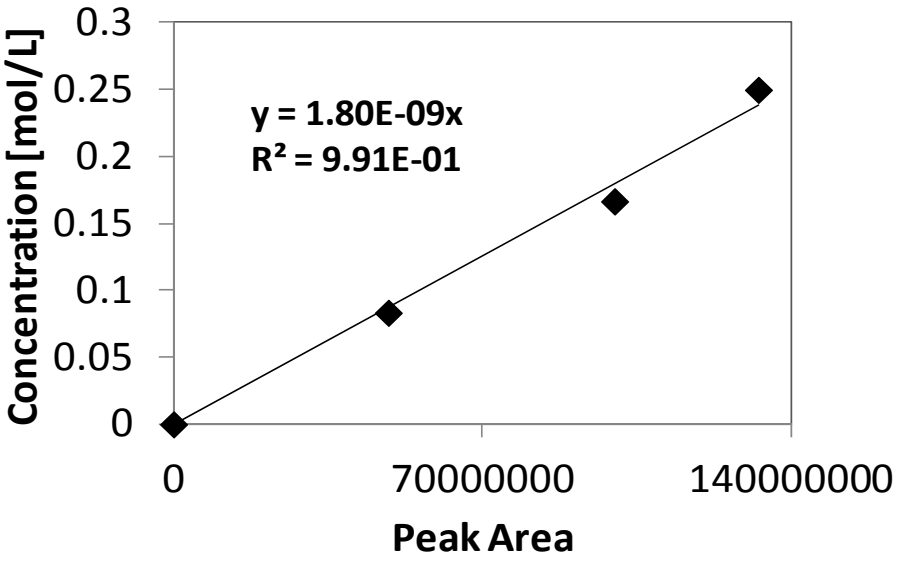

Figure 8.5: Tartronic acid calibration curve

VI. Glyceraldehyde

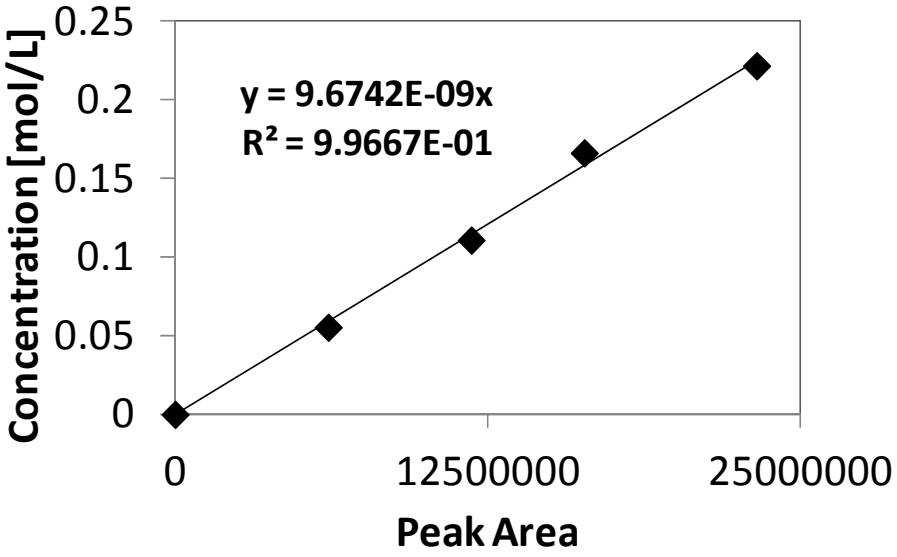

Figure 8.6: Glyceraldehyde calibration curve

VII. Acetic acid

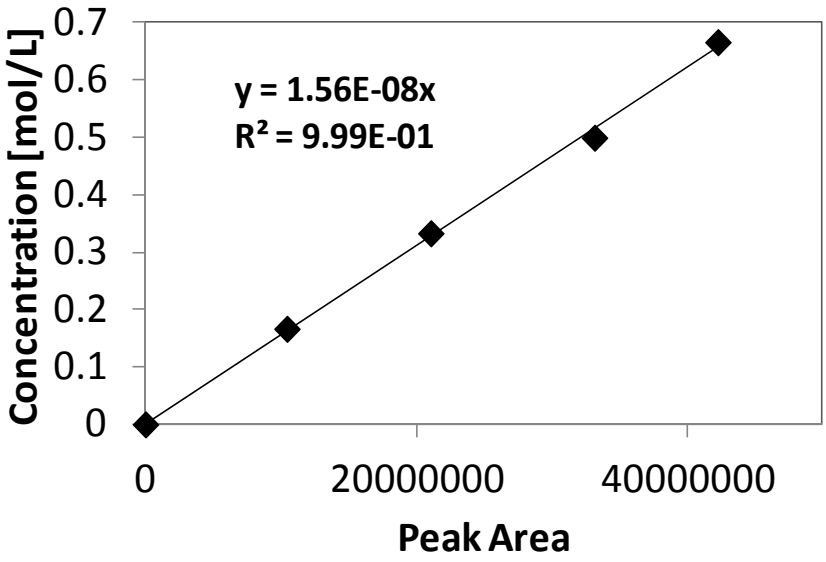

Figure 8.7: Acetic acid calibration curve

VIII. Formic acid

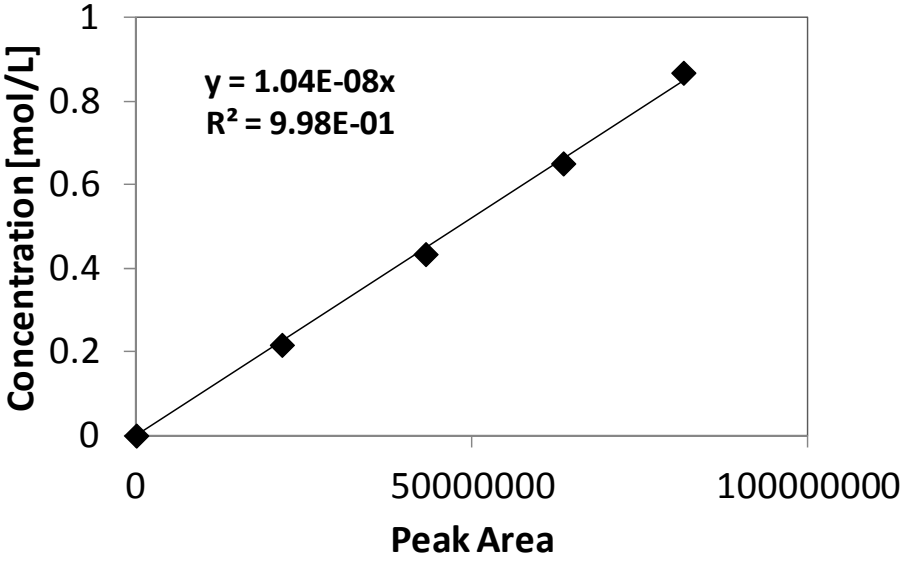

Figure 8.8: Formic acid calibration curve

IX. Lactic acid

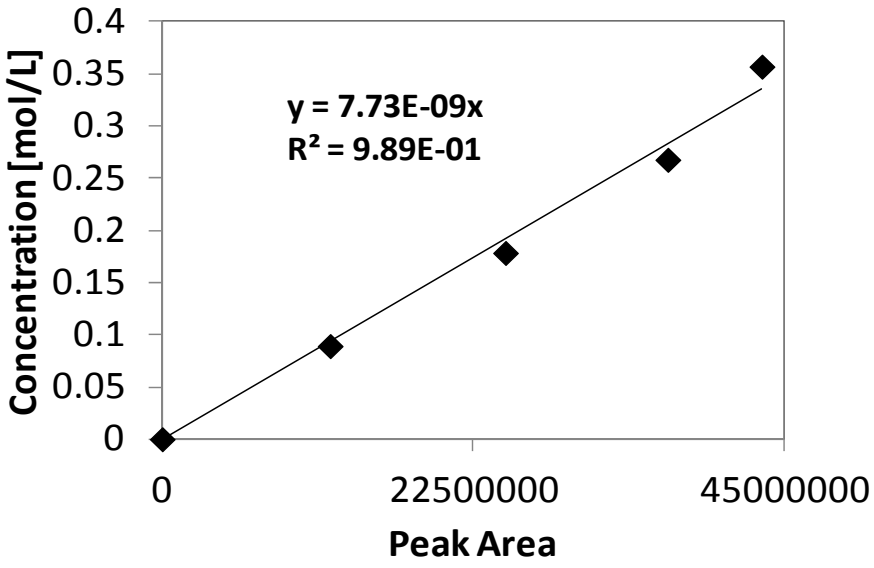

Figure 8.9: Lactic acid calibration curve

X. Carbonic acid

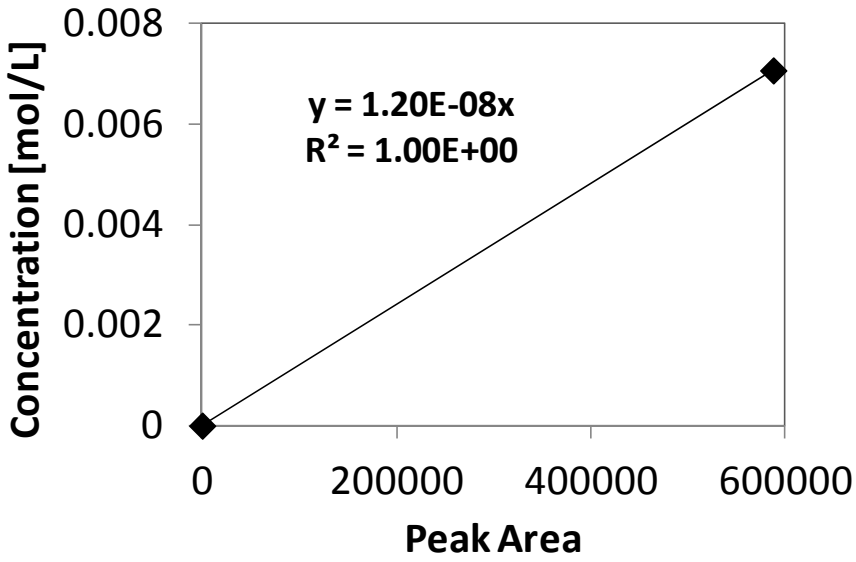

Figure 8.10: Carbonic acid calibration curve

Appendix II

Calculation of catalyst loading for bimetallic catalyst

- A known mass of Au/Al_2O_3 catalyst was digested and a standard solution of known volume was made up
- This solution was analysed by AAS to obtain he concentration of gold in that solution
- The gold loading could then be calculated from this using the mass of catalyst digested and molar masses of the precursor solution, $HAuCl_4$.

Using $Au_{63}Pt_{37}$ as an example:

- 3.92g of $(NH_3)_4PtCl_2$ salt was dissolved in 25ml of deionised water
  = 0.44 M of $(NH_3)_4PtCl_2$ solution
- In 10g of catalyst, with a loading of 1.4 wt%, there is 0.14g of Au. Since it is necessary to have a total metal loading of 2.2 wt%, the deficit (0.08g) is to be made up by the addition of Pt
- The volume of Pt solution to be added is calculated as follows:

Mass of Pt required	Concentration of solution	Molar mass of Pt	Conversion to ml
0.08g Pt	**L**	**mol**	**1000 ml**
	0.44 mol salt	**196 g Pt**	**1 L**

≈ 1 ml